Discovery and Mechanistic Studies of Triamterene-Induced Naïve Conversion of Late-Stage Epiblast Stem Cells

DISSERTATION

Von

Dipl.-Chem.

Damir Jacob Illich

aus Banja Luka

Discovery and Mechanistic Studies of Triamterene-Induced Naïve Conversion of Late-Stage Epiblast Stem Cells

Zur Erlangung des akademischen Grades eines
Doktors der Naturwissenschaften
(Dr. rer. nat.)
von der Fakultät für Chemie und chemische Biologie
der Universität Dortmund
angenommene

Dissertation

Von
Dipl.-Chem.
Damir Jacob Illich
aus Banja Luka

1. Gutachter: Prof. Dr. Herbert Waldmann
2. Gutachter: Prof. Dr. Hans R. Schöler

Tag der mündlichen Prüfung: 18. September 2014

To my mother Ljilja and Miao

Eidesstattliche Erklärung

Hiermit versichere ich an Eides statt, dass ich die vorliegende Arbeit selbstständig und nur mit den angegebenen Hilfsmitteln angefertigt habe.

Münster, Juli 2014

Damir Jacob Illich

Die vorliegende Arbeit wurde unter Anleitung von Prof. Dr. Herbert Waldmann und Prof. Dr. Hans R. Schöler am Max-Planck Institut für molekulare Biomedizin in Münster in der Zeit von Januar 2010 bis July 2014 angefertigt.

Acknowledgements

Table of Contents

Table of Contents

_____

III

Table of Contents

1.   Introduction

1.1   Chemical Genetics

1.1.1 Definition

Chemical genetics is the study of the function of gene products using perturbation by small molecules. A more detailed explanation of certain terms within the given definition shall facilitate better understanding.

Chemical genetics is often used interchangeably with the term chemical genomics. In most cases both mean the same field and scientific approach. However, there is a certain distinction very similar to the difference between the fields of genetics and genomics. In general, the suffix -ome, such as in genome, proteome, or metabolome, indicates the entire pool of a certain type of molecules within a biological system. Omics aims at the global study of the entire pool, e.g. the global transcription analysis to study structural and functional differences between two cell types. In the analogous sense, the extension from chemical genetics to chemical genomics is the aim to identify a specific inhibitor for each gene product in the human genome (Schreiber, 2005).

In chemical biology and medicinal chemistry small molecules are used to inhibit specific protein functions. Chemical biology applies small molecules to study biological phenomena by identifying the protein targets that cause or prevent a biological effect. The aim of medicinal chemistry is to identify selective and potent inhibitors of protein targets that cause a pathological outcome. This process certainly includes the study of the pathological mechanism, as well as the mechanism of action of the inhibitor. Both, however, contain the three main components of chemical genetics which are

the synthetic generation and expansion of small molecule libraries, development of screening assays, and target identification and validation.

Next, the meaning of gene product within the above definition of chemical genetics shall be explained. A gene is the sequence of nucleic acids within the DNA encoding a protein. The DNA is packaged into chromosomes and contains intron and exon regions in eukariotes. According to the central dogma of molecular biology the nucleic acid sequence from the DNA is irreversibly transcribed into the messenger RNA, which is then irreversibly translated into protein. During the process of splicing the introns are removed, and only the exons encode the protein. In brief, DNA makes RNA, and RNA makes protein. Hence, it becomes obvious that gene products can be twofold, since DNA encodes both RNA and protein. To clarify this ambiguity within the above given definition of chemical genetics and the following content of the presented thesis, by gene product solely protein is meant.

A specific feature of chemical genetics lies within the tools used to perturb a biological system. These tools are in particular small molecules. Small molecules are defined as substances with a molecular weight below 800 Da. Some definitions of chemical genetics include also other exogenous ligands. These could potentially be antisense RNA, or DNA-targeting reagents. Here, we shall focus on protein-binding reagents and small molecules only. This specification is essential since the generation and modification of small molecule libraries by means of synthetic chemistry is a crucial topic in the field of chemical genetics as will be explained further below.

Small molecules are used to perturb a biological system, but how? The question itself already provides one half of the answer, namely that small molecule compounds are the elementary parts that perturb the system. This appears natural to us, but although plants and their extracts have been used for thousands of years to treat diseases, the insight that it is individual molecules that reside within the plants that cure the diseases did not come until the isolation of morphin from opium by Sertürner in 1804, which marked the isolation of the first active compound (Klockgether-Radke, 2002). The

second premise, namely that small molecule compounds bind to specific protein receptors came 100 years later through the works of Paul Ehrlich and Emil Fischer who developed the ideas of a molecular receptor and the lock-and-key principle (Stockwell, 2000). This insight, that there is a specific interaction between the small molecule and the target protein is key to the field of chemical genetics. Today, it is known which forces enable the small molecule to interact with the target protein. These are noncovalent electromagnetic and electrostatic interactions such as hydrogen bonds and salt bridges, and hydrophobic interactions, and steric interactions of the partners. There were many crucial steps toward this discovery. On the one hand, there was the development of protein sequencing, NMR and cristalography methods to study protein structure and the properties of binding pockets. On the other hand, there were advances in our understanding of the physical forces at the atomic level, as well as progress in organic synthesis that allowed chemical modification of the small molecule inhibitors to study structure-activity-relationships (SAR). Computational chemistry and molecular modeling have equally become valuable modern investigation methods to study inhibitor-target interaction.

Taken together, chemical genetics is the study of gene product functions through perturbation with small molecule compounds. Chemical genetics is predominantly focused on the perturbation of proteins as gene products. Chemical biology and medicinal chemistry also apply small molecules to perturb protein functions. Small molecules are used as exogenous ligands to perturb protein functions.

1.1.2 Why Chemical Genetics

Conventional gene technology methods have been developed to include very sophisticated technologies that allow conditional gene knockouts and inducible gene expression. New methods using zink finger nucleases,

TALENs, and CRISPR offer elegant ways to modify the genome by homologous recombination. These techniques offer convenient ways to study genes in a conventional genetic approach. So why do we need chemical genetics?

The chemical genetic approach entails several advantages over conventional genetics (Spring, 2005). One very obvious advantage is the simplicity of the approach. Gene knockout and knockout mouse technology are laborious and tissue consuming. Compared to that, the perturbation by using a small molecule inhibitor barely involves more than the step in which the compound is added.

Following the same line, small molecules act instantly and rapidly. Small molecules are cell permeable and diffuse directly to their target protein to inhibit its function. The inhibition of kinases, for example, by using small molecules takes not much longer than 15 min, and the results can be made visible by western blotting. Transfections of plasmids can take several hours, and viral transductions are usually done over night. After the foreign DNA has been introduced into the host it still takes 12 - 48 hours for the introduced sequence to be processed. In some cases the cells that need to be analyzed do not live long enough, or do not exist long enough in a particular developmental state, to allow genetic modifications (Hakkim et al., 2011).

An important advantage of using small molecules is the fact that the inhibiting effect is reversible. If cells are treated with an inhibitor in cell culture all that needs to be done is to replace the medium by new medium that is not containing the compound, i.e. the small molecule can be washed out. The remaining compounds inside the cells will be metabolized or actively transported outside the cells. On the other side, if a genetic modification has been introduced into the genome it cannot be made reversible. Transient transfections have to be analyzed by sequencing to reliably exclude integrations into the genome, and inducible or conditional genetic perturbations are often accompanied by the problem of "leaking".

Chemical genetics allows us to study critical genes where genetic knockouts are lethal for the organism or the cell. A genetic knockout might also cause a cell type to change, for example by differentiation, so that the cell type of interest cannot be studied anymore. Small molecules act instantly and rapidly and can be applied to study the gene product of interest at different stages, e.g. different developmental stages, to determine the moment at which the function of the studied gene product is indispensable. Stat3 knockout mouse embryos, for example, die before gastrulation which makes investigations on cells derived from Stat3 knockout mice impossible (Takeda et al., 1997). By using a small molecule Stat3 inhibitor the role of Stat3 could potentially be dissected during embryo development, in embryonic stem cells, as well as epiblast stem cells, and even later during differentiation (Schust et al., 2006). Chemical genetics also allows the simultaneous study of multiple gene products by the application of multiple small molecule inhibitors at the same time. Thus, the interaction of several gene products that cause a biological effect in a concerted fashion can be studied. Genetic techniques are not as convenient for this purpose. Random and multiple integrations, and the uncontrolled distribution of the transfected plasmids significantly complicate this approach.

Small molecules can be added at different concentrations, thus, allowing the study of dose-dependent effects. The argument of simplicity is here especially valid. By adding different amounts of the compound to the biological system the function of the gene product can be quantified. This is possible if the small molecule acts via noncovalent inhibition which is, however, mostly the case.

Other relevant arguments in favor of the chemical genetic approach deserve to be mentioned such as the possibility to study posttranslational function of gene products, safety issues, and practical reasons concerning storage, handling and the applicability for high-throughput screening. One argument, however, that is of significant and fundamental importance needs to be emphasized that is of particular importance for the field of medicinal chemistry. As outlined earlier, small molecule inhibitors can be applied to

inhibit gene products that cause diseases. The majority of the drugs on the market are small molecule inhibitors that have improved life quality and increased life expectancy considerably during the course of the 20th century. Genetic approaches are obviously very difficult to implement and not comparable to the simplicity of orally available drugs for the use at home. The originally promising gene therapy is not feasible for the treatment of most diseases and has failed to cope with the broad expectations.

The main disadvantage of chemical genetics as compared to the conventional genetic approach is probably the fact that inhibitors are still not available for each single gene product. However, there is a global coordination of the efforts toward a real chemical genomics through databases like ChemBank and PubChem. Another argument is that certain gene products are not "druggable" because they are too small and do not have a real binding pocket for small molecules. However, although transcription factors have been considered as not being target proteins for small molecule inhibition recently several successful attempts have been made to target transcription factors with small molecules (Koehler, 2010). Finally, although small molecules are optimally designed to be specific and potent toward their target protein it is sometimes impossible to introduce a perfect selectivity in particular among conserved isoforms of protein families so that some small molecules exhibit a certain promiscuity among a group of target proteins.

1.1.3 Small Molecule Libraries

The chemical genetic approach can be devided into three main steps: generation and expansion of a small molecule library, screening, and target identification and validation. That means that certain tools are indispensable at each of these three steps. The first such tool is the chemical library of small molecule compounds. Small molecule libraries are collections of diverse small molecules containing thousands and sometimes millions of compounds.

These are stored and tested in automated processes in high-throuput screening. Probably the largest and best known libraries are those of big pharmaceutical companies that have collected their compounds over decades. But compound libraries become increasingly available to academic institutions as well through automated screening facilities or smaller commercial libraries. Chemical genetics involving high-throughput screening is a relatively new field since it was not possible before certain technological advances that enabled automated processing, as well as advances in synthetic chemistry that made it possible to generate huge compound collections in a time and labor efficient manner.

Probably the biggest step toward chemical diversity was the development of solid-phase synthesis of small molecules (Bunin and Ellman, 1992). A starting material was attached to an insoluble bead which simplified purification and isolation of intermediate products significantly. Earlier chemists focused their efforts on the total synthesis of complex natural products. The synthetic approach aiming at the generation of one target compound was termed target-oriented synthesis (TOS). This allowed chemists to synthesize focused libraries by using sequential fragment-coupling reactions.

The expansion of the applicability of solid-phase synthesis, which was initally developed for peptide synthesis only (Merrifield, 1997), to non-peptide chemistry marked the beginning of combinatorial chemistry of small molecules (Bunin and Ellman, 1992). Combinatorial chemistry includes strategies such as parallel synthesis and split-and-pool synthesis and aims at the generation of the highest possible number of compounds in as few synthatic steps as possible. For the generated compounds the highest possible structural diversity and complexity are wanted. This approach with the ultimate goal to synthesize an inhibitor for each protein function, i.e. the biologically active chemical space, is called diversity-oriented synthesis (DOS) (Schreiber, 2000). In contrast to TOS which applies retrosynthesis to plan a synthatic strategy, i.e. a planning starting from the target compound, DOS sets up the synthesis starting from the building blocks. The reactions used are equally

important since they should encompass stereochemistry and branching pathways to accomplish a fast and efficient synthetic pathway toward chemical diversity and complexity (Tan et al., 1998).

DOS aims at the synthesis of the biologically active chemical space to generate an inhibitor for each gene product. A third approach toward this end has developed that is mainly concerned with the question how to identify the areas in chemical space that are enriched with biologically active compounds instead of blindly synthesizing every conceivable substance. It argues that a complete synthesis of the entire chemical space is not possible and that there is a rational and logical method for the discovery of biologically relevant subspace. This approach was termed biology-oriented synthesis (BIOS) (Wetzel et al., 2011). In principle, it is a natural product-inspired concept. The idea behind it is that natural products have evolved to interact with various proteins. First, they specifically interact with the active sites of the enzymes that are involved in their biosynthesis. And later, they interact with their functional target proteins which they are supposed to inhibit within their biological activity. Hence, both natural products as well as the binding pockets of proteins are evolutionary tailored to each other. Because of that, within the chemical space natural products entail evolutionary designed "privileged structures" for biological activity in particular because of their structural complexity and widespread presence of stereogenic centers (Wetzel et al., 2011). These structures have highly conserved scaffolds as it is evident from the scaffold trees of the structural classification of natural products (SCONP), basically a charter of the chemical space of natural products (Koch et al., 2005). This bioactive chemical space can be explored through the computer-based tool Scaffold Hunter (http://scaffoldhunter.sourceforge.net/) (Wetzel et al., 2009). The synthesis efforts according to biology-oriented synthesis should be oriented around these evolutionary favoured scaffolds. Since, both natural products as well as the binding pockets of proteins are evolutionary tailored to each other then ligands with similar structures should have an affinity to binding pockets of proteins with similar structures. This hypothesis

lays the ground for protein structure similarity clustering (PSSC) which is in a way the protein analogue of SCONP, a classification of proteins according to evolutionary conservation of their binding sites. Both methods of analysis, SCONP and PSSC, complement each other in the BIOS approach to select relevant scaffolds for the synthesis of focused diversity around the biologically active starting point (Wetzel et al., 2011).

1.1.4 Screens

The second tool that is required for chemical genetics are high-throughput screening assays. Through the advances in chemical synthesis large libraries of small molecules can be synthesized which requires automated and miniaturized screening platforms for a time and cost efficient identification of active compounds. Therefore, large screening assays are usually performed fully automated in 1536-well plates with working volumes of 3 - 10 μl. In forward chemical genetics libraries of diverse small molecule inhibitors are screened aiming at the discovery of a specific phenotype. This approach is analogous to forward genetics where random mutations are introduced into a large number of organisms. Then the mutants are screened for the desired phenotype of interest, and the mutations of specific genes are analysed that caused the phenotype. In forward chemical genetics this involves screening of a large library of ligands (mutation equivalents) for a specific phenotype of interest followed by target identification to uncover the specific protein that caused the phenotype. Target identification will be introduced in the next section.

In contrast to forward genetics where the identification of the mutated gene that caused the phenotype of interest is the last step and is not known at the onset of the screening assay, in reverse genetics the mutation of a specific gene is the starting point. What is not known at the beginning is the phenotype that the introduced mutation will cause. In analogy to that, in

reverse chemical genetics first the inhibitor of a specific protein of interest has to be identified. If the inhibitor is not known yet, an *in vitro* protein-based assay has to be developed to identify the inhibitor of the protein of interst. Once the target-based assay has yielded a specific inhibitor of the protein of interest a cell-based (*in vivo*) assay can be performed to analyze the resulting phenotype. Depending on the specificity and potency of the discovered inhibitor it could be optimized through synthetic modification toward more desired features before it is applied in the call based assay.

An important issue in screening of active compounds is the read-out or detection of compound activity that will ultimatelly define the assay quality. The field has agreed to use the Z'-factor as a standard method of quality assessment of screening assays (Zhang et al., 1999). It is, in brief, a statistical coefficient between 0 and 1 that describes the screening window of the assay depending on the means and standard deviations of the positive and negative controls of the screening assay.

There are multiple detection methods for *in vitro* target-based assays. Depending on the type of target protein, for example, fluorescence-based methods for the determination of enzymatic activity. These include fluorogenic enzyme substrates, FRET donor/acceptor pairs, oxygen and pH-sensitive probes, and immunoassays.

Detection methods for cell-based assays, on the other side, include high-content imaging, marker gene analysis, and functional assays. High-content imaging is based on microscopic imaging to detect phenotypic changes. Marker gene or protein analysis includes reporter-gene assays and antibody-based cellular immunoassays. In functional assays changes in the functional activities of cells are detected, such as growth rate, metabolism, or apoptosis.

1.1.5 Target Identification and Validation

The third step in the forward chemical genetic approach is target identification (target ID) and validation. Target ID is necessary only in forward chemical genetics, since reverse chemical genetics starts with the specific perturbation of the protein of interest. There have been significant advances in the field of target identification during the course of the last two decades. Nevertheless, compared to the progress in synthetic chemistry and the technological progress leading to fully automated and miniaturized high-throughput screening, target ID still remains the most challenging step in chemical genetics. This is mainly due to the fact that in contrast to its genetic counterpart where advanced whole genome sequencing technology allows the rapid and straightforward detection of single mutations that cause an observed phenotype, in chemical genetics such a general universally applicable protocol for the identification of ligand-protein interactions still does not exist. Instead, target identification in chemical genetics employs a variety of different approaches toward this end.

The most common methods currently applied can be divided into proteomics, genetics, and bioinformatics (Ziegler et al., 2013). Affinity-based proteomics, commonly referred to as "pulldown", is probably the most widely applied method. In principal, a pulldown probe is immobilized on an insoluble carrier and exposed to a protein cell lysate to bind the target protein. Subsequently, the carriers are washed to remove unspecific binding, the attached proteins are separated on an SDS-PAGE, digested with trypsin, and the resulting peptides are analyzed by mass spectrometry. The pulldown probes are generated by synthetically attaching a linker, e.g. alkyl, triethylenglycol, or peptide groups, connecting the hit compound to the insoluble bead. Before the linker can be attached to the hit compound a structure-activity-relationship (SAR) analysis has to be performed to identify the inactive site of the hit compound at which the linker can be attached without disturbing the compound's activity. An important point in protein pulldown are control

experiments. Since pulldowns can result in a lot of unspecific binding stringent washing steps are essential as well as the inclusion of control experiments using only the linker attached to the carrier resin and a slightly modified hit compound that exhibits a significantly reduced activity. The final analysis by mass spectrometry should result in a list of candidate proteins for further confirmation. Quantitative proteomics by isotope labeling, such as SILAC, are very powerful methods to quantify the affinity of the attached proteins to the pulldown probe (Ong et al., 2002).

Another protein-based method for target identification are *in vitro* profiling experiments against a target subclass such as kinases, phosphatases, or G protein-coupled receptors (GPCR). Profiling assays against various target classes are commercially offered by different companies. This step is usually taken once there are hints that indicate a certain target class. An additional advantage of profilings is the simultaneous target validation, i.e. assessment of the specificity of the profiled compound to a particular target protein.

Microarray technology is a very efficient tool among the genetic methods for target identification. It allows an examination of the global changes in gene transcription patterns that are caused by a small molecule compound. Through the use of proper control inhibitors micro array analyses can help to identify the perturbed signaling pathways by subjecting the differentially expressed genes to gene ontology (GO) analysis. If the specific modulation of target genes of a particular signaling pathway is observed known components of that signaling cascade can be investigated by biochemical methods to identify the specific protein target. A disadvantage of micro array-based target identification methods is the fact that only changes at the RNA level can be observed. Hence, one can only indirectly deduce the protein target from the perturbed signaling pathways and the affected target genes which is mostly not straightforward. Proper control compounds, statistically relevant technical and biological repetitions, and treatments for only very short time periods to detect instant effects are indispensable to obtain reliable data. Once a

potential target protein is identified it needs to be validated, i.e. scientific evidence needs to be provided to confirm that the candidate protein

is undoubtedly causing the phenotype. Multiple methods must be applied simultaneously toward this end. The affinity of the hit compound toward the candidate protein must be verified in an *in vitro* assay, and a dose response curve should be generated. Selectivity of the hit compound is equally important and can be assessed by profiling against members of various protein families and different isoforms of the same protein family. Global transcriptome analyses are also suitable to analyse the caused effects within the cellular environment. Structurally diverse inhibitors of the same target protein could then be applied to reproduce the phenotype, or the affected signalling pathway could be modified upstream or downstream using suitable inhibitors. The gold standard, however, to confirm the protein target within the cell environment is a gene knockdown of the target protein that results in the same phenotype. If possible, the mechanism of action of the hit compound should be validated in a suitable *in vivo* assay, for example using a transgenic model organism. Eventually, it depends on the given project which experiments are most suitable to substantiate the data in support of a candidate protein.

1.2   Pluripotent Stem Cells

1.2.1 Mouse Embryonic Stem Cells (mESC)

Pluripotent stem cells share two common features that distinguish them from other cell types: self-renewal and pluripotency. Self-renewal is defined as the cells' ability to maintain their pluripotent cell state indefinitely. It is a sort of immortality that allows the cells to be expanded in cell culture for an extended period without losing their pluripotency. Pluripotency, on the other hand, is the cells' capacity to give rise to all somatic cell types of an adult organism. The

derivation of somatic cells from pluripotent stem cells is called differentiation. Cells with these two features do not exist in the adult human body. Solely, cells with a limited differentiation capacity capable of self-renewal are found in the adult body (Wagers and Weissman, 2004). These cells are called adult stem cells, or multipotent stem cells to emphasize their limited differentiation potential. Examples include haematopoietic or mesenchymal stem cells residing in the bone marrow. During development pluripotent stem cells exist solely during a narrow time frame and in the early embryo.

Embryonic stem cells were isolated from the mouse embryo and maintained in cell culture in 1981 (Evans and Kaufman, 1981; Martin, 1981). Briefly, after the fertilization of the zygote in the oviduct up to the 8-cell stage the embryo remains totipotent, i.e. capable of generating extraembryonic tissue, the placenta, as well as all somatic cells of the embryo proper. Subsequently, the blastocyst is formed containing the trophoectoderm and the inner cell mass (ICM) in which the embryonic stem cells reside that will eventually form the embryo. It is at this stage of development that embryonic stem cells are derived. For mouse this is in most cases at E3.5 of the preimplantation embryo, but could be also half a day earlier, or later.

Two types of tests are widely applied to assess the pluripotency of cells: the teratoma formation assay and the chimera assay. Pluripotent cells that are injected into the flanks of immunodeficient mice form teratomas that contain somatic cells of all three germ layers that result from the differentiation of the injected cells. Histological analysis is used to confirm the proper development into all three germ layers. On the other hand, if pluripotent cells are injected into the blastocysts of host embryos, and the blastocysts are subsequently transferred into pseudo-pregnant foster mice the injected pluripotent cells will contribute to the development of all somatic cell types of the developing embryo (Bradley et al., 1984). The resulting mice will be derived from two types of cells, those that were injected and those from the host embryo. Hence, the derived mice will be chimeric. Chimerism can be made obvious from the firm color of the derived mice if the injected cells and the host

embryos are selected properly. The gold standard test for pluripotency is tetraploid complementation in which all cells in the ICM of the host embryo are replaced by the cells to be tested so that the resulting embryo is completely derived from the injected cells.

In cell culture mouse embryonic stem cells grow in small, oval, dome-shaped colonies. They are usually grown on a feeder cell layer of mouse embryonic fibroblasts (MEF) or feeder-free, e.g. on gelatin-coated cell culture plates. They are passaged as single cells using trypsin and exhibit high clonogenicity. Mouse embryonic stem cells have both active X chromosomes in female cells. Their pluripotency is maintained through a core regulatory network of the key transcription factors *Oct4*, *Sox2*, *Nanog*, *Klf2*, and *Klf4*. This core regulatory network is extrinsically controlled through the LIF/STAT3 and BMP4 pathways (Niwa et al., 2009; Ying et al., 2003). In contrast to that, it has been found that stimulation of ERK signaling primes mESC for differentiation (Burdon et al., 1999; Kunath et al., 2007; Stavridis et al., 2007). Examples of specific gene markers that characterize mESC include *Rex1*, *Esrrb*, *Dppa3*, *Dppa5*, *Klf2*, and *Gbx2*, and prominant cell-surface markers are SSEA1 and alkaline phosphatase.

1.2.2 Human Embryonic Stem Cells (hESC)

It was not until 1998 that human embryonic stem cells were derived and maintained in cell culture (Thomson et al., 1998). Their potential to give rise to all somatic cell types principally opened doors toward cell replacement therapies of dysfunctional or damaged tissues (Kehat et al., 2001; Zhang et al., 2001). Especially the arrival of human induced pluripotent stem cells (iPSC), which are human pluripotent cells that are indistinguishable from embryonic stem cells that are derived, however, from somatic cells through nuclear reprogramming, caused a tsunami of scientific activity in this field (Takahashi et al., 2007).

Like mESC, hESC are derived from the ICM of the preimplantation embryo. The human embryo, however, reaches the blastocyst stage at E4 - 5. Human ESC are cultured on MEF feeder cells or matrigel-coated cell culture plates. However, although hESC, like mESC, are derived at the blastocyst stage from the ICM of preimplantation embryos they have certain features that distinguish them from mESC. Distinctions are apparent already at the morphology level. While mESC grow in small, oval, dome-shaped colonies, hESC form large, round, flat, colonies. The maintenance of mESC pluripotency works through LIF/STAT3 and BMP4 signaling (Niwa et al., 2009; Ying et al., 2003), whereas hESC are maintained through Activin A and FGF2 (Greber et al., 2011; Greber et al., 2010; Xu et al., 2008). In contrast to that, ERK stimulation primes mESC for differentiation (Burdon et al., 1999; Kunath et al., 2007; Stavridis et al., 2007). HESC exhibit low clonogenicity when passaged as single cells. Usually a ROCK inhibitor is applied to inhibit apoptosis if hESC are dissociated into single cells (Watanabe et al., 2007). HESC are either passaged mechanically as small clumps, or by using collagenase or accutase. On the gene level hESC share the pluripotency core regulatory network consisting of *OCT4*, *NANOG*, and *SOX2*, and also express the mESC marker genes *REX1*, *ESRRB*, *DPPA3*, *DPPA5*, *KLF2*, and *GBX2*. While mESC express the cell-surface marker SSEA1, but not the cell-surface markers SSEA3, SSEA4, and Tra-1-60, hESC do not express SSEA1, but SSEA3, SSEA4, and Tra-1-60 (Pera and Tam, 2010). HESC are, like mESC, positive for alkaline phosphatase. As mentioned earlier the gold standard experiment for the verification of pluripotency is tetraploid complementation. Chimera experiments are obviously not possible with hESC. HESC do, however, give rise to teratomas with cells of all three germ layers when injected into immunodeficient mice.

1.2.3 Epiblast Stem Cells (EpiSC)

Epiblast stem cells represent another mouse pluripotent cell type. They were first isolated in 2007 (Brons et al., 2007; Tesar et al., 2007). However, in contrast to mESC and hESC, which are derived from the ICM of preimplantation embryos, EpiSC are derived between E5.5 - 7.5 from postimplantation mouse embryos. Since EpiSC can be maintained stably in prolonged cell culture they provide a convenient and relevant system for the study of developmental events in the pregastrulation embryo through investigations of the changes in cell fate between mESC and EpiSC.

EpiSC are pluripotent stem cells capable of indefinite self-renewal and differentiation into all somatic cell types. They readily form teratomas. The pluripotency core regulatory network consists of *Oct4*, *Nanog*, and *Sox2*, as in mouse and human ESC. However, there are significant differences between mESC and EpiSC that clearly distinguish the two cell types. While mESC grow in small, oval, dome-shaped colonies EpiSC grow in large, round, and flat colonies very similar to hESC colonies. They are passaged using accutase, collagenase, or mechanically as small clumps since they do not tolerate well single cell dissociation like hESC. Furthermore, like hESC they are maintained pluripotent by Activin A and FGF2, in contrast to LIF and BMP4 in mESC (Greber et al., 2010). On a genetic level they do not express the ICM marker genes *Rex1*, *Esrrb*, *Dppa3*, *Dppa5*, *Klf2*, and *Gbx2,* but some early differentiation markers like *Fgf5, Fgf8,* and *T brachyury* (Pera and Tam, 2010)*.* EpiSC do express the cell-surface marker SSEA1, however not SSEA3, SSEA4, and alkaline phosphatase. Also, when mESC develop into EpiSC one X chromosome undergoes random inactivation in female cells. The most important difference between mESC and EpiSC, however, is the fact that EpiSC are not chimera competent in contrast to mESC (Bradley et al., 1984; Guo et al., 2009; Tesar et al., 2007). EpiSC only form teratomas.

In light of the above mentioned similarities EpiSC, rather than mESC, appear to be the counterpart of hESC. However, there are also crucial differences

between the two cell types. In contrast to EpiSC hESC do express all the ICM markers such as *REX1*, *ESRRB*, *DPPA3*, *DPPA5*, *KLF2*, and *GBX2* similar to mESC. Furthermore, EpiSC do not express the cell-surface markers SSEA3, SSEA4, and alkaline phosphatase unlike hESC (Pera and Tam, 2010). On grounds of the described discrepancies the different pluripotent states continue to be studied intensively.

1.2.4 Naïve and Primed Pluripotency

Two distinct pluripotent states have been described in the mouse system: one is represented by mESC and the other by EpiSC. HESC appear to share more similarities with mouse EpiSC than with mESC despite some non-neglectable differences. mESC are distinct from EpiSC on several levels including derivation, morphology, clonogenicity, signaling, marker expression, and epigenetic markup. Most importantly, however, while both mESC and EpiSC readily form teratomas only mESC can contribute to chimera development while EpiSC can not (Bradley et al., 1984; Guo et al., 2009; Tesar et al., 2007). This is consistent with the earlier finding that epiblast cells cannot contribute to chimeras when injected into the blastocyst (Rossant, 2008). This developmental restriction in EpiSC together with the presence of early lineage markers has come to be called primed pluripotency, in the sense of primed for differentiation (Nichols and Smith, 2009). In contrast, the cells of the ICM with fully unrestricted developmental capacity have been said to represent the ground state of pluripotency, or naïve pluripotency.

The two distinct states of pluripotency represented by mESC and EpiSC have been intensively investigated since by profiting from the fact that both cell types can be stably maintained in cell culture. Hence, through interconversion of the two cell types, for example, the distinct features could be explored. EpiSC could be derived from mESC through differentiation by adapting mESC to the culture conditions of EpiSC, i.e. Activin A, FGF2 and withdrawal of LIF (Guo et al., 2009). The conversion of EpiSC to mESC through ectopic

expression of ICM-specific transcription factors has equally been reported (Festuccia et al., 2012; Gillich et al., 2012; Guo and Smith, 2010; Guo et al., 2009; Hall et al., 2009; Silva et al., 2009; Tai and Ying, 2013). Other studies have reported that transgenic expression is not required, and that EpiSC could be converted into ESC by a change in the culture conditions only (Bao et al., 2009; Chou et al., 2008; Greber et al., 2010; Hanna et al., 2009; Ware et al., 2009). Among these methods the most widely established protocol for the conversion is based on the simultaneous inhibition of GSK3β and MEK in the presence of LIF, which came to be known as 2i/LIF (Greber et al., 2010). This is based on the previous finding that inhibition of GSK3β and MEK with small molecule inhibitors can capture and maintain naïve pluripotency independent of other factors (Ying et al., 2008).

The similarity between hESC and EpiSC has prompted researchers to investigate whether a mESC-like hESC state could exist. Different attempts using ectopic expression and extrinsic factors have been made to generate naïve hESC (Buecker et al., 2010; Gafni et al., 2013; Hanna et al., 2010; Ware et al., 2009). However, to this date no transgene-free stable cells have been generated. Furthermore, it is still widely disputed whether a mESC-like equivalent naturally exists in humans. In rodents a natural developmental arrest at the late preimplantation stage occurs that prevents the implantation of the embryo into the uterus called diapause. At this developmental stage the self-renewal of the naïve epiblast from which mESC are derived is facilitated in these species. Diapause does not occur in humans.

1.2.5 Early-Stage and Recalcitrant Late-Stage EpiSC

It has previously been shown that EpiSC display heterogeneity within a population (Han et al., 2010; Tsakiridis et al., 2014) and between different cell lines (Bernemann et al., 2011). The heterogenous cell populations exhibit distinct functional features such as the propensity to convert to an ESC-like

state under culture conditions. Part of this heterogeneity is probably due to the broad developmental window of derivation. In this regard, it has been suggested that early-stage EpiSC are susceptible to cellular reprogramming towards an ESC-like state, whereas late-stage EpiSC are recalcitrant to this process (Han et al., 2010; Hayashi and Surani, 2009). However, the majority of EpiSC display functional features of late-stage postimplantation epiblast development. The very small subpopulation which respresents early-stage EpiSC capable of undergoing reversion to an ESC-like state under 2i/LIF is even chimera competent when injected into the ICM (Han et al., 2010). Given their chimera competence which is the hallmark feature of naïve pluripotency their ESC conversion by 2i/LIF represents merely a switch in the signaling pathways that maintain their pluripotency network from TGFβ/Activin A and FGF2 to LIF/STAT3 and BMP4. The vast majority of EpiSC fail to respond to 2i/LIF-induced ESC conversion indicating their inertness toward chemical modulation of the ERK and WNT pathway in this process. To our knowledge until now nobody has explored the mechanistic accounts for the recalcitrance of late-stage EpiSC toward ESC-conversion by chemical means only.

2.   Aims and Objectives

It has previously been reported that mouse EpiSC lines comprise heterogenous populations, which can be functionally equivalent to cells of either the early or the late stages of postimplantation development. So far, late-stage EpiSC which represent the vast majority of EpiSC were not susceptible to chemical reprogramming to naïve pluripotency as represented by mESC.

At the onset of the presented research project the goal of the thesis was to elucidate the molecular mechanism governing the reversion from primed to naïve pluripotency. Toward this end, three different questions needed to be answered: Can recalcitrant late-stage EpiSC be reverted to a naïve ESC-like state by chemical means alone, i.e. without genetically invasive methods? If so, which extrinsic factors can accomplish naïve conversion of late-stage EpiSC? What is the mechanism-of-action of the extrinsic factor?

It was hypothesized that it may be possible to revert late-stage EpiSC by using appropriate small molecule inhibitors that would modify certain signaling pathways in a way that would result in the necessary switch in the gene expression pattern that will eventually enforce naïve conversion.

In order to identify a small molecule compound capable of converting late-stage EpiSC a forward chemical genetic approach was followed. Toward this end, first a small molecule screening assay was developed. In order to ensure cell penetration and bioactivity of the used substances and to facilitate potential subsequent target validation I planned to screen the LOPAC library of known pharmacologically active compounds. The read-out should be based on fluorescent reporter gene expression. The OCT4-GFP EpiSC-GOF18 line was used for this purpose. An automated high-content imager could be used for the detection of converted OCT4-GFP positive cells.

The potential hit compound should first be validated on various late-stage EpiSC to confirm its activity. The putative converted cells should be characterized to confirm their naïve pluripotency including teratoma and chimera assays. As a way to elucidate the mechanism-of-action the direct protein target of the hit compound should be identified using various methods for target identification including protein pulldown. Structure-activity-relationship analyses were to be performed toward structure optimization and possible pulldown probe generation. Finally, microarray analyses, biochemical assays, and gene knockdown experiments should be applied to investigate perturbed pathways and crucially involved genes as part of the elucidation of the mechanism-of-action of the hit compound.

3.   Experimental Part

3.1   Materials

3.1.1 Cell Culture

PBS w/o Ca/Mg (PAA)

DMEM high glucose (PAA)

Knockout - DMEM (Invitrogen)

DMEM/F12 (Invitrogen)

Neurobasal (Invitrogen)

FCS Gold (PAA)

Knockout - Serum Replacement (Invitrogen)

L-Glutamine with Pen/Strep (PAA)

Non-essential amino acids (PAA)

2-Mercaptoethanol (Invitrogen)

0.25% Trypsin (Invitrogen)

Accutase (PAA)

N2-Supplement (Invitrogen)

B27-Supplement (Invitrogen)

24

3.1.2 Growth Factors and Small Molecule Inhibitors

Human basic fibroblast growth factor (bFGF) (Peprotech)

Human leukemia inhibitory factor (LIF) (own production)

Human/murine/rat Activin A (Peprotech)

Human bone morphogenetic protein 4 (BMP4) (Peprotech)

CHIR99021 (CH) (Tocris)

PD0325901 (PD) (Tocris)

SB431542 (SB) (Tocris)

XAV939 (Tocris)

IWR-1 (Sigma)

Amiloride (Sigma)

Triamterene (Sigma)

D4476 (Tocris)

AS605240 (Alexis)

LY294002 (Sigma)

TG100-115 (in house synthesis)

Jak Inhibitor 1 (EMD Millipore)

Y-27632 (Tocris)

Hoechst 33258 (Sigma)

DAPI (Invitrogen)

Sodium butyrate (Sigma)

AU49 (in house synthesis)

AU52 (in house synthesis)

AU58 (in house synthesis)

LOPAC1280 library (Sigma)

3.1.3 Cell Culture Media

- ESC medium
  Knockout-DMEM
  20% Knockout - Serum Replacement
  1x L-Glutamine with Pen/Strep
  1x Non-essential amino acids
  100 μM 2-Mercaptoethanol
  2000 units/mL LIF

- ESC medium (N2B27)
  50% DMEM/F12
  50% Neurobasal
  1x N2 Supplement
  1x B27 Supplement
  1x L-Glutamine with Pen/Strep (PAA)
  1x Non-essential amino acids
  100 μM 2-Mercaptoethanol
  10 ng/mL LIF
  10 ng/mL BMP4

- EpiSC medium (MEF-conditioned; CM)
  Knockout-DMEM
  20% Knockout - Serum Replacement (KOSR)
  1x L-Glutamine with Pen/Strep
  1x Non-essential amino acids
  100 μM 2-Mercaptoethanol
  5 ng/mL bFGF (before and after conditioning over MEFs)

- EpiSC medium (N2B27 medium)
  50% DMEM/F12
  50% Neurobasal
  1x N2 Supplement
  1x B27 Supplement
  1x L-Glutamine with Pen/Strep (PAA)
  1x Non-essential amino acids
  100 μM 2-Mercaptoethanol
  20 ng/mL Activin A
  12 ng/mL bFGF

- MEF medium
  DMEM high glucose
  10% FCS Gold
  1x L-Glutamine with Pen/Strep

- HEK293 medium
  DMEM high glucose
  10% FCS Gold

- Cryopreservation medium
  45% culture medium of cell type to be cryopreserved
  45% FCS or Knockout - Serum Replacement (same as in culture medium)
  10% DMSO

3.1.4 Cell Lines

- EpiSC-GOF18

  E3

  (C57BL/6 X DBA/2) X 129/Sv

  derived at E5.5

  OCT4-GFP under control of 18kb (DE and PE) Oct4 promoter

  (Bernemann et al., 2011; Greber et al., 2010; Yeom et al., 1996)

- EpiSC-OG2

  (CBA/CaJ X C57BL/6J)F2X129 X C57BL/6J

  derived at E5.5

  OCT4-GFP under control of ΔPE Oct4 promoter

  (Bernemann et al., 2011; Greber et al., 2010; Yeom et al., 1996)

- EpiSC-T9

  129S2/SvHsd

  derived at E5.5

  (Tesar et al., 2007)

- EpiSC-C1a1

  B6XCBA F1

  derived at E5.5

  (Brons et al., 2007)

- ESC-OG2

  C57BL/6J

  derived at E3.5

  OCT4-GFP under control of ΔPE Oct4 promoter

  (Yeom et al., 1996)

- Bcatenin$^{fl/fl}$ ESC

  (provided by Dr Ian Chambers and Dr Rodrigo Osorno)

  Rosa26-CreERT2

  C57/B6

  derived at E3.5

  Upon treatment with 4-OH cells become Bcatenin$^{-/-}$, and GFP

  expression is acquired constitutively.

  (Brault et al., 2001; Tsakiridis et al., 2014)

- Stat3$^{-/-}$ ESC

  (provided by Dr Ian Chambers and Dr Rodrigo Osorno)

  MF1

  derived at E3.5

  (Ying et al., 2008)

- TNGETC1 ESC

  (provided by Dr Ian Chambers and Dr Rodrigo Osorno)

  Homologous recombination was used to insert eGFP at the Nanog

  AUG codon in E14Tg2a ES cell (Chambers et al., 2007).

  Subsequently, TdtTomato was inserted just before the 3' UTR of the

  Esrrb (Festuccia et al., unpublished).

  (Chambers et al., 2007)

- Mouse embryonic fibroblasts (MEF)

  CF1

  derived at E12.5

- HEK293T cells

3. Experimental Part

3.1.5 Antibodies

For immunocytochemistry:

- Nanog
  ab70482
  1:500 dilution
  (Abcam)

- Nanog
  14-5761-80
  1:500 dilution
  (eBioscience)

- Sox2
  sc17320
  1:500 dilution
  (Santa Cruz)

- Sox2
  sc-17320
  1:500 dilution
  (Santa Cruz)

- Stella/Dppa3
  ab19878
  1:300 dilution
  (Abcam)

- Esrrb
  PP-H6705-00
  1:500 dilution
  (Persaeus Proteomics)

- Klf4
  AF 3158
  1:500 dilution
  (R&D Systems)

- Oct4
  sc-5279
  1:500 dilution
  (Santa Cruz)

For Western blot analysis:

- β-catenin
  C19220-050
  1:500 dilution
  (BD Biosciences)

- p-S33/S37/T41-β-catenin
  #9561
  1:1000 dilution
  (Cell Signaling)

- Smad2/3
  #3102
  1:1000 dilution
  (Cell Signaling)

- p-S465/467-Smad2
  #3101
  1:1000 dilution
  (Cell Signaling)

- ERK
  #9102
  1:2000 dilution
  (Cell Signaling)

- p-ERK
  #4370
  1:2000 dilution
  (Cell Signaling)

- Stat3
  sc482
  1:1000 dilution
  (Santa Cruz)

- p-Stat3
  sc8059
  1:1000 dilution
  (Santa Cruz)

- Alpha-tubulin
  T6199
  1:10000 dilution
  (Sigma)

For FACS analysis:

- CD31/Pecam1
  551262
  1:100 dilution
  (BD Biosciences)

3.1.6 qRT-PCR Primers

All qRT-PCR primers were synthesized by Metabion International AG, Martinsried, Germany.

- Axin2
  F: TAGGCGGAATGAAGATGGAC
  R: CTGGTCACCCAACAAGGAGT

- Beta-actin
  F: ACTGCCGCATCCTCTTCCTC
  R: CCGCTCGTTGCCAATAGTGA

- Cdx1
  F: GGGGTCACTGTGGACAAACT
  R: GGCCTAGGACACAAGAGCTG

- Csnk1delta

  F: ATGCCATTTGGGTTTGTCAT

  R: CACCACACCTTTCTGGAGGT

- Csnk1epsilon

  F: GCTCGAATGTGTGAAGACGA

  R: CGTCTTGAGGCTGAACTTCC

- Dppa4

  F: CGGGCGTCATAACCAGTTCA

  R: GACATGCATGCGGAGGCTAC

- Dppa5

  F: TGTGTCTCCGACCTGGATGC

  R: CACATCAGAATGCGCAGCAG

- Esrrb

  F: AGGCTCTCATTTGGGCCTAGC

  R: ATCCTTGCCTGCCACCTGTT

- Fgf5

  F: CCTTGCGACCCAGGAGCTTA

  R: CCGTCTGTGGTTTCTGTTGAGG

- Fgf8

  F: TCGCGAAGCTCATTGTGGA

  R: GCCGTTGCTCTTGGCAATTAG

- Gapdh

  F: CCAATGTGTCCGTCGTGGAT

  R: TGCCTGCTTCACCACCTTCT

- Klf2

  F: AGGCCTGTGGGTTCGCTATAAA

  R: GGCAAATTATGGCTCAAAGTAGCAG

- Klf4

  F: TGTGTCGGAGGAAGAGGAAGC

  R: ACGACTCACCAAGCACCATCA

- Nanog

  F: GAACGGCCAGCCTTGGAAT

  R: GCAACTGTACGTAAGGCTGCAGAA

- Oct4

  F: TGTTCCCGTCACTGCTCTGG

  R: TTGCCTTGGCTCACAGCATC

- Rex1

  F: GGCTGCGAGAAGAGCTTTATTCA

  R: AGCATTTCTTCCCGGCCTTT

- Sox1

  F: GGCCGAGTGGAAGGTCATGT

  R: TCCGGGTGTTCCTTCATGTG

- Sox2

  F: TTCGAGGAAAGGGTTCTTGCTG

  R: TCCTTCCTTGTTTGTAACGGTCCT

- Stella

  F: GCCGCACAGCAGATGTGAA

  R: AAATCTGGATCGTTGTGCATCCT

- T brachyury

  F: TTGAACTTTCCTCCATGTGCTGA

  R: TCCCAAGAGCCTGCCACTTT

3.1.7 Primers for Bisulfite Sequencing

All primers for bisulfite sequencing were synthesized by Metabion International AG, Martinsried, Germany.

- OCT4-GFP
  F1: GTTTTTTTATTTATTTAGGGGG
  R1: AAATAAACTTCAAAATCAACTTACC
  F2: GGGGTTAGAGGTTAAGGTTAGAGG
  R2: ACCAAAATAAACACCACCCC

- Oct4 endo
  F1: TTTGTTTTTTTATTTATTTAGGGGG
  R1: ATCCCCAATACCTCTAAACCTAATC
  F2: GGGTTAGAGGTTAAGGTTAGAGGG
  R2: CCCCCACCTAATAAAAATAAAAAAA

- Esrrb
  F1: TGTAAAAGATAGGGTTTTTGATTTGA
  R1: AAAACAATACCAAAACCACCACTAA

- Rex1
  F1: TATATTAATGTTGGAAAAAGTTTAGGTAAT
  R1: AACTCCTTAAACCCCTCCCTTTTTAAATAA
  F2: GTTTAGGTAATTAGTGTATTTTGTAG
  R2: TAAACCCCTCCCTTTTTAAATAAAC

- Dppa3/Stella

  F1: ATTTTGTGATTAGGGTTGGTTTAGAA

  R1: CCAAAACATCCTCTTCATCTTTCTTCT

  F2: TTTTTGGAATTGGTTGGGATTG

  R2: CTTCTAAAAAATTTCAAAATCCTTCATT

- Dppa5

  F1: GGTTTGTTTTAGTTTTTTTAGGGGTATA

  R1: CCACAACTCCAAATTCAAAAAAT

  F2: TTTAGTTTTTTTAGGGGTATAGTTTG

  R2: CACAACTCCAAATTCAAAAAATTTTA

- Vasa

  F1: ATAATGGAATTGATGAGTTTTTGGA

  R1: AAAACAACAAATAACATCAAAC

  F2: GGTTTTAATAAAGGTGGAGAA

  R2: AAAACAACAAATAACATCAAAC

- Pecam1

  F1: TTTTTAGTTTGGAGGTTTGTATTTG

  R1: CCCAAACCTCATTATTCTTAATTTC

3.1.8 Other Materials and Kits

- RNeasy Micro/Mini Kit for total RNA extraction (Qiagen)
- ZR plasmid miniprep kit (Zymo Research)
- NucleoBond Xtra plasmid midi/maxiprep kit (Macherey-Nagel)
- DNAse I (Macherey-Nagel)
- M-MLV Reverse Transcriptase (USB)
- Oligo-dT16 primers (Metabion)
- dNTPs (USB)
- 5x RT buffer (USB)
- SYBR green PCR master mix (Biorad)
- mouseRef-8 V2 expression BeadChips (Illumina)
- linear TotalPrep RNA amplification kit (Ambion)
- Dual-Glo luciferase assay (Promega)
- Super TOP/FOP plasmids (Addgene)
- Lipofectamin 2000 (Invitrogen)
- FuGENE 6 (Promega)
- Opti-MEM medium (Invitrogen)
- DNeasy Blood & Tissue kit (Qiagen)
- QIAquick gel extraction kit (Qiagen)
- EpiTect bisulfite kit (Qiagen)
- DNA proofreading polymerase (NEB)
- TOPO cloning kit for sequencing (Invitrogen)
- KinaseProfiler / IC50Profiler Services (Merck/Millipore; now Eurofins)
- shRNA plasmids (Sigma)
- Fast Red chromogen (Sigma)
- Naphthol phosphate solution (Sigma)
- Mounting medium (Invitrogen)

3.2   Methods

3.2.1   Derivation and Culture of MEF Feeder Cells

It is important to ensure that sterilized surgery instruments are used and that the surgical dissection is performed under a sterile hood. For the generation of MEF feeder cells E12.5 embryos from CF1 mice were dissected out from the uterus and washed in a 10cm cell culture dish containing prewarmed PBS. The washed embryos were then transfered to a new 10cm dish with prewarmed MEF medium and the heads and livers were of each embryo was removed. Then the remaining embryo tissue of three embryos was cut into small pieces in a microtube using scissors. 500 µl of fresh MEF medium was added to the minced embryo material and the whole content was transferred onto a 100 µm cell strainer in a 6-well plate. The material was gently passed through the mesh with the syringe plunger, while making sure that the filter membrane was immersed in media. The filtrate from the 6-well plate was transferred to a 50 ml Falcon tube filled with MEF media and the cell suspension was homogenized by trituration. Then the entire cell suspension was transferred to a 15cm cell culture plate and was incubated at 37 °C. The medium was changed after 6-7 hrs to remove floating cells and debris. The confluent cell monolayers were split 1:4 after 48 hrs and the susequent confluent cultures were frozen until they were used. The derived MEFs were expanded by passaging up to six times using trypsin before they were used as feeder cells for ESC culture.

3.2.2   Generation of MEF-Conditioned Medium

For feeder free culture of EpiSC on FCS-coated dishes EpiSC medium based on 20% KOSR in KO-DMEM was conditioned over CF1 MEFs. For this purpose CF1 MEFs were seeded out in gelatin-coated 15cm plates at a density of 50,000 cells/cm^2. The next day the MEFs were γ-irradiated by

exposure to 4000 rads from a γ-radiation source for mitotic inactivation. After removing the MEF medium and washing with 1x PBS (w/o Ca2+ and Mg2+) 80 ml of unconditioned EpiSC medium containing 5 ng/ml bFGF were added to the 15cm plate and the cells were kept for 24 hrs at 37 °C. Subsequently, the conditioned medium was collected from the culture dishes and new unconditioned medium was added conditioning. This process was repeated for six consecutive days. After that the collected conditioned madium was pooled together and filtered through a 0.22 μm sterile filter, aliquoted into 50 ml Falcon tubes, and stored at -20 °C. Prior to use bFGF was additionally added directly to the culture dish at a concentration of 5 ng/ml.

3.2.3 Culture of EpiSC

EpiSC were routinely cultured in MEF-conditioned medium on feeder-free dishes that had been precoated with fetal calf serum (FCS) for 15 min at RT. After precoating the FCS was aspirated and the culture dishes were washed with plenty of PBS. EpiSC were passaged as soon as individual colonies were about to grow into each other initiating differentiation. Prior to their dissociation using accutase the differentiated areas were removed mechanically with an injection needle under a stereo microscope in a laminar flow hood. The dissociated colonies were seeded as single cells at approximately 15,000 cells per 6cm dish if not indicated otherwise, and new bFGF was added directly into the cell culture dish. The cells were kept at 37 °C and the cell culture medium was replaced daily.

3.2.4 Culture of ESC

ESC were routinely cultured either on MEF feeder cells, or on feeder-free cell culture dishes that were precoated with 0.1% gelatin in PBS for at least 1 hr at RT. MEF feeder cells were seeded at a density of 50000 cells/cm^2 on 0.1% gelatin-coated dishes and were cultured overnight at 37 °C before they

were mitotically inactivated by γ-radiation the next day. ESC were passaged at 90% confluency using trypsin, and the single cells were seeded at 150,000 cells per 6cm dish if not otherwise indicated. If the ESC were cultured on MEF feeder cells, before they were reseeded on a new MEF feeder layer they were cultured for 2 x 1 hr on a gelatin-coated dish to remove the previous MEF cells by faster attachment to the gelatin-coated surface. The cells were kept at 37 °C and the cell culture medium was replaced every other day.

3.2.5 Freezing and Thawing of Cells

Cells were dissiociated to single cells using the appropriate dissociation enzyme. Prior to dissociation differentiated cell colonies were mechanically removed with an injection needle or a pipette under a stereo microscope in a laminar flow hood. Usually the EpiSC or ESC cells of one confluent 6cm dish were equally distributed to 5-10 cryovials containing. Once the cells were centrifuged after dissociation the cell pellet was resuspended in the appropriate amount of cryopreservation medium, and 1 ml aliquots of the cell suspension were frozen in cryovials at -80 °C. ROCK inhibitor was added to the cryopreservation medium when EpiSC were frozen. For long term storage the cells were stored at -150 °C in liquid nitrogen.

The cryopreserved cells were thawed quickly at 37 °C in a water bath until most of the content was liquid, and the cell suspension was diluted at least 1:10 in the corresponding culture medium of the thawed cell type. The cells were centrifuged, the medium was aspirated thoroughly, and the cell pellet was resuspended in prewarmed culture medium. The EpiSC or ESC from one vial were seeded into one 6cm dish.

3.2.6 Small Molecule Screening Assay

96-well plates with black walls and clear bottoms were precoated with FCS for 15 min at RT. The FCS was aspirated and the 96-well plates were washed

with 200 μl of PBS per well using a multichannel pipette. EpiSC were dissociated into single cells using accutase and the cells were seeded out at 2000 cells per well in 150 μl of EpiSC CM. The plates were incubated for 48 hrs at 37 °C. The culture medium was replaced by 90 μl of fresh CM and the compounds of the LOPAC library were added in 10 μl samples so that the final concentration of each compound was 10 μM. The cells were incubated with the compounds for six days at 37 °C. After the incubation the medium was thoroughly aspirated and 50 μl per well of trypsin was added without washing the cells and the plates were incubated for 30 min at 37 °C. The dissociation of the colonies was further facilitated through rocking and vortexing the plate, and pipetting up and down the trypsin cell suspension. Then 50 μl of MEF medium containing Hoechst nuclei dye was added to each well and the plates were read out by a high-content imager. The quantitative readout using high-content imaging was based on the number of single cells with a GFP intensity above a preset minimum value. The threshold for the GFP intensity was set according to the level in ESC. As a positive control, 2i/LIF-supplied ESC medium was used, whereas EpiSC CM containing bFGF was used as negative control. The quality of the assay was validated using the Z-factor, which was calculated to be 0.57.

3.2.7 Conversion of EpiSC

EpiSC were plated either on γ-irradiated MEF feeder cells or on FCS-coated tissue culture plates at low density (≤10000 cells per well of 6-well plate) and cultured overnight in MEF-conditioned EpiSC medium supplemented with bFGF. The next day the EpiSC medium was replaced by the conversion medium. If not otherwise indicated the conversion medium consisted of MEF-conditioned EpiSC medium containing 5 μM TR or AU52 without additional bFGF. The cells were cultured in the conversion medium for eight days, and after the first three days medium was changed every day. OCT4-GFP positive

colonies usually started to appear on day 6. On day 8 the cells were dissociated with trypsin and replated at low density on MEF feeder cells or on a gelatin-coated cell culture dish to allow single colony formation, and were cultured in standard ESC medium supplemented with PD. For the first 3-5 passages the newly formed ESC-like colonies were manually selected, dissociated with trypsin, and replated in a new culture dish.

3.2.8 FACS

Tissue culture cells for flow cytometry analysis were first dissociated using an appropriate enzyme. ESC and converted EpiSC were dissociated using trypsin, for EpiSC accutase was used. Around one million cells were resuspended in 500 μl of cell culture medium and the cell suspension was passed through a 40 μm cell strainer to remove debris and undissociated tissue. DAPI dye was added to detect dead cells. The readout was based on OCT4-GFP expression.

If cells were stained for the expression of PECAM1/CD31 usually one million of the dissociated cells was resuspended in 100 μl of 3% FCS in PBS. The conjugated antibody was added and the cell suspension was incubated on ice for 30 min with short vortexing disruptions after each 10 min. After the incubation the cells were washed twice with 300 μl of 3% FCS in PBS, resuspended in 500 μl of cell culture medium containing DAPI dye, and passed through a 40 μm cell strainer before they were submitted for analysis.

3.2.9 Total RNA Isolation

Total RNA from tissue culture cells was isolated using the RNAeasy Mini/Micro Kit (Qiagen) following the manufacturer's instructions that are briefly described here. Cells grown in a monolayer in a cell culture dish were lysed directly in the culture vessel using the RLT lysis buffer. The lysate was pipetted directly onto a QIAshredder spin column placed in a 2 ml collection

tube, and centrifuged for 2 min at maximum speed. One volume of 70% ethanol was added to the homogenized lysate, mixed well by pipetting, and applied to an RNeasy mini column placed in a 2 ml collection tube, and centrifuged for 15 s at 10000 rpm. The flow-through was discarded since the RNA was bound to the silica-gel membrane of the RNeasy mini column. The RNA was washed twice with RW1 buffer before DNAse I in Buffer RDD was pipetted directly onto the RNeasy silica-gel membrane for a 15 min incubation at RT. The RNA was washed once again with buffe RW1, and twice with buffer RPE. The RNA was eluted by pipetting a small amount of RNAse-free water directly onto the silica-gel membrane, and centrifugation for 1 min at 10000 rpm. The concentration of RNA was determined using the NanoDrop spectrophotometer.

3.2.10 cDNA Synthesis

For qRT-PCR, 200 to 1000 ng of total RNA were used in one reverse transcription reaction. A 25 μl reaction mixture with up to 1 μg of total RNA consisted of 5 μl RT-buffer, 0.5 μl oligo-dT, 0.5 μl dNTP mix, 0.2 μl M-MLV reverse transcriptase, and water. The reaction mixture was incubated in a thermo cycler for 60 min at 42 °C, and then for 10 min at 75 °C to inactivate the enzyme. The 25 μl of cDNA that was made from 200 ng of total RNA was diluted by adding 675 μl of nuclease-free water before it was used in a qRT-PCR reaction. The cDNA was stored at -20 °C, and the RNA was stored at -80 °C.

3.2.11 qRT-PCR

qRT-PCR was performed using the Applied Biosystems 7500 Real-Time PCR instrument. The 20 μl reaction mix contained 10 μl SYBR green PCR master mix, 7 μl of cDNA prepared as discribed under 3.2.9, and 3 μl of the primer mix. The primer mix was prepared by adding together 5 μl of a 100 mM

solution of each, the forward and reverse primer, and 190 μl of water. The reactions were performed over 40 cycles, and the relative expression levels were calculated using the $2^{-\Delta\Delta Ct}$ method. *Gapdh* and *Actb* were used as housekeeping genes, and the expression levels were normalized to technical and biological reference samples. Primer sequences are shown under 3.1.6.

3.2.12 Microarray Analysis

Total RNA for global transcriptome microarray analysis was isolated as described under 3.2.9 using Qiagen RNeasy columns with on-column DNA digestion. 300 ng of total RNA per sample was used as input into a linear amplification protocol (Ambion) which involved synthesis of T7-linked double-stranded cDNA and 12 hours of in vitro transcription incorporating biotin-labelled nucleotides. The 2100 Bioanalyzer (Agilent) was used for quality control. Purified and labeled cRNA was then hybridized for 18h onto Illumina MouseRef-8 v2 expression BeadChips following the manufacturer's instructions. After washing as recommended, chips were stained with streptavidin-Cy3 (GE Healthcare) and scanned using the iScan reader (Illumina) and accompanying software. Samples were exclusively hybridized as biological replicates.

For microarray data processing the bead intensities were mapped to gene information using BeadStudio 3.2 (Illumina). Background correction was performed using the Affymetrix Robust Multi-array Analysis (RMA) background correction model (Irizarry et al., 2003). Variance stabilization was performed using the log2 scaling and gene expression normalization was calculated with the method implemented in the lumi package of R-Bioconductor. Data post-processing and graphics was performed with in-house developed functions in Matlab. Hierarchical clustering of genes and samples was performed with one minus correlation metric and the unweighted average distance (UPGMA) (also known as group average) linkage method.

3.2.13 DNA Isolation

Tissue culture cells were lysed using the ATL buffer from the DNeasy Blood & Tissue kit. Proteinase K was added and the microcentrifuge tube was placed in a thermomixer at 55 °C for overnight incubation. One volume of nuclease-free water was added and then one volume of a phenol:chloroform:isoamylalcohol mixture, and the content was mixed thoroughly. The tube was centrifuged for 10 min at 12000 rpm at RT, and the separated upper phase was transferred to a new tube. One volume of phenol:chloroform:isoamylalcohol was added, the content was mixed thoroughly, and centrifuged for 10 min at maximum at 20 °C, and the resulting upper phase was transferred to a new tube. Two volumes of ice-cold 96% ethanol and 1/10 volume of a 3 M sodium acetate solution were added and the sample was kept for 30 min at -80 °C. After centrifugation for 15 min at 10000 rpm at 5 °C the supernatant was removed, and the DNA pallet was washed with ice-cold 70% ethanol. After another centrifugation for 15 min at 10000 rpm at 5 °C the supernatant was removed, and the DNA pellet was air-dried. The DNA pellet was then dissolved in nuclease-free water by incubation at 55 °C in a thermomixer for six hours .

3.2.14 DNA Methylation Analysis

To determine DNA promoter methylation status, bisulfite conversion was carried out on 2 µg of isolated genomic DNA using the EpiTect Bisulfite kit (Qiagen) according to the manufacturer's protocol. The two step protocol, consisting of bisulfite DNA conversion and cleanup of bisulfite converted DNA are briefly described here. DNA to be used in the bisulfite reactions was thawed. The required amount of Bisulfite Mix was dissolved by adding 800 µl RNase-free water to each aliquot. The Bisulfite Mix was completely dissolved by vortexing. The bisulfite reactions were prepared in 200 µl PCR tubes according to the instructions provided by the manufacturer. The PCR tubes

were closed tightly and mixed thoroughly at RT. The DNA protect buffer turned from green to blue indicating sufficient mixing and correct pH for the bisulfite conversion reaction. The bisulfite DNA conversion was performed in a thermal cycler following the program indicated by the manufacturer. After the bisulfite conversion was completed the PCR tubes containing the bisulfite reaction were briefly centrifuged, and then the complete bisulfite reaction was transferred to a clean 1.5 ml microcentrifuge tube. 560 μl of freshly prepared Buffer BL containing 10 μg/ml carrier RNA were added to each sample. The solutions were mixed by vortexing and then centrifuged briefly. Then, the entire mixture from each 1.5 ml microcentrifuge tube was transferred into the corresponding EpiTect spin column. The spin columns were centrifuged at maximum speed for 1 min. The flow-through was discarded. The spin column was then washed once with 500 μl of Buffer BW. 500 μl Buffer BD was added to each spin column, and incubated for 15 min at RT. The spin column was centrifuged at maximum speed for 1 min, the flow-through was discarded, and the spin column was washed twice with 500 μl of Buffer BW. To remove any remaining liquid the spin column was centrifuged at maximum speed for 1 min in a new 2 ml collection tube, and subsequently incubated for 5 min at 56 °C in a heating block. The purified DNA was then eluted with 20 μl Buffer EB and centrifugation.

The bisulfite converted DNA was amplified by PCR using the primers provided under 3.1.7. Bisulfite PCR was performed using DNA proofreading polymerase according to manufacturer's instructions. 20 μl reaction mixtures comprised of DNA proofreading polymerase, primers for methylation analysis, bisulfite converted DNA, and nuclease-free water. The PCR cycling conditions were 95 °C for 5 min followed by 40 cycles (95 °C for 30 sec, Xoptimal °C for 45 sec, 72 °C for 1 min) and a final extension step at 72 °C for 5 min. Optimal annealing temperature (Xoptimal °C) was empirically determined for each primer set using the Primer3web software.

PCR products were purified using QIAquick gel extraction kit, cloned into the pCRII TOPO vector according to the manufacturer's protocol, and

subsequently transformed into TOP10 Escherichia coli. Individual colonies were inoculated into LB medium containing Kanamycin (50 µg/ml) and cultured overnight in a 37 °C shaking incubator. Plasmids were extracted using the ZR plasmid miniprep kit.

Individual clones were sequenced by GATC-biotech using the M13 primers (http://www.gatc-biotech.com/en/index.html). Sequences were analyzed using the Quantification Tool for Methylation Analysis (QUMA, http://quma.cdb.riken.jp).

3.2.15 Immunocytochemistry

Cells grown in a 12-well plate were rinsed with PBS and fixed with 4% PFA/PBS for 10 min at RT. The PFA solution was aspirated, the cells were rinsed with PBS, and permeabilized with 0.2% Triton X-100/PBS for 10 min at RT. The Triton X-100 solution was aspirated, the cells were rinsed with PBS, and the blocking solution, consisting of 2% BSA/5% FCS/PBS, was added for 1 hour at RT. The blocking solution was aspirated, the cells were rinsed with PBS, and the cells were incubated with the primary antibody (given under 3.1.5) either overnight at 5 °C, or for one hour at RT. The primary antibody was diluted as indicated under 3.1.5 in 0.5% BSA/PBS. The cells were washed three times rocking for 5 min with PBS, and the secondary antibody was applied for one hour at RT in a 1:1000 dilution in 0.5% BSA/PBS. The cells were washed three times rocking for 5 min with PBS. Hoechst dye was added during the second washing step. The cells were covered with mounting medium and a cover slide, and pictures were taken on a Leica fluorescense microscope.

3.2.16 Alkaline Phosphatase Staining

The staining solution was prepared by adding 40 µl of naphthol phosphate solution to 1 ml of Fast Red chromogen. Cells grown in a monolayer in a

culture vessel were rinsed with PBS and fixed with 4% PFA/PBS for 10 min at RT. The PFA solution was aspirated, the cells were rinsed with PBS, and covered with the staining solution. The cells were incubated with the staining solution for 15 min at RT in dark. The staining solution was aspirated, and the cells were rinsed with Milli-Q water and allowed to air-dry.

3.2.17 Teratoma Assay and H&E Staining

The teratoma assay was used to assess the *in vivo* pluripotency of cells. Cultured cells were dissociated into single cells using an appropriate enzyme, and one million cells were collected in about 250 µl of cell culture medium. The cell suspension was injected subcutaneously into the flanks of immunodeficient SCID mice. The development of the teratomas was carefully observed, and the mice were usually sacrificed 4-6 weeks following the injection. The teratomas were excised and fixed in 4% paraformaldehyde at 4 °C overnight, and paraffin embedded at 4 °C until they were sectioned (4 µm) and stained with hematoxylin & eosin for histological analysis according to standard procedures.

3.2.18 ESC Aggregation

Cells were aggregated and cultured with denuded post-compacted eight-cell stage mouse embryos. Briefly, eight-cell embryos were flushed from [(C57BL/6 x C3H) F1 females x CD1 males] at 2.5 dpc and placed in M2 medium. Clumps of loosely connected cells (10-20 cells each) with short trypsin-treatment were chosen and transferred into microdrops of potassium simplex optimized medium (KSOM) with 10% FCS under mineral oil. Each clump was placed in a depression in the microdrop. Meanwhile, batches of 30-40 embryos were briefly incubated in acidified Tyrode's solution until dissolution of their zona pellucida. A single embryo was placed on the clump. All aggregates were assembled in this manner, and cultured overnight at

37 °C and 5% CO2. After 24 hours of culture, the majority of aggregates had formed blastocysts. 11-14 embryos were transferred into one uterine horn of a 2.5 dpc pseudopregnant recipient.

3.2.19 Kinase Profiling Assay and IC50 Determination

The kinase profiling assay and the IC50 determination have been performed by the KinaseProfiler and IC50Profiler Services at Merck/Millipore, which at the time this thesis was written belonged to Eurofins. A radiometric assay was used for all protein kinases, and a FRET-based assay, called HTRF assay, was applied for the lipid kinases. The screening conditions and protocols used in the KinaseProfiler radiometric protein kinase assays and HTRF lipid kinase assays as provided by Merck/Millipore are briefly described here.

Dilution buffer compositions prior to addition to reaction mix:

- FAK:
  15 mM MOPS, 0.75 mM EDTA, 0.0075% Brij-35, 3.75% Glycerol, 150 mM NaCl, 0.1% β-mercaptoethanol, 1 mg/mL BSA

- PKCα, PKCβI, PKCβII, PKCγ, PKCδ, PKCε, PKCμ, PKCι, PKCη:
  20 mM HEPES, 0.03% Triton X-100

- CK2, CK2α2:
  20 mM HEPES, 0.15 M NaCl, 0.1 M EDTA, 5 mM DTT, 0.1% Triton X-100, 50% Glycerol

- MEK1:
  25 mM TRIS, 0.1 mM EGTA, 0.1% β-mercaptoethanol, 1 mg/mL BSA

- mTOR:

  500 mM HEPES, 10 mM EGTA, 0.1% Tween 20

- PDK1:

  50 mM TRIS, 0.1% β-mercaptoethanol, 1 mg/mL BSA

- JNK1α1, JNK2α2, JNK3, ROCK-II:

  50 mM TRIS, 0.1 mM EGTA, 0.1% β-mercaptoethanol, 1 mg/mL BSA

- Lyn, MAPK1, MAPK2, MKK4, MKK6, MKK7β, Syk:

  50 mM TRIS, 0.1 mM EGTA, 0.1 mM Na3VO4, 0.1% β-
  mercaptoethanol,
  1 mg/mL BSA

- all other profiled kinases:

  20 mM MOPS, 1 mM EDTA, 0.01% Brij-35, 5% Glycerol,
  0.1% β-mercaptoethanol, 1 mg/mL BSA

- The dilution buffer composition for the lipid kinase assays is
  proprietary.

All compounds were prepared to 50x final assay concentration in 100% DMSO. This working stock of the compound was added to the assay well as the first component in the reaction, followed by the remaining components as detailed in the general assay protocols below. In the standard KinaseProfiler service, there was no pre-incubation step between the compound and the kinase prior to initiation of the reaction. The positive control wells contained all components of the reaction, except the compound of interest; however, DMSO (at a final concentration of 2%) was included in these wells to control for solvent effects. The blank wells contained all components of the reaction, with a reference inhibitor replacing the compound of interest. This abolished

kinase activity and established the base-line (0% kinase activity remaining). The reference inhibitors used to generate the blank signal for each kinase are given below. For lipid kinase assays, the blank wells were generated by omitting the enzyme (rather than by including a reference inhibitor to abolish the signal).

General kinase assay protocol for the radiometric assay:

The majority of the kinases was incubated with 8 mM MOPS pH 7.0, 0.2 mM EDTA, 50 µM EAIYAAPFAKKK, 10 mM MgAcetate and [γ-33P-ATP] (specific activity approx. 500 cpm/pmol, concentration as required). The reaction was initiated by the addition of the MgATP mix. After incubation for 40 minutes at room temperature, the reaction was stopped by the addition of 3% phosphoric acid solution. 10 µl of the reaction was then spotted onto a P30 filtermat and washed three times for 5 minutes in 75 mM phosphoric acid and once in methanol prior to drying and scintillation counting. Modifications to this protocol include the buffer composition (see above) and the substrate and substrate concentration.

General kinase assay protocol for the FRET-based assay:

The lipid kinases were incubated in assay buffer containing 25 µM phosphatidylinositol 4-phosphate/75 µM phosphatidylserine and MgATP (concentration as required). The reaction was initiated by the addition of the ATP solution. After incubation for 30 minutes at room temperature, the reaction was stopped by the addition of stop solution containing EDTA and biotinylated phosphatidylinositol 4,5-bisphosphate. Finally, detection buffer was added, which contained europium-labelled anti-GST monoclonal antibody, a GST-tagged PH domain and streptavidin allophycocyanin. The plate was then read in time-resolved fluorescence mode and the homogenous

time-resolved fluorescence (HTRF) signal was determined according to the formula HTRF = 10000 x (Em665nm/Em620nm).

3.2.20 Luciferase Assays

To assess the relative *Oct4* enhancer activities luciferase vectors containing the proximal (PE) and distal (DE) enhancers in the pGL3-promoter were used (Greber et al., 2010). The investigated cells were transfected as single cells with the luciferase vectors together with a renilla vector by Amaxa nucleofection (Program A-23, 4 µg of DNA, $1x10^6$ cells). The cells were cultured feeder-free, and EpiSC were cultured with the ROCK inhibitor after nucleofection. 48 hours after the transfection the cells were assayed using the Dual-Glo Luciferase assay according to the manufacturer's instructions. The read out was performed in 96-well plates with white walls and flat, white bottoms. The luciferase values were normalized to the renilla values and divided by the signals for the empty vector.

The TOP/FOP luciferase assay was performed in a 96-well cell culture plate. EpiSC were plated feeder-free on FCS-coated surface at a density of 5000 cells/well. The next day, the cells were transfected in Opti-MEM medium with 100 ng per well of the TOP/FOPFlash vectors together with 0.4 ng per well of a renilla vector using Lipofectamin 2000 according to the manufacturer's instructions. After 24 hours the cells were treated with 10 µM AU52, 3 µM CH, and DMSO control. The cells were incubated for 24 hours and subsequently reporter activity was quantified using the Dual-Glo Luciferase assay. The firefly signals were normalized to renilla luciferase activity, and then the TOP/FOP ratio was calculated.

3.2.21 shRNA-Based Gene Knockdown

The MISSION TRC shRNA constructs were received as bacterial glycerol stocks and were used with packaging plasmids to produce lentiviral

transduction particles. Bacterial cultures were amplified from the glycerol stocks for use in purification of the shRNA plasmid DNA using the ZR plasmid miniprep kit and the NucleoBond Xtra plasmid midi/maxiprep kit following the manufacturers' instructions. HEK293T cells were used as packaging cells for lentiviral particle production by co-transfection with compatible packaging plasmids using FuGENE 6 following standard procedures. EpiSC were seeded as single cells on FCS-coated tissue culture dishes at low density 12 hours prior to the infection. The attached single cells were transduced by the lentiviral particles overnight. The transduction medium was replaced by normal EpiSC MEF-conditioned medium, and the cells were cultured overnight before puromycin selection was initiated. Knockdown efficiency was assessed by qRT-PCR.

3.2.22 Western Blotting

Protein isolation was performed on ice to avoid protein degradation. Adherent cells were washed with cold PBS, and lysed with RIPA lysis buffer containing protease inhibitors (250 μl per well of 6-well plate). Cells were scraped from the culture dish using a pre-cooled cell scraper and placed into a microcentrifuge tube. To shear DNA to reduce viscosity the sample was sonicated 3 times for 15 seconds, and subsequently centrifuged at 16000g for 20 min at 4 °C. The supernatant was transferred to a new tube, and the pellet was discarded. A Bradford assay with BSA as protein standard was used to determine the protein concentration. Protein concentrations of the samples were equalized by adding lysis buffer, and the lysates were boiled in Laemmli sample buffer at 95 °C for 5 min to denature the protein. Equal amounts of protein (20 μg) were loaded into the wells of an SDS-PAGE gel (gel percentage depending on the size of the protein), and the electrophoresis was run in running buffer at 100-150 V to complete the run in about 1 hour. The proteins were blotted on a PVDF membrane overnight in a cold room at a

constant current of 10 mA. The membrane was blocked in 5% milk powder in TBST at RT for 1 hr. The primary antibody was diluted in the blocking solution, and the membrane was incubated overnight at 4 °C. The blot was rinsed 3 times for 5 min with TBST and incubated in blocking solution containing the HRP-conjugated secondary antibody for 1 hour at RT. The membrane was rinsed 3 times for 5 min with TBST, and the chemiluminescence signal was captured using the chemiluminescent HRP substrate and ECL Hyperfilm in an autoradiography cassette. The films were developed and scanned in for digital editing. The primary antibodies for Western blotting are given under 3.1.5.

- RIPA lysis buffer:
  50 mM Tris-HCl pH 8.0
  150 mM NaCl
  0.1% Triton X-100
  0.5% sodium deoxycholate
  0.1% sodium dodecyl sulphate (SDS)
  1 mM sodium orthovanadate
  1 mM NaF
  Protease inhibitors tablet

- Laemmli sample/loading buffer
  4% SDS
  10% 2-mercaptoethanol
  20% glycerol
  0.004% bromophenol blue
  0.125 M Tris-HCl pH 6.8

- Running buffer
  25 mM Tris pH 8.3
  190 mM glycine
  0.1% SDS

- TBST
  20 mM Tris pH 7.5
  150 mM NaCl
  0.1% Tween 20

3.2.23 Zebrafish Developmental Assay

Zebrafish were maintained in a recirculating aquaculture system under standard laboratory conditions at 27 °C. For mating, a male and a female fish were kept overnight in a 1 liter tank, separated by a grid. The next morning, as the grid was removed, the female laid eggs that were immediately fertilized by the male´s sperm. Embryos were harvested and kept in petri dishes filled with 1 x E3 embryo medium at 28.5 °C. They were staged by hours post fertilization (hpf) at 28.5 °C. Wild type embryos were dechorionated at 5 hpf and kept in E3 medium in 2% agarose/E3-coated petri dishes. At 7 hpf the medium was exchanged to E3 medium supplemented with either 20 µM IWR-1, 3 µM CH, 5 µM TR, 5 µM AU52, or the same volume of DMSO as control. Embryos were incubated at 28.5 °C and imaged at 48 hpf with a stereomicroscope. 60 x E3: 17.2 g NaCl, 0.75 g KCl, 2.9 g CaCl2×2H2O, 4.9 g MgSO4×7H2O, ddH2O up to 1 liter.

4.   Results

4.1   Late-Stage EpiSC are Recalcitrant as They Do Not Revert Under the 2i/LIF Condition

EpiSC-GOF18   contain a GFP transgene that is driven by at least three regulatory elements of the *Oct4* gene (Yeom et al., 1996). The upstream area contains two enhancers, namely the distal enhancer (DE) and the proximal enhancer (PE), as well as a TATA-less promoter. In ESC-OG2, the GFP reporter depends on the DE of *Oct4* for transcription, i.e., the transgene lacks the proximal enhancer (*Oct4*-ΔPE-GFP) (Yeom et al., 1996). The DE of *Oct4* contains a dense binding locus for key ESC-specific transcription factors (Chen et al., 2008). EpiSC preferentially utilize the PE over the DE, and the *Oct4*-ΔPE-GFP is active only in ESC, and not in EpiSC—both findings suggesting that EpiSC must lack some key ESC-specific transcription factors (Tesar et al., 2007; Yeom et al., 1996). The two Oct4 reporter lines (GOF18, which has the entire *Oct4* regulatory region, and OG2, which lacks the proximal enhancer, PE) were used to study naïve pluripotency (Yeom et al., 1996). Naïve pluripotent cells of both the GOF18 and OG2 reporter lines express GFP when cultured in ESC conditions (Figures 1, ESC samples). The corresponding primed pluripotent cells when cultured in EpiSC conditions do not express GFP, except for the small subpopulation which was previously shown to be chimera competent (Han et al., 2010) (Figures 1, EpiSC samples).
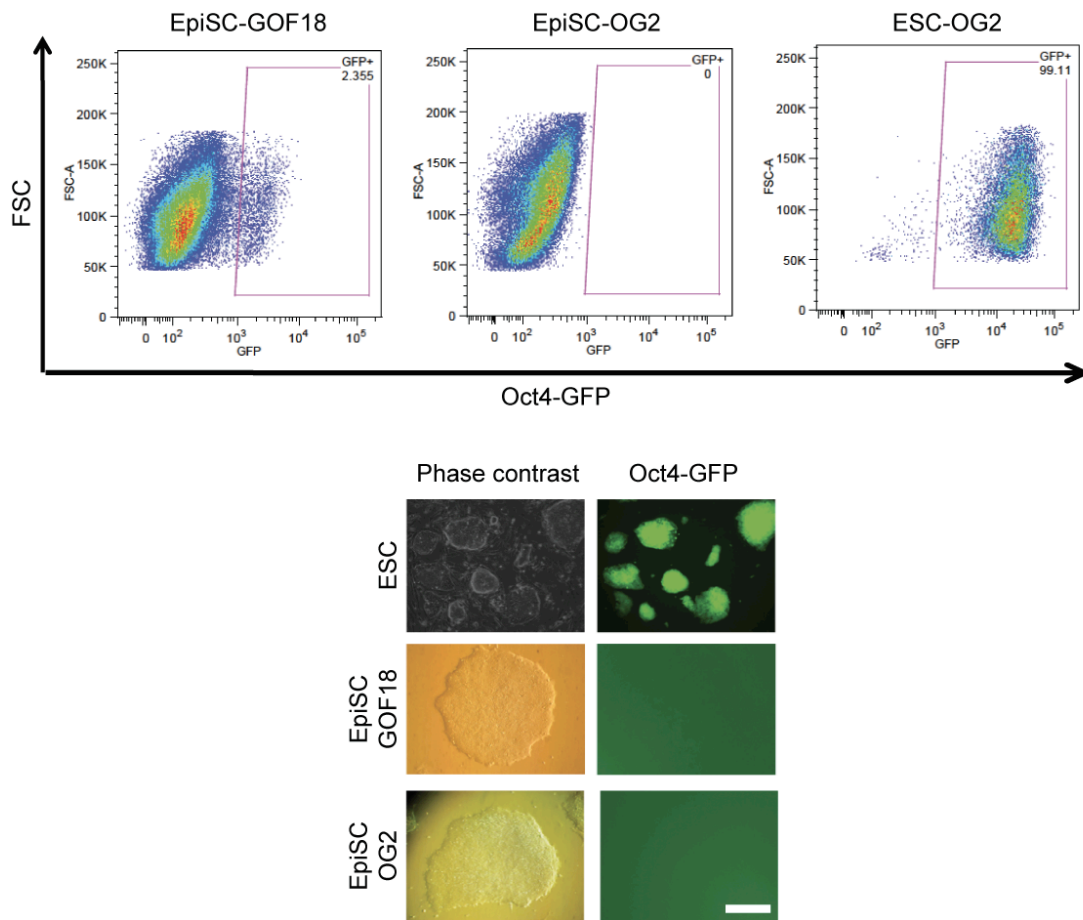
Figure 1. OCT4-GFP expression in naive and primed pluripotent stem cells.
Upper panel: Percentage of *OCT4-GFP*–positive cells in EpiSC-GOF18 (left), EpiSC-OG2 (middle), and ESC-OG2 (right) as measured by FACS. Lower panel: Morphology and *OCT4-GFP* expression in ESC-OG2, EpiSC-GOF18, and EpiSC-OG2 (Scale bar: 300µm).

Global gene expression analysis revealed that EpiSC-GOF18 exhibited a gene expression pattern distinct from that of ESC-OG2 (Figure 2). Certain genes were specifically expressed in ESC that were not present in EpiSC, such as *Zfp42/Rex1* and *Dppa3*. Since they respresent the naïve cell type that was originally derived from the ICM, they were termed ICM markers. The bioinformatics analysis of microarray data was performed by Dr Marcos Jesus Arauzo Bravo.
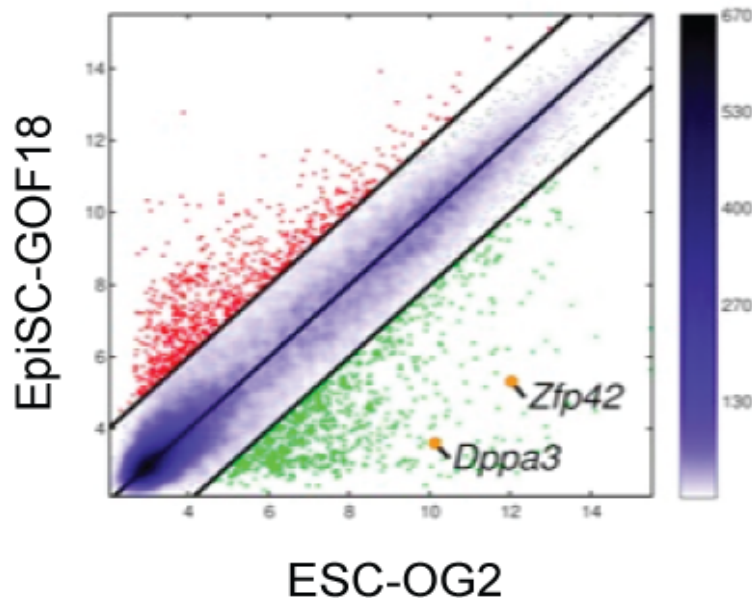
Figure 2. Scatter plot of global gene expression microarrays comparing EpiSC-GOF18s with ESC-OG2.

The black lines delineate the boundaries of 4-fold difference in gene expression levels. Genes highly expressed in EpiSC samples compared with ESC samples are shown as red dots; those less expressed are shown as green dots. Positions of the pluripotent cell marker *Zfp42*/*Rex1* and the germ cell marker *Dppa3*/*Stella* are indicated as orange dots. The color bar to the right indicates the scattering density; the higher the scattering density, the darker the blue color. Gene expression levels are depicted on $\log_2$ scale.

Quantitative RT-PCR analysis confirmed that a set of genes including *Klf4*, *Rex1*, *Stella*, *Esrrb, Dppa4* and *Dppa5* were expressed at much lower levels in EpiSC compared with ESC, whereas lineage specific markers such as *T-brachyury, Fgf5* and *Fgf8* were expressed at higher levels (Figure 3).
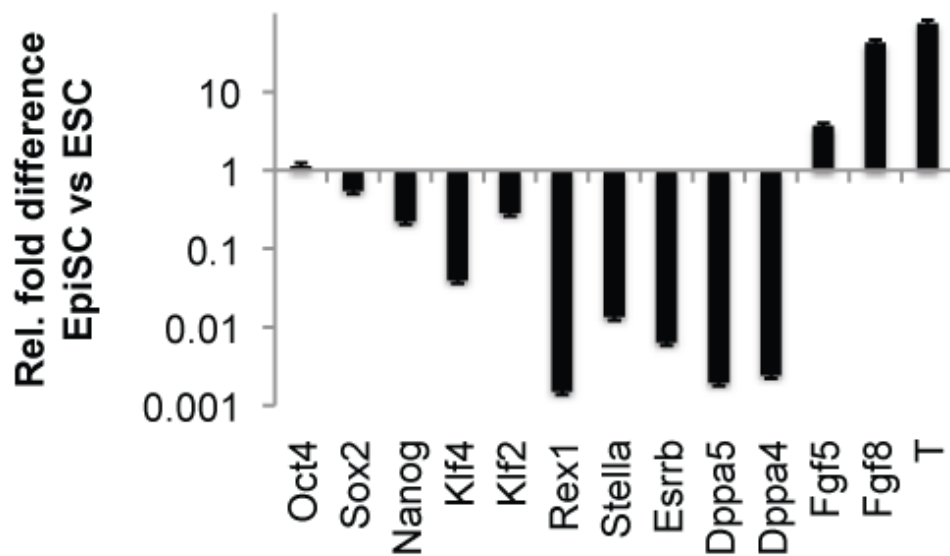
Figure 3. Comparison of gene expression patterns in EpiSC versus ESC.
Expression levels are normalized to the ESC levels (Data represent mean ± SD of triplicates; n = 3).

As reported previously (Han et al., 2010), when unsorted EpiSC-GOF18 containing OCT4-GFP–positive and –negative cells were cultured in 2i/LIF, I observed an increase in OCT4-GFP–expressing cells that resembled ESC (about 6-fold; compare left panels of Figures 1 and 4, vehicle control in lower left panel of Figure 4). When sorted OCT4-GFP–negative EpiSC-GOF18 or EpiSC-OG2 were cultured under the same conditions, namely 2i/LIF, I did not detect an increase in OCT4-GFP–positive cells, demonstrating that these GFP-negative cells were recalcitrant to conversion (Figure 4, compare middle panels for EpiSC-GOF18 and right panels for EpiSC-OG2).
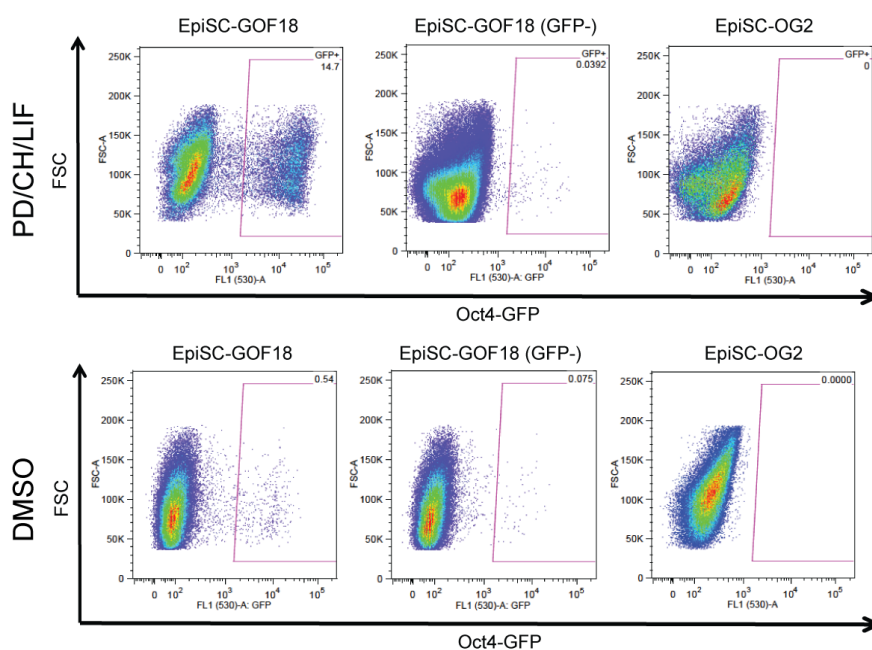
Figure 4. FACS analysis of 2i/LIF-induced ESC conversion.
Upper panel) Percentage of *OCT4-GFP*–positive cells after ESC conversion with PD/CH/LIF in unsorted EpiSC-GOF18 (left), sorted *OCT4-GFP*–negative EpiSC-GOF18 (middle), and EpiSC-OG2 (right) as measured by FACS. Lower panel) DMSO controls for the conversion with PD/CH/LIF in unsorted EpiSC-GOF18 (left), sorted *OCT4-GFP*–negative EpiSC-GOF18 (middle), and EpiSC-OG2 (right) as measured by FACS.

The 2i/LIF converted cells could be maintained under ESC culture condition, exhibited an ESC morphology, and also showed increased expression of the ICM/ESC marker *Rex1,* which was neither increased in FACS-sorted OCT4-GFP–negative cells, nor in EpiSC-OG2 (Figure 5).
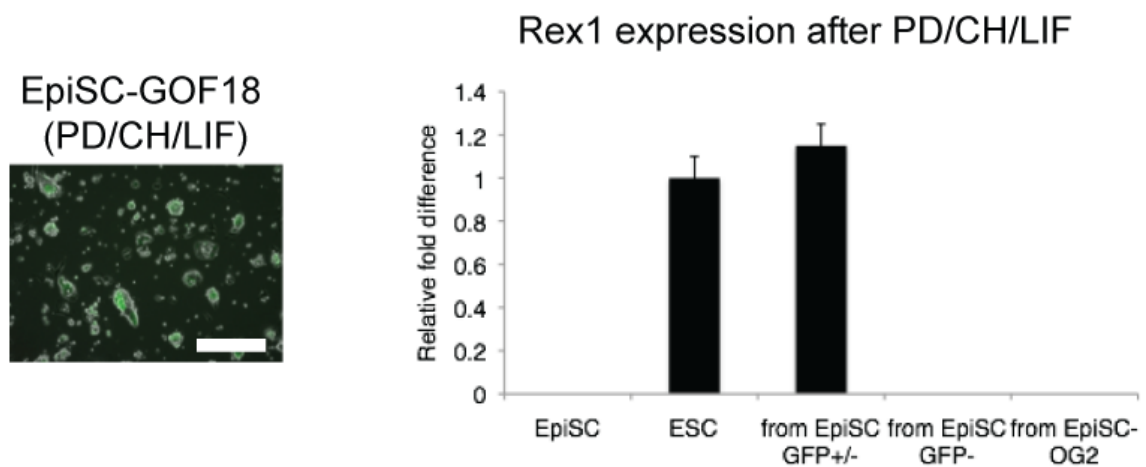
Figure 5. 2i/LIF converted EpiSC-GOF18.

Left panel) OCT4-GFP expression in PD/CH/LIF-converted EpiSC-GOF18 (Scale bar: 250µm). Right panel) Expression of the ICM marker gene Rex1 (Zfp42) in unsorted EpiSC, OCT4-GFP–negative EpiSC, and EpiSC-OG2 after conversion with PD/CH/LIF compared to EpiSC and ESC. Expression levels are normalized to the ESC levels (Data represent mean ± SD of triplicates; n = 3).

4.2   Small Molecule Screen Identifies Triamterene (TR)

To identify small molecules capable of converting recalcitrant late-stage EpiSC into an ESC-like state, I developed a screening platform in a 96-well format (Figure 6). Three crucial parameters had to be optimized for establishing a robust and reproducible assay. I plated 2,000 single EpiSC per well and cultured the plates under EpiSC culture conditions (mouse embryonic fibroblast [MEF] conditioned medium containing bFGF) for two days to allow the cells to attach and start forming colonies. Plating 2,000 cells/well proved optimal in terms of growth characteristics, efficiency of the positive control (2i/LIF), and standard deviation of the readout. Moreover, I determined that six days of incubation resulted in optimum values for the positive control.
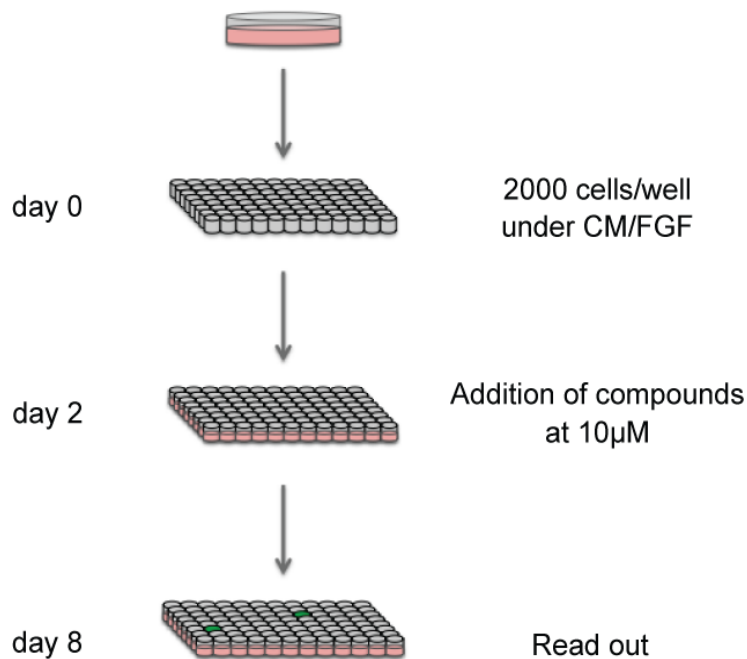
Figure 6. Schematic representation of the assay workflow.

The quantitative readout using high-content imaging was based on the number of single cells with a GFP intensity above a preset minimum value which was based on the OCT4-GFP intensity in ESC (Figure 7).
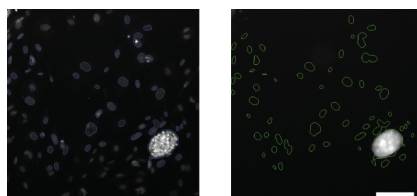
Figure 7. Readout system based on consequent fluorescence imaging for Hoechst nuclei stain (left) and OCT4-GFP (right) with Arrayscan®.
(Scale bar: 100 μM)

The threshold for the GFP intensity was set according to the level in ESC. As a positive control, I used 2i/LIF-supplied ESC medium. As a negative control I used EpiSC culture medium, i.e. MEF conditioned medium containing bFGF, in which spontaneous conversion was not observed (Figure 8).
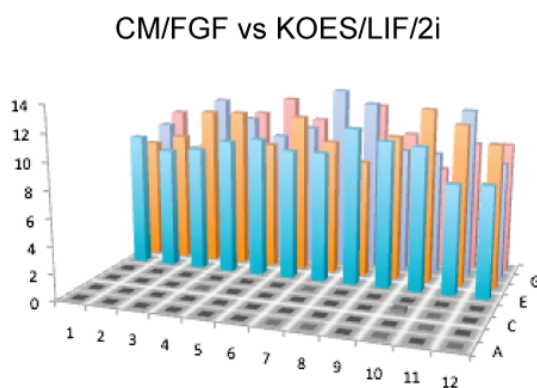
Figure 8. Positive and negative controls of the small-molecule screening assay as measured by the Arrayscan®.
ESC as positive controls, were cultured under PD/CH/LIF condition; EpiSC as negative controls, were kept under EpiSC culture conditions, i.e. on FCS-coated surface with MEF-conditioned medium and bFGF.

The quality of the assay was validated using the Z'-factor, which was calculated to be 0.57 (Zhang et al., 1999) (Figure 9).
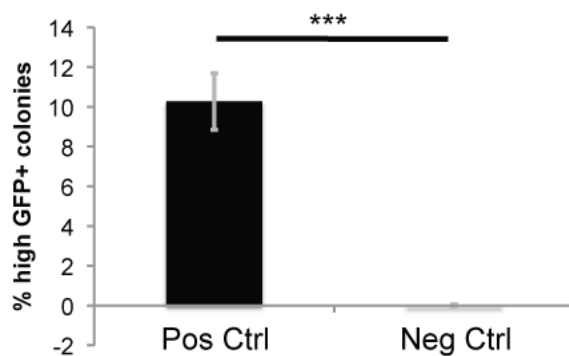

Figure 9. Z-factor of the developed small-molecule screening assay. (Data represent mean ± SD of triplicates; n = 3; p < 0.001).

Then the LOPAC[TM] library containing about 1,200 pharmacologically active compounds was screened at 10 μM screening concentration, and an active compound capable of inducing *OCT4-GFP* expression in EpiSC under EpiSC culture conditions was identified (Figure 10).
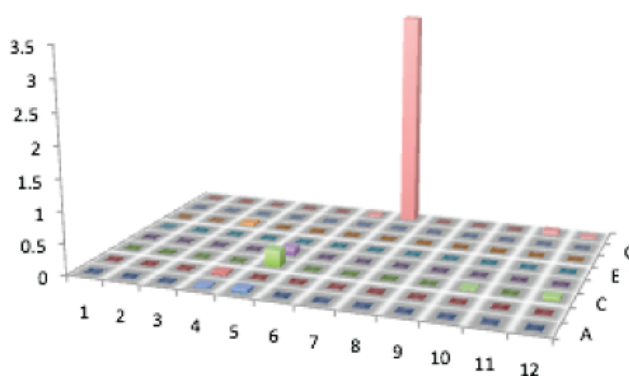
Figure 10. Hit compound Triamteren.
The hit compound Triamterene was located in rack number 15, position H07 of the LOPAC® library.

The hit compound was found to be a pteridine derivative known as Triamterene (TR), which blocks the epithelial sodium channel (ENaC), and is therefore used as a diuretic in the treatment of hypertension (Figure 11) (Busch et al., 1996). I subsequently evaluated the ability of the hit compound to convert late-stage EpiSC into an ESC-like state.
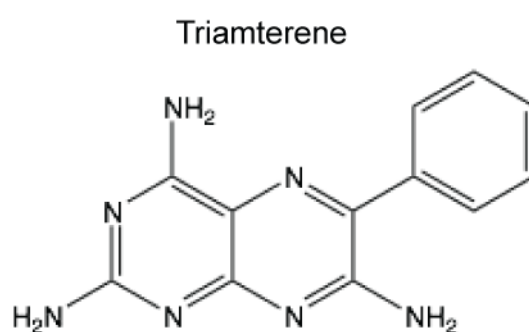

Figure 11. Chemical structure of the hit compound Triamterene.

4.3   TR Induces ESC Conversion of Recalcitrant EpiSC

TR was intially identified using unsorted EpiSC-GOF18. Next I tested the effect of TR on the recalcitrant OCT4-GFP–negative fraction of GOF18 cells. After culturing the OCT4-GFP–negative EpiSC-GOF18 with TR for seven days, flow cytometry analysis revealed a strong induction of OCT4-GFP expression, despite the presence of bFGF and ActivinA (Figure 12 left panel). Furthermore, TR induced OCT4-GFP reactivation in EpiSC-OG2 with an efficiency comparable to that of the sorted OCT4-GFP-negative EpiSC-GOF18 (Figure 12, compare left and right panels).
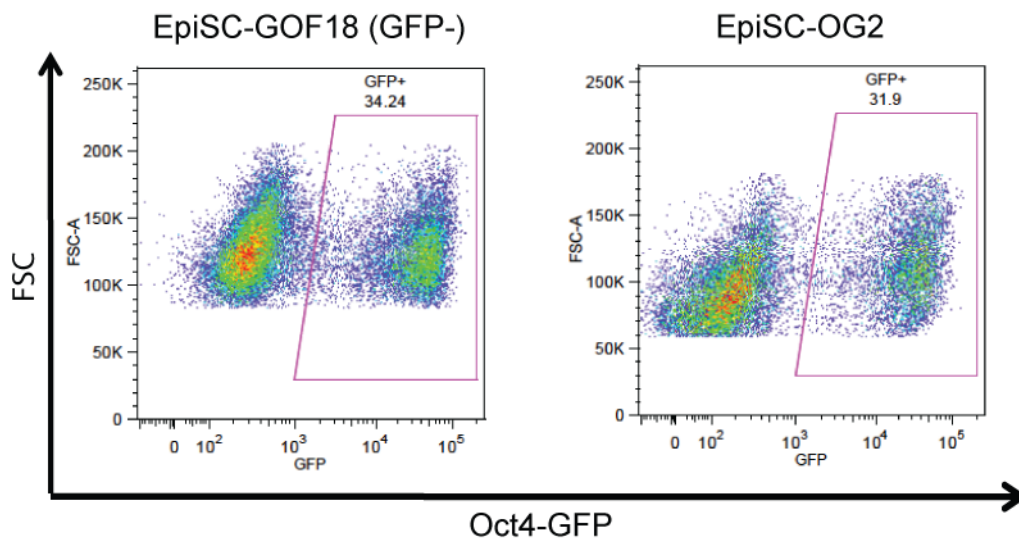

Figure 12. Triamterene induces ESC conversion in recalcitrant late-stage *OCT4-GFP*–negative EpiSC-GOF18 and EpiSC-OG2.
Percentage of *OCT4-GFP*–positive cells after treatment with Triamterene in sorted *OCT4-GFP*–negative EpiSC-GOF18 (left) and EpiSC-OG2 (right) as measured by FACS.

Clonal lines from the TR-reverted EpiSC-GOF18 ESC-like cells (TR-GOF18) were maintained for a prolongued period in ESC medium containing LIF in the absence of TR, and were passaged as single cells using trypsin. The cells exhibited a cell morphology and OCT4-GFP expression similar to ESC (Figure 13).
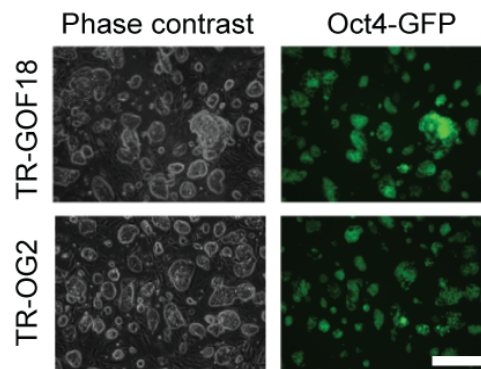

Figure 13. Morphology and *OCT4-GFP* expression in clonally expanded converted TR-GOF18 and TR-OG2 cells.
(Scale bar: 200µm).

Reverted cells from both EpiSC-GOF18 and EpiSC-OG2 and ESC were also similar with respect to ALP expression and their proliferation rates (Figure 14).
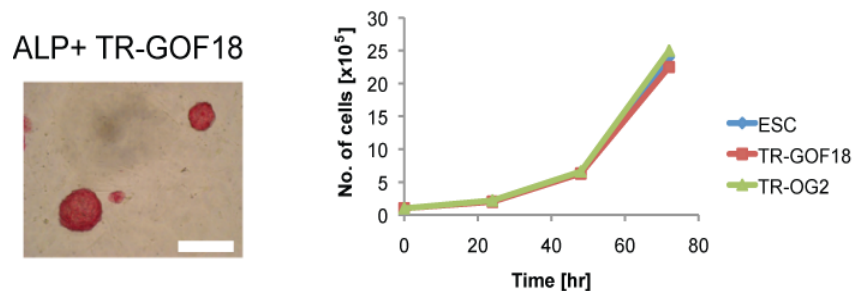

Figure 14. AP expression and growth curves of TR-GOF18 and TR-OG2 cells.
Left panel) Expression of ALP in converted TR-GOF18 cells (Scale bar: 200µm).
Right panel) Comparison of cell growth curves of TR-GOF18 and TR-OG2 cells with ESC.

Moreover, when cultured in the presence of CM/FGF, TR-converted cells dramatically changed their morphology toward bigger flat colonies, and also lost OCT4-GFP expression, two features consistent with an EpiSC phenotype (Figure 15).
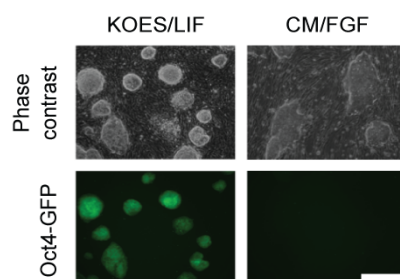

Figure 15. Morphology and *OCT4-GFP* expression of TR-GOF18 cells cultured under ESC conditions (KOES/LIF) and EpiSC conditions (CM/FGF).

(Scale bar: 300µm).

Additionally, TR-converted EpiSC (re)-expressed ESC-specific markers, such as *Rex1*, *Stella*, *Klf2*, *Klf4* and *Esrrb* (Figure 2B). In contrast, genes upregulated in EpiSC, such as *T-brachyury, Fgf5,* and *Fgf8*, were downregulated in TR-induced cells.
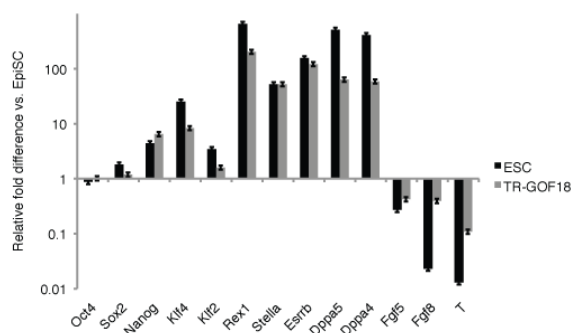

Figure 16. Comparison of gene expression patterns in ESC, TR-GOF18 cells, and EpiSC.

Expression levels are normalized to those of EpiSC (Data represent mean ± SD of triplicates; n = 3).

Most importantly, global gene expression analysis showed obvious assimilation of the gene expression profiles between TR-converted cells and ESC (Figure 17; see also Figure 29). The bioinformatics analysis of microarray data was performed by Dr Marcos Jesus Arauzo Bravo.
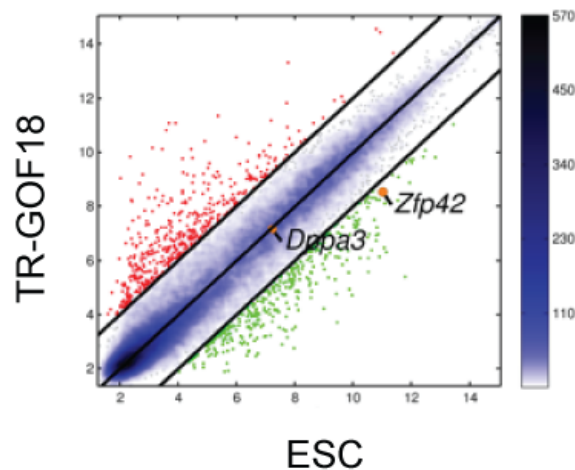

Figure 17. Scatter plot of global gene expression microarrays comparing TR-GOF18 cells with ESC.

The black lines delineate the boundaries of 4-fold difference in gene expression levels. Genes highly expressed in TR-GOF18 samples compared with ESC samples are shown as red dots; those less expressed are shown as green dots. Positions of the pluripotent cell marker *Zfp42*/*Rex1* and the germ cell marker *Dppa3*/*Stella* are indicated as orange dots. The color bar to the right indicates the scattering density; the higher the scattering density, the darker the blue color. Gene expression levels are depicted on $\log_2$ scale.

Then the ability of TR to convert EpiSC lines (T9 and C1a1), which were previously shown to be basically resistant to media-induced conversion using 2i/LIF, was assessed (Bernemann et al., 2011). TR efficiently induced the reactivation of ESRRB and KLF4 proteins in EpiSC-T9 and EpiSC-C1a1, promoted a change in morphology to small dome-shaped colonies, and upregulated Pecam1 (Figure 18). The immunocytochemical analysis of TR-converted EpiSC-T9 and EpiSC-C1a1 was performed by Dr Miao Zhang.
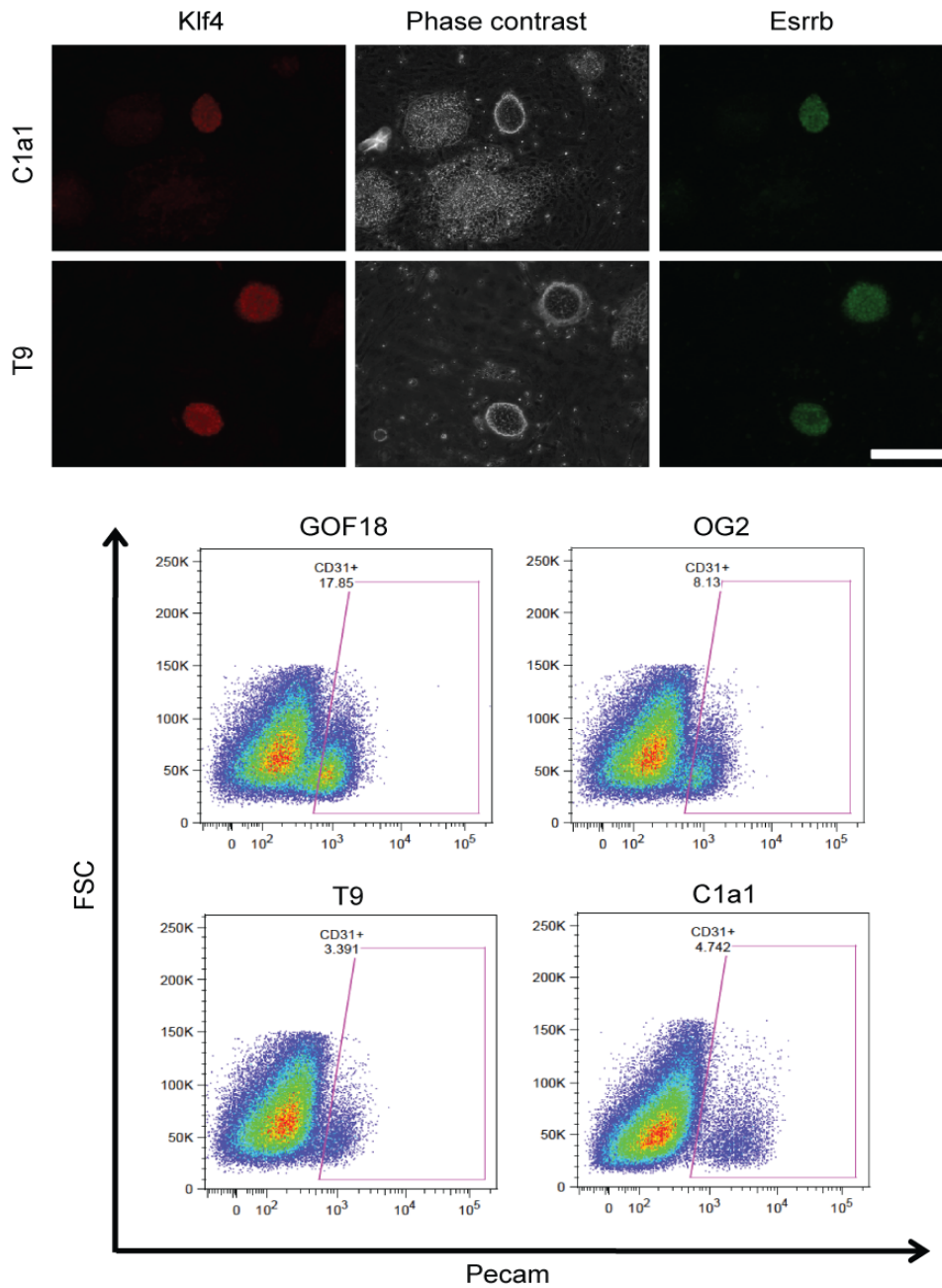
Figure 18. Immunocytochemical analysis of KLF4, ESRRB, and PECAM1 expression in TR-converted recalcitrant late-stage EpiSC.

Upper panel) Immunofluorescence analysis for the ICM markers *Klf4* and *Esrrb* in the TR-converted EpiSC lines C1a1 and T9 (Scale bar: 200µm). Lower panel) Percentage of *Pecam1*–positive (*CD31*) cells after treatment of EpiSC-GOF18, EpiSC-OG2, EpiSC-T9, and EpiSC-C1a1 with Triamterene as measured by FACS.

The effectiveness of TR to re-instate naïve pluripotency in EpiSC was further tested using an X-Chromosome-GFP reporter in female EpiSC. Culturing these EpiSC in ESC media containing LIF did not reactivate XChr-GFP on the silent X-chromosome, consistent with lack of reprogramming, whereas TR successfully promoted XChr-GFP reactivation (Figure 19). Taken together, TR induced the efficient conversion of recalcitrant late-stage EpiSC toward a cellular state that is similar to that of ESC. The immunocytochemical analysis of TR-converted EpiSC-T9 and EpiSC-C1a1 was performed by Dr Miao Zhang.
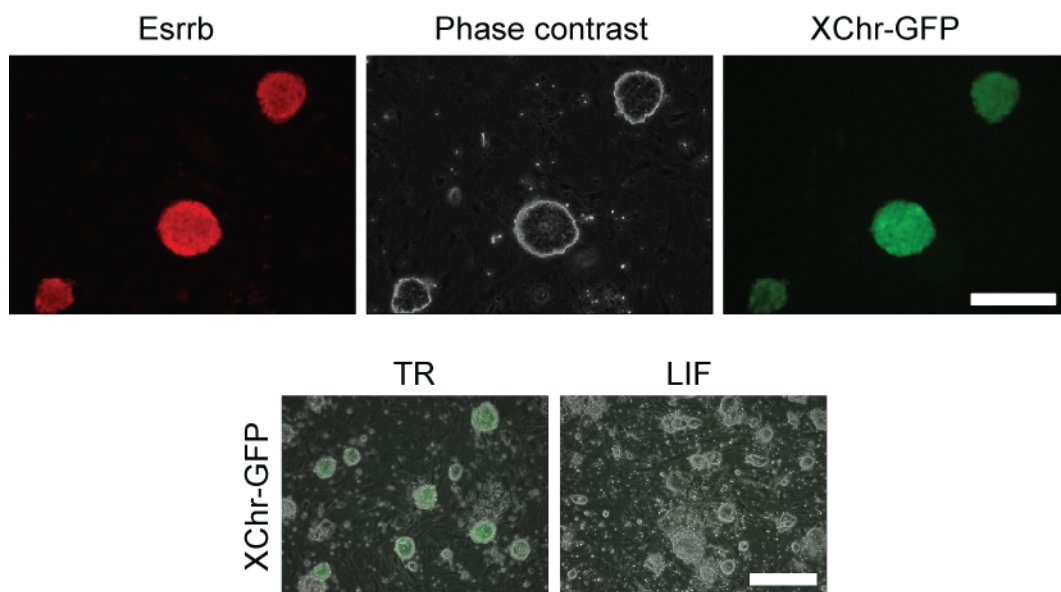

Figure 19. TR-induced X-Chromosome reactivation in EpiSC.
Upper panel) X-chromosome reactivation and immunofluorescence analysis for the ICM marker *Esrrb* after TR-conversion (Scale bar: 200µm).
Lower panel) X-Chromosome reactivation induced by TR as compared to LIF treatment alone (Scale bar: 200µm).

4.4   Combined Treatment With TR/PD Improves the Transition to Naïve Pluripotency

Althought TR-converted cells and ESC had many traits in common, the clonal populations displayed some OCT4-GFP-negative cells, which are not observed to such an extend in ESC cultured in KO-DMEM/KOSR/LIF (Figure 20, compare left and middle panels). In order to overcome this deficiency, I treated the TR-converted cells with a select set of chemical inhibitors known to support ESC self-renewal/cell reprogramming as well as a collection of compounds synthesized in house (Nie et al., 2012). I found that culturing the TR-converted cells in KO-DMEM/KOSR/LIF, together with the MEK inhibitor PD0325901 (PD) dramatically increased the proportion of OCT4-GFP-positive cells (Figure 20, compare middle and right panels).
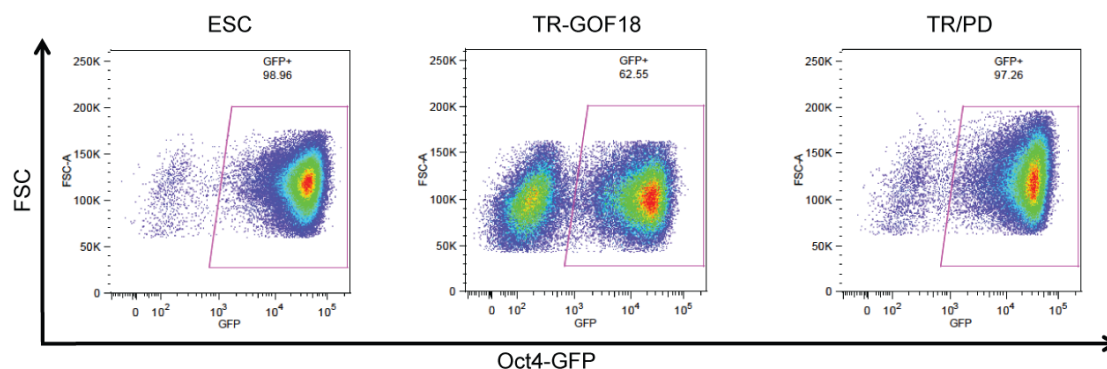
Figure 20. Percentage of *OCT4-GFP*–positive cells in ESC, TR-GOF18 cells, and TR/PD-converted cells.

These TR/PD-converted cells and ESC were indistinguishable wth respect to cell morphology, growth characteristics, AP activity and OCT4-GFP expression (Figure 21).

Figure 21. Morphology, *OCT4-GFP* expression, and ALP expression in ESC, TR-GOF18 cells, and TR/PD-converted cells grown on a MEF feeder layer and on a gelatin-coated surface.

(Upper scale bar: 350µm, lower scale bar: 5mm).

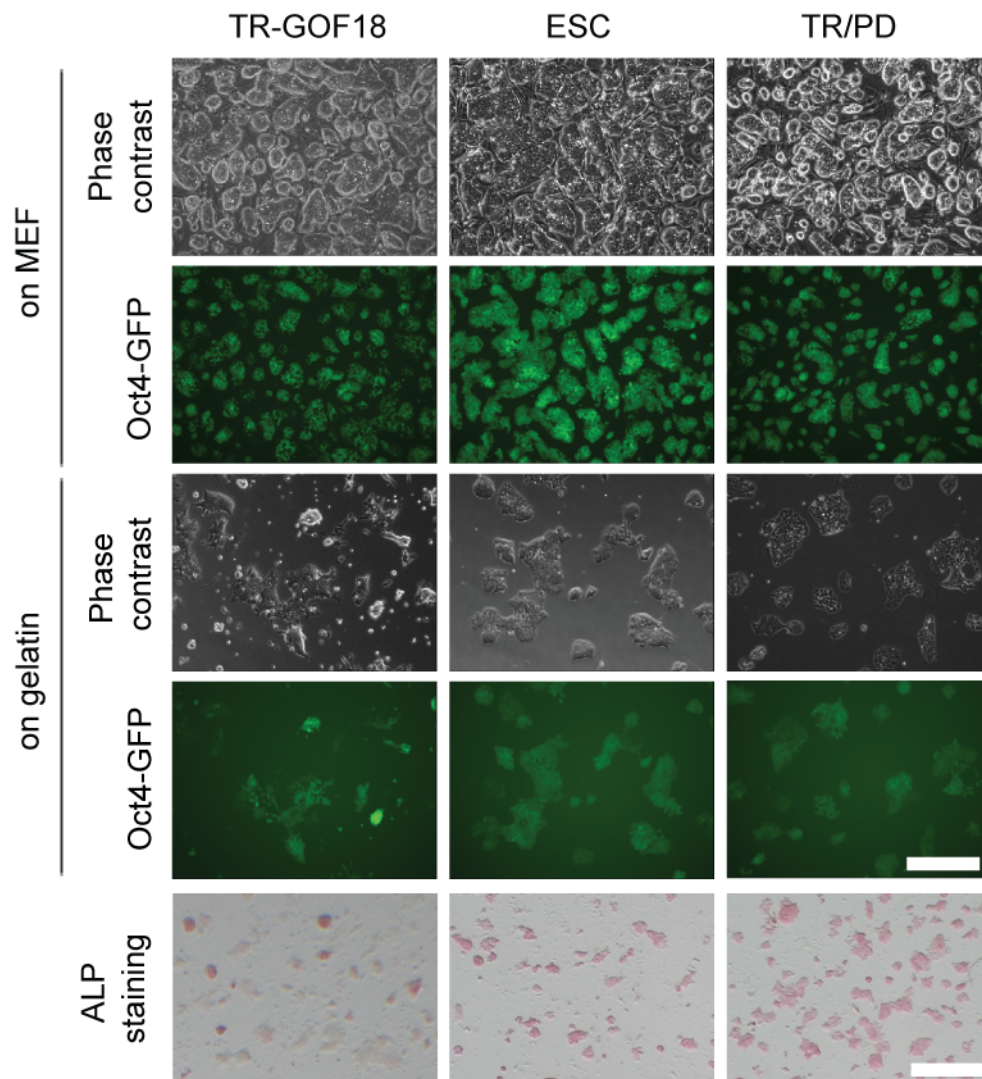At the molecular level, TR-GOF18 cells clearly expressed ICM-specific markers such as *Rex1*, *Stella*, and *Esrrb* which are not expressed in EpiSC (Figures 16 and 22). However, the expression levels of several ICM markers, such as *Sox2*, *Klf4*, *Dppa4* and *Dppa5* did not reach those of ESC (Figures 16 and 22). On the other hand, some lineage markers, including *T*, *Fgf5*, and *Fgf8* were still higher expressed than in ESC (Figures 16 and 22). This deficiency could be overcome by ERK inhibition in TR-GOF18 cells (Figure 22). TR/PD-converted cells (re)-expressed ESC-specific markers, while EpiSC markers were downregulated (Figure 22).
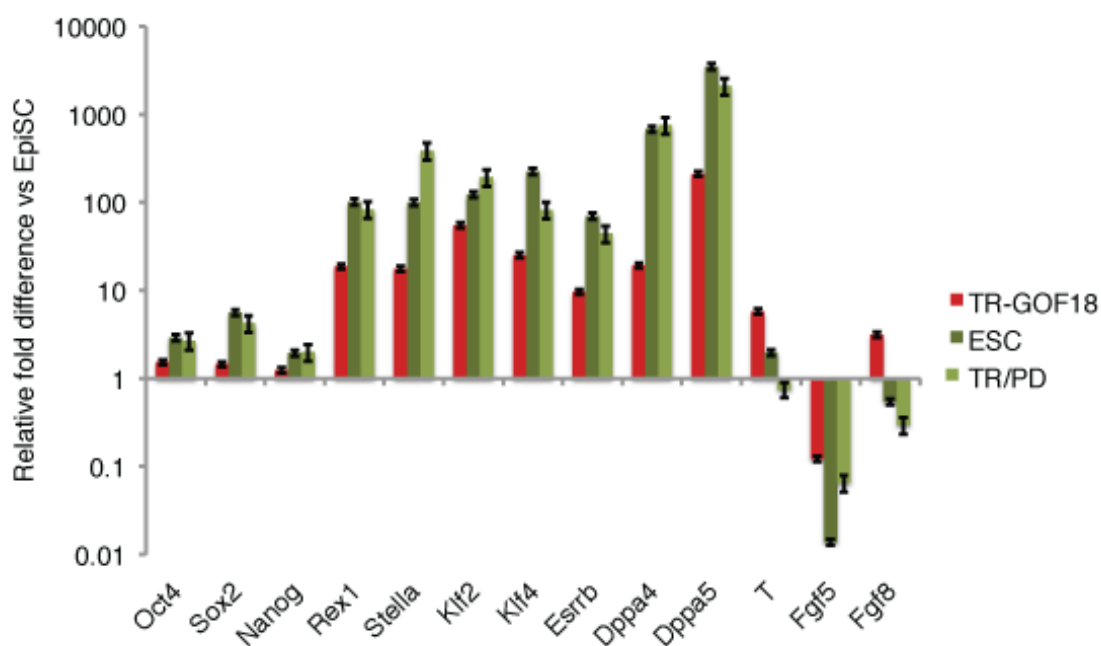
Figure 22. Comparison of gene expression patterns in ESC, TR-GOF18 cells, EpiSC, and TR/PD-converted cells.

Expression levels are normalized to those of EpiSC (Data represent mean ± SD of triplicates; n = 3).

In contrast to EpiSC, colonies of TR/PD-converted cells exhibited homogeneously expressed protein levels of Sox2, Nanog, and Stella (Figure 23). The immunocytochemical analysis of TR-converted EpiSC-T9 and EpiSC-C1a1 was performed by Dr Miao Zhang.
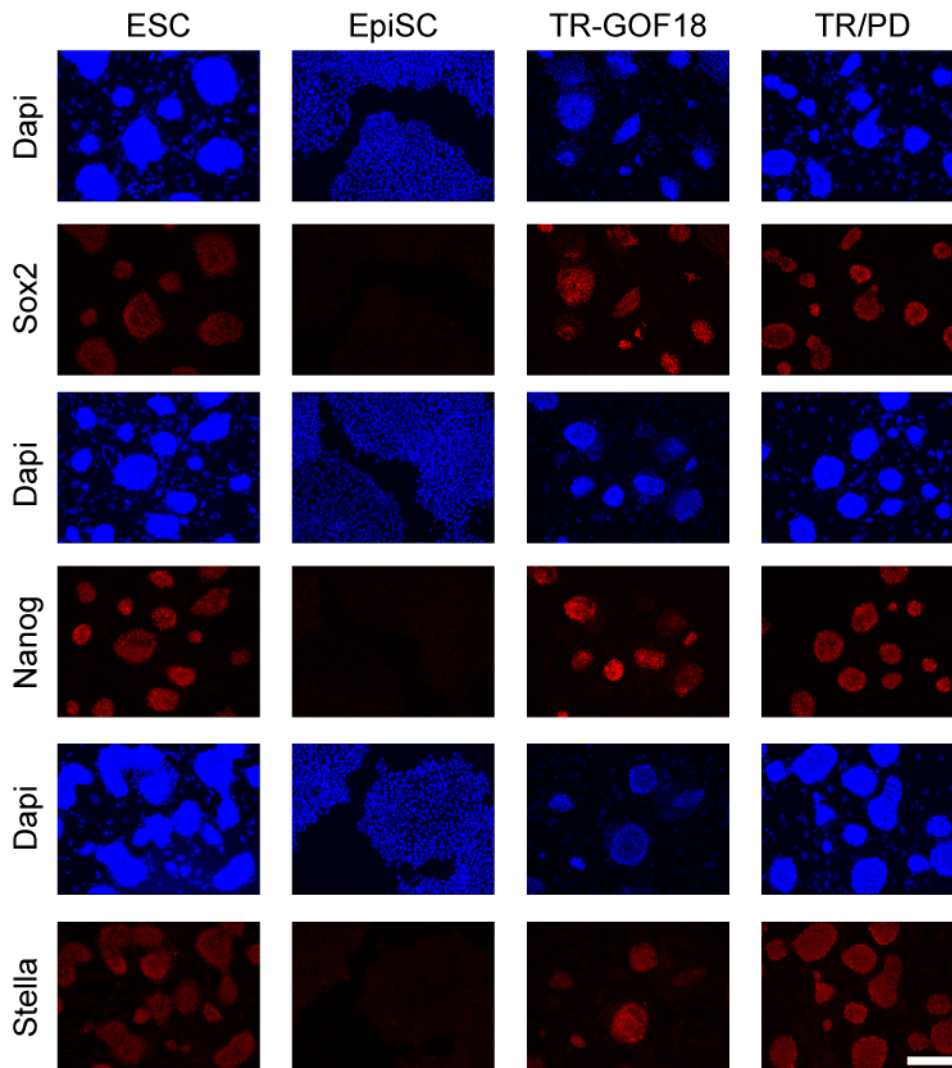
Figure 23. Immunofluorescence analysis for SOX2, NANOG, and STELLA (DPPA3) in ESC, TR-GOF18 cells, EpiSC, and TR/PD-converted cells. DAPI was used for DNA staining.

(Scale bar: 350µm).

ESC preferentially use the distal enhancer (DE) to drive *Oct4* expression, while EpiSC use the proximal enhancer (PE) (Tesar et al., 2007; Yeom et al., 1996). Using a luciferase assay, I compared *Oct4* enhancer activity in the converted cells with that of ESC and EpiSC. The PE/DE ratio in TR/PD-converted cells was tilted toward the preferential use of the *Oct4* DE, reminiscent of ESC, but in contrast to EpiSC (Figure 24).

Figure 24. Evaluation of the Oct4 enhancer activity in ESC, TR-GOF18 cells, EpiSC, and TR/PD-converted cells.

Relative luciferase activity was normalized to the activity of an empty vector (Data represent mean ± SD of triplicates; n = 3; p < 0.001).

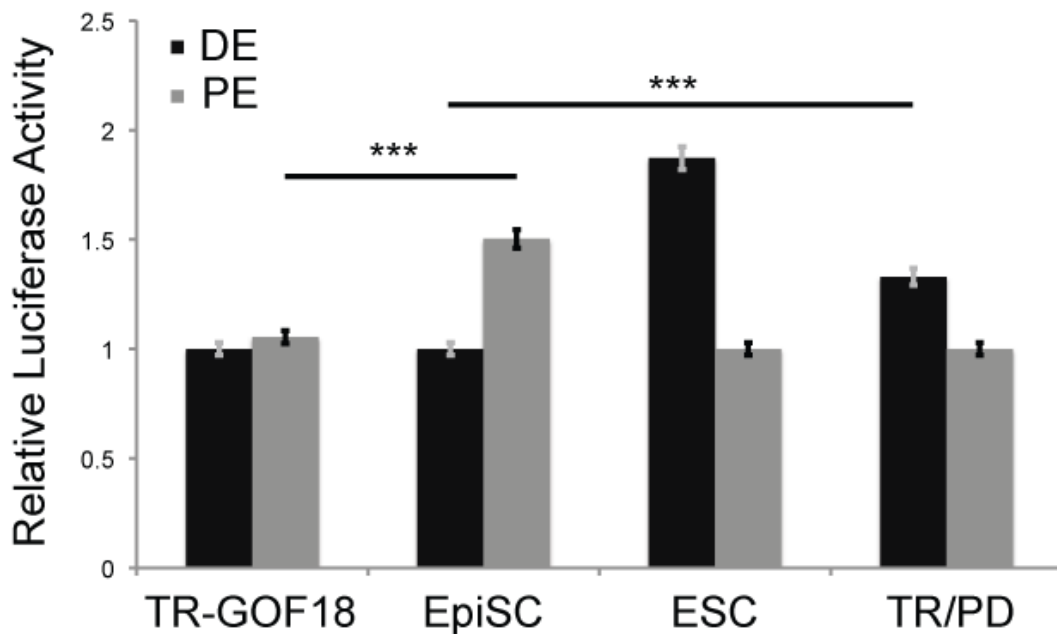In accordance, TR/PD cells exhibited a global gene expression pattern that closely resembled the one of ESC (Figure 25, see also Figures 27 and 28). The bioinformatics analysis of the microarray data was performed by Dr Marcos Jesus Arauzo Bravo.

Figure 25. Scatter plot of global gene expression microarrays comparing TR/PD cells with ESC.

The black lines delineate the boundaries of 4-fold difference in gene expression levels. Genes highly expressed in TR/PD samples compared with ESC samples are shown as red dots; those less expressed are shown as green dots. Positions of the pluripotent cell marker *Zfp42*/*Rex1* and the germ cell marker *Dppa3*/*Stella* are indicated as orange dots. The color bar to the right indicates the scattering density; the higher the scattering density, the darker the blue color. Gene expression levels are depicted on $\log_2$ scale.

Next, the responsiveness of the reverted cells to ESC- and EpiSC-related signaling pathways was assessed (Figure 26). EpiSC are dependent on TGFβ/SMAD2/3 signaling, whereas ESC require stimulation of the LIF/STAT3 pathway for their propagation. Inhibition of LIF/STAT3 signaling in ESC induces differentiation, i.e. pluripotency markers are downregulated, and early differentiation markers upregulated as compared to the untreated control (Figure 26 left panel, see ESC+JAKi). In contrast to that, EpiSC differentiation is induced when TGFβ/SMAD2/3 signaling is inhibited (Figure 26 right panel, see EpiSC+SB). Upon inhibition of these two pathways TR/PD cells reacted in both cases similar to ESC and different from EpiSC which indicates a switch in the signaling pathways toward those related to naïve pluripotency (Figure 26, see TR/PD+JAKi in left panel, and TR/PD+SB in right panel). Notably, TR-converted cells exerted in both cases a more moderate response than ESC and TR/PD-converted cells (Figure 26, see TR-GOF18+JAKi in left panel, and TR-GOF18+SB in right panel).
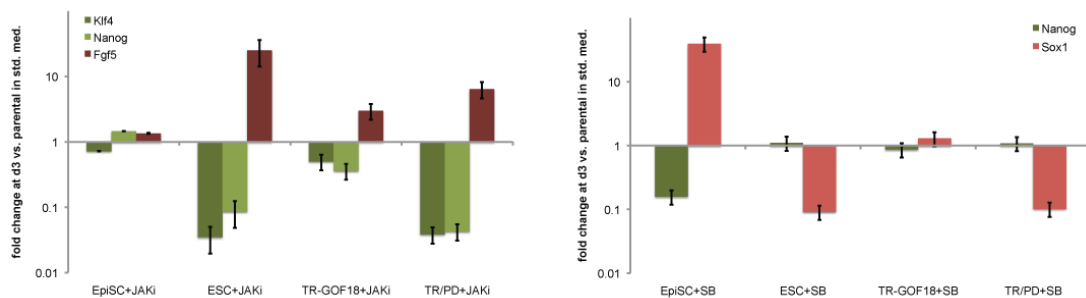
Figure 26. RT-qPCR analysis of the effects of LIF/STAT3 (left) and SMAD2/3 (right) inhibition in ESC, TR-GOF18 cells, EpiSC, and TR/PD-converted cells.
(Data represent mean ± SD of triplicates; n = 3).

4.5   Germline Competence is Restored in TR/PD-Converted Cells

The converted cells were compared to EpiSC and ESC by global gene expression analysis. The heat maps of TR/PD cells were very similar to those of ESC (Figures 27). The bioinformatics analysis of the microarray data was performed by Dr Marcos Jesus Arauzo Bravo.

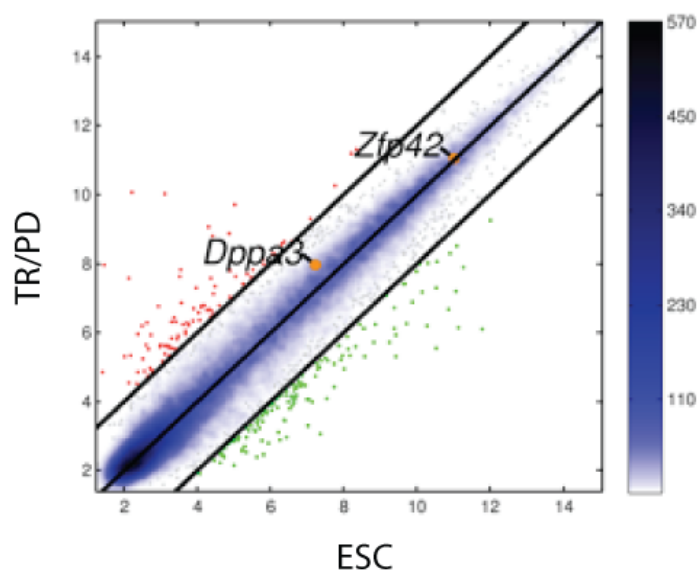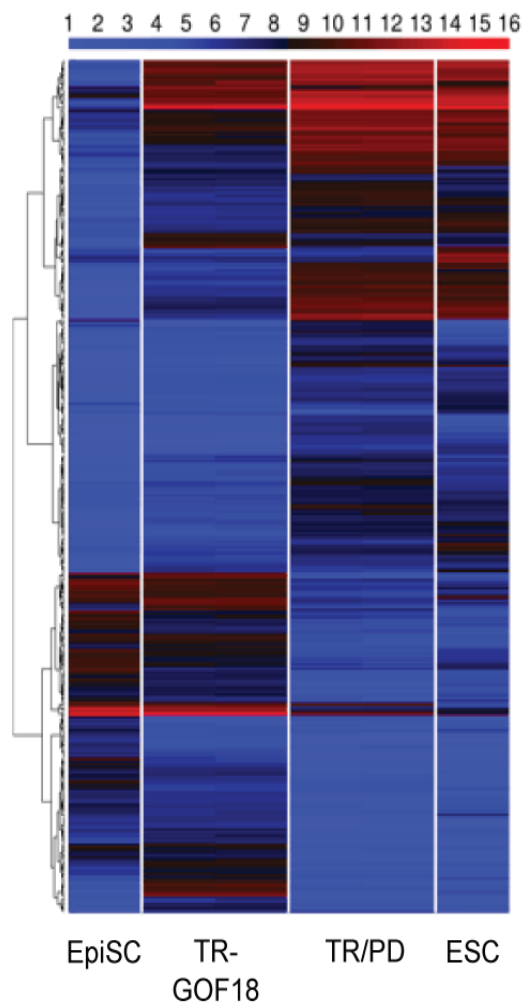**Figure 27. Heat map of global gene expression patterns in ESC, TR-GOF18 cells, EpiSC, and TR/PD-converted cells.**

The color bar at top codifies the gene expression in $\log_2$ scale. Red and blue colors indicate high and low gene expression levels, respectively.

The close correlation between TR/PD cells and ESC was also confirmed by hierarchical clustering analysis (Figure 28). The bioinformatics analysis of the microarray data was performed by Dr Marcos Jesus Arauzo Bravo.
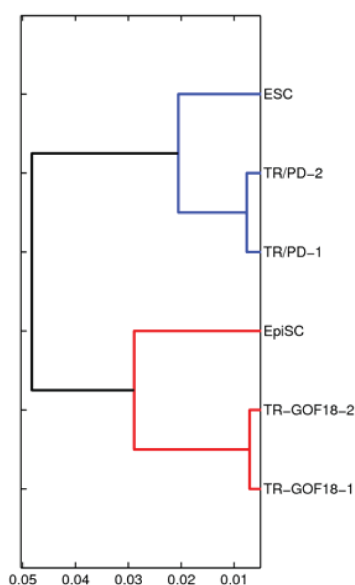
Figure 28. Hierarchical clustering shows that TR/PD-converted cells cluster close to ESC.

The most significantly differentially expressed genes between TR-converted and TR/PD cells give insight into the specific changes at the genetic level that distinguish the two cell types (Figure 29). For example, the ICM markers *Dppa5*, *Esrrb*, *Dppa4*, *Klf2*, and *Nr5a2* are expressed in TR-GOF18 cells at levels comparable to those in ESC. Other ICM markers, such as *Tcl1*, *Tbx3*, and *Klf4*, are also strongly induced in TR-GOF18 cells as compared to EpiSC, but reach the expressio levels of ESC only upon addition of PD. MEK inhibition also results in the suppression of early differentiation markers, such as *Fgf5* and *Fgf8*, which were still elevated in TR-GOF18 cells.

81
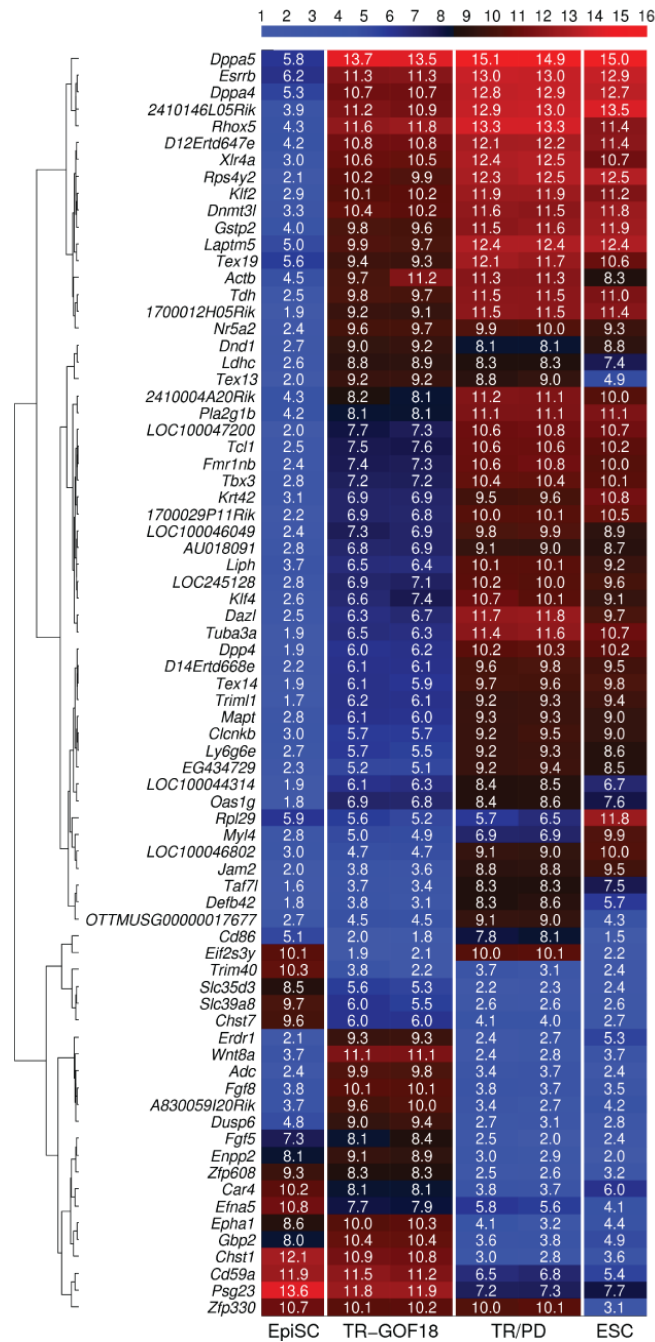
Figure 29. The 75 most significantly differentially expressed genes among the four samples EpiSC (GOF18), TR-GOF18, TR/PD and ESC (OG2).

The color bar at top codifies the gene expression in log2 scale. Red and blue colors indicate high and low gene expression levels, respectively.

Then, it was assessed whether the aforementioned switch in gene expression was accompanied by a global change in the methylation state of TR/PD-converted cells. Consistent with the gene expression data (Figures 3, 16, 22), the endogenous *Oct4* promoter was completely unmethylated in both ESC and EpiSC, while the OCT4-GFP transgene promoter was mainly unmethylated in ESC and highly methylated in EpiSC (Figure 30). In TR/PD cells the OCT4-GFP transgene promoter was basically unmethylated, whereas in TR-converted cells the transgene promoter was only partially unmethylated. Demethylation was also observed for other marker genes analyzed in TR/PD-converted cells (Figure 30). Analysis of DNA methylation was performed by Dr Kee Pyo Kim.
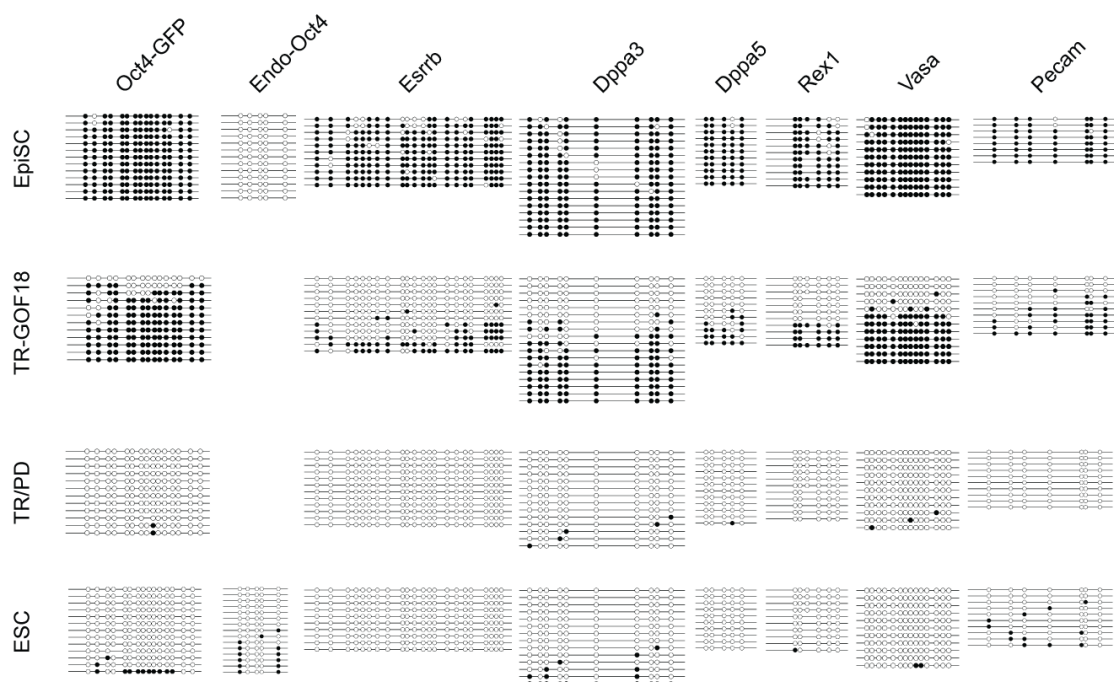
Figure 30. DNA methylation status of the promoter regions of ICM marker genes in ESC, TR-GOF18 cells, EpiSC, and TR/PD-converted cells.

Following global gene expression and methylation analysis, *in vivo* differentiation assays were used to functionally characterise the reverted cells. TR/PD-converted cells gave rise to teratomas containing tissues of all germ layers (Figure 31). Cell were injected, and teratomas were excised by Dr Davood Sabour.
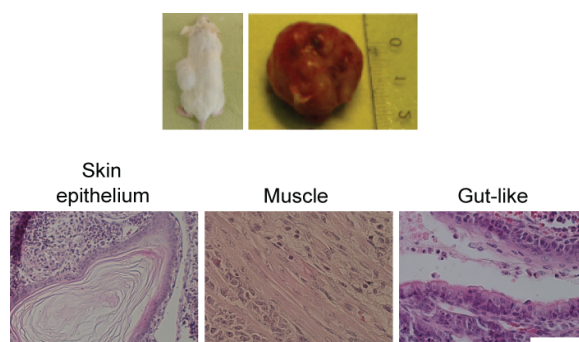
Figure 31. Teratoma assay with TR/PD cells.

Upper panel) Representative image of a teratoma derived from TR/PD cells in a teratoma assay. Lower panel) Representative tissues of ectodermal (skin epithelium), mesodermal (muscle), and endodermal (gut-like) lineages in teratomas obtained from TR/PD-converted cells (Scale bar: 50µm).

Most importantly, upon injection into blastocysts, TR/PD-converted cells showed successfull integration into the ICM, and consequently germline contribution (Figure 32).

Figure 32. Germline contribution of TR/PD cells.

ICM integration of TR/PD-converted cells in blastocyst (left, scale bar: 50µm), embryonic day (E)14.5 pups obtained after embryo transfer (middle), and germline contribution of TR/PD-converted cells (right, scale bar: 450µm).

4.6   TR Targets CK 1δ/ε

Then, efforts were focused on the identification of the molecular target of TR, a well-known ENaC inhibitor (Busch et al., 1996). Amilorid, another structurally diverse ENaC inhibitor failed to induce OCT4-GFP expression in EpiSC-GOF18, thus ruling out ENaC as the effective target of TR-induced ESC conversion (Figure 33) (Canessa et al., 1994).
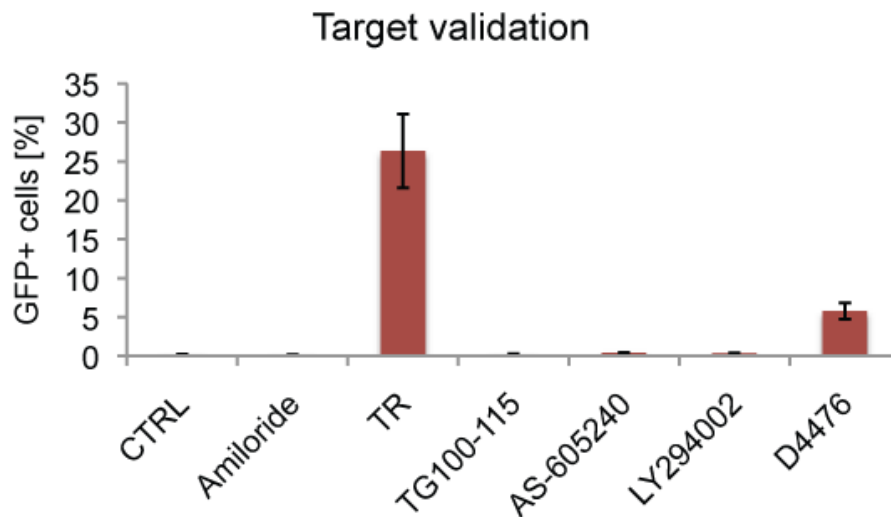
Figure 33. ENaC and PI3K inhibition in EpiSC.

Influence of ENaC and PI3K inhibitors on the induction of OCT4-GFP expression in EpiSC as determined by flow cytometry (Data represent mean ± SD of triplicates; n = 3).

Previously, several pteridin derivatives were reported to inhibit different protein kinases (Doukas et al., 2009; Gomtsyan et al., 2004; Leung et al., 2006). Therefore, it was hypothesized that a kinase may be the target of TR. A kinase profiling assay against a selected panel of more than 100 protein kinases and their isoforms, covering the majority of the signaling pathways reported to govern stem cell fate was performed with TR (Appendix 1). According to this screen TR specifically inhibited casein Kinase 1δ (CK1δ) and phosphatidylinositide 3-kinase class 2γ (PI3KC2γ). To validate CK1δ and PI3KC2γ as possible targets of TR during ESC conversion I selected the pan-PI3K inhibitor LY294002, the potent and selective PI3K gamma inhibitors AS-605240 and TG100-115, and the CK1δ/ε inhibitor D4476. While inhibition of PI3K did not lead to induction of OCT4-GFP expression, using D4476 to inhibit CK1δ/ε resulted in a significant number of OCT4-GFP–positive cells (Figures 33 and 34).
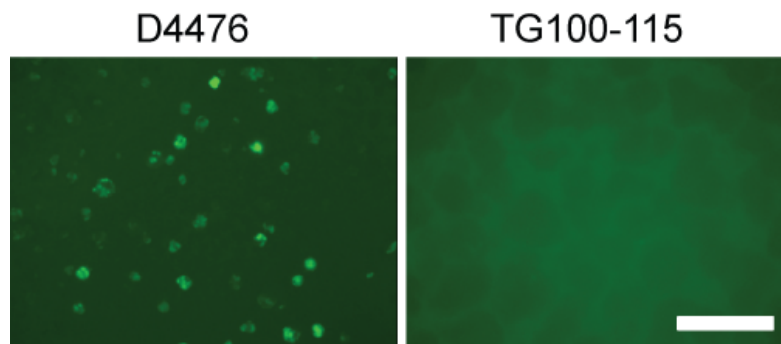
Figure 34. OCT4-GFP expression in EpiSC after 8 days treatment with the CK1 inhibitor D4476 and the PI3K inhibitor TG100-115.
(Scale bar: 300 µm).

Having identified CK1δ as a target of TR, Andrei Ursu then chemically synthesized a library of about 80 derivatives around the pteridine scaffold in an attempt to study the structure-activity-relationship for inhibition of CK1δ, and to produce a more potent inhibitor that would further augment conversion (Ursu, 2014). I tested the synthesized compounds in an EpiSC conversion assay based on OCT4-GFP and PECAM1 expression as readout using FACS. The SAR study revealed that modifications of the phenyl ring in position 6 of the pteridine scaffold resulted in significant changes in compound activity. Interestingly, while any modifications in the *para*-position of the phenyl ring reduced compound activity dramatically, introducing substituents in the *meta*-position such as fluorine, chlorine, bromine, or methyl produced more active compounds with the chlorine derivative showing the highest conversion efficiency (Figures 35 and 36). Detailed information concerning the synthesis of the derivatives will be part of the doctoral dissertation of Andrei Ursu, and are not further discussed in this thesis (Ursu, 2014).
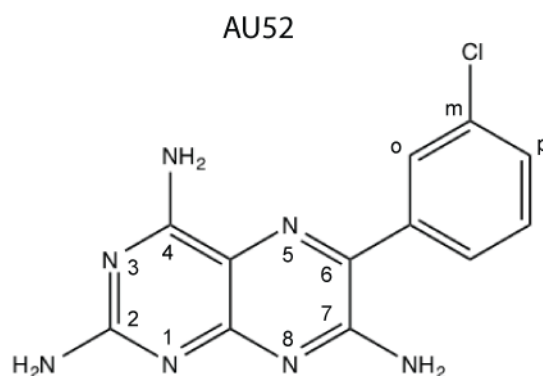
Figure 35. Chemical structure of the Triamterene derivative AU52.
(o: ortho, m: metha, p: para).

The potential of AU52 to convert EpiSC was assessed based on the induction of PECAM1 and OCT4-GFP upon treatment. AU52 clearly demonstrated the highest conversion efficiency among the selected inhibitors (Figure 36). It achieved a 3-fold higher conversion efficiency than 2i/LIF. Wnt inhibition alone did not yield PECAM1/OCT-GFP double-positive cells, and neither did sodium butyrate which was previously reported to be capable of ESC-conversion of EpiSC (Figure 36).
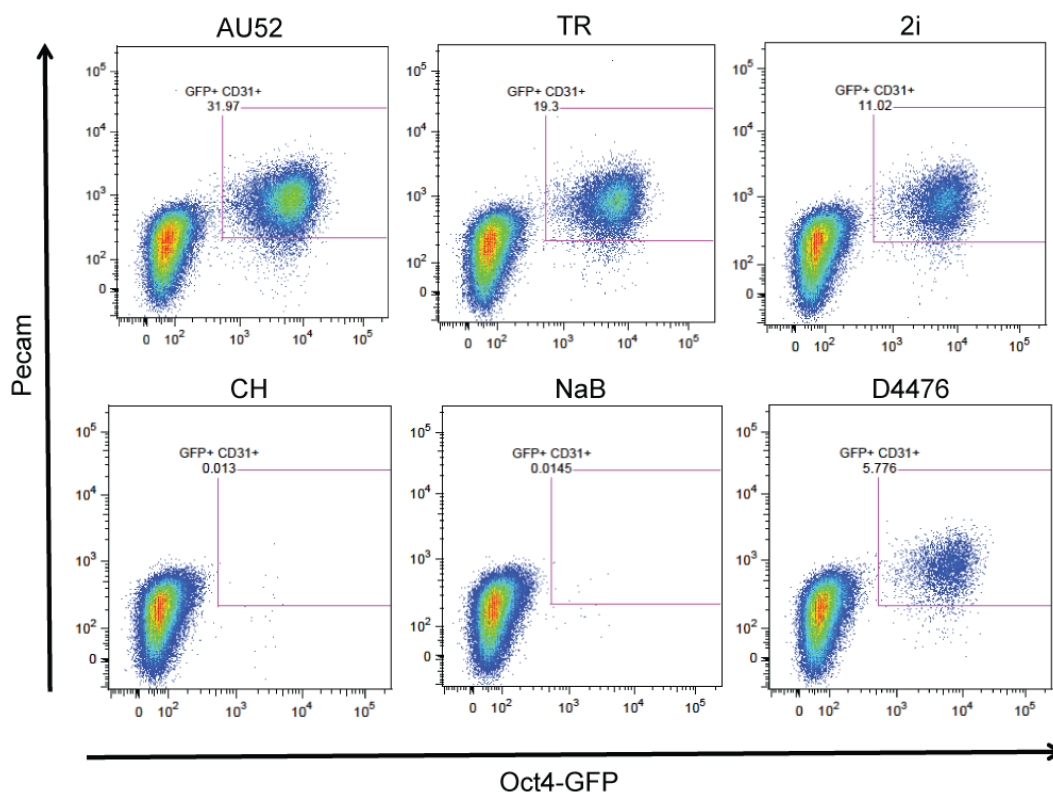
Figure 36. Conversion efficiency of AU52 compared to other inhibitors.
Percentage of OCT4-GFP and PECAM1 (CD31) double–positive cells after 7 days ESC conversion with AU52, TR, 2i, CH, NaB, and D4476 in EpiSC-GOF18 as measured by flow cytometry.

Consistently, the derivative AU52 which demonstrated the highest biological activity clearly showed stronger inhibition of CK1δ, with IC_{50} values of 7.95 µM for TR, and 5.79 µM for AU58 (Figure 37). The graph in figure 37 was generated by Andrei Ursu.
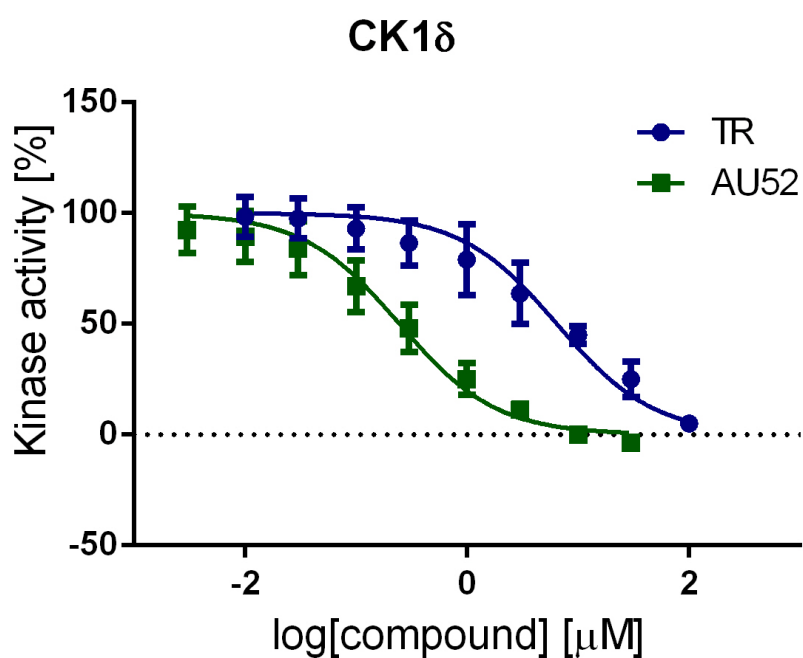
Figure 37. Dose-response curves of Triamterene and its derivative AU52 for the inhibition of CK1δ.

The IC_{50} values were calculated to be 7.95 µM for TR and 0.44 µM for AU52.

Having identified AU52 as the derivative with the highest conversion efficiency and a nearly 20 times higher affinity for CK1δ than TR, the selectivity of AU52 and TR among the selected panel of kinases, particularly among the CK family members, were then assessed (Figure 38 and Appendix 1). AU52 displayed a selectivity very similar to that of TR (Appendix 1). Although TR and AU52 both displayed stronger inhibition of CK1δ, they also inhibited CK1ε, suggesting a potential role also for CK1ε in ESC conversion (Figure 38).
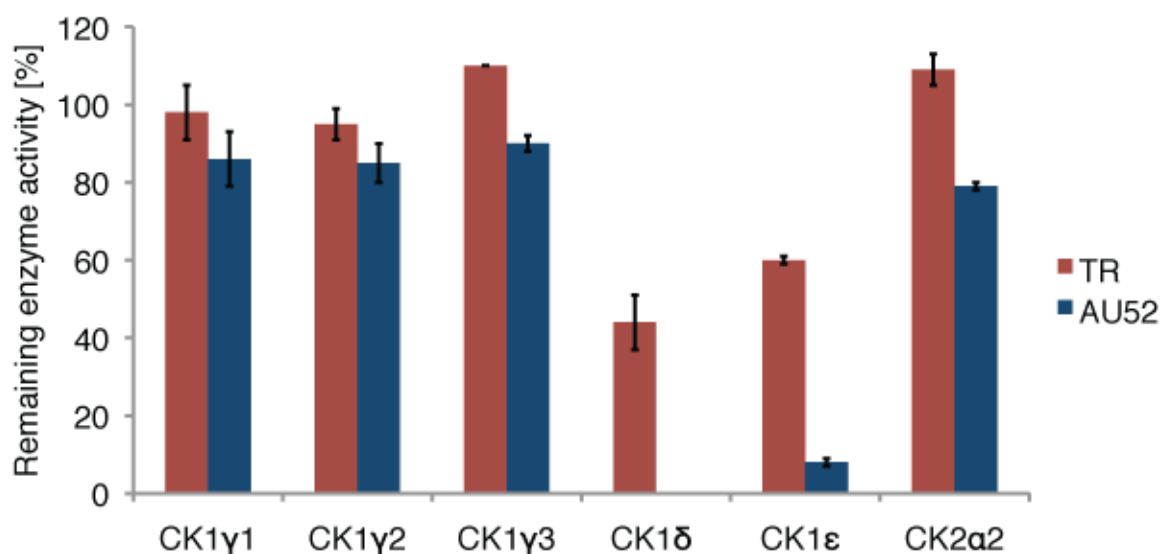
Figure 38. Kinase acitivity profiling of Triamterene against representatives of the casein kinase family.

(Compound concentration = 10 µM; data represent mean ± SD of triplicates; n = 3).

The IC$_{50}$ values against CK1ε were calculated to be 23.65 µM for TR and 5.36 µM for AU52 (Figure 39). The graph in figure 39 was generated by Andrei Ursu.
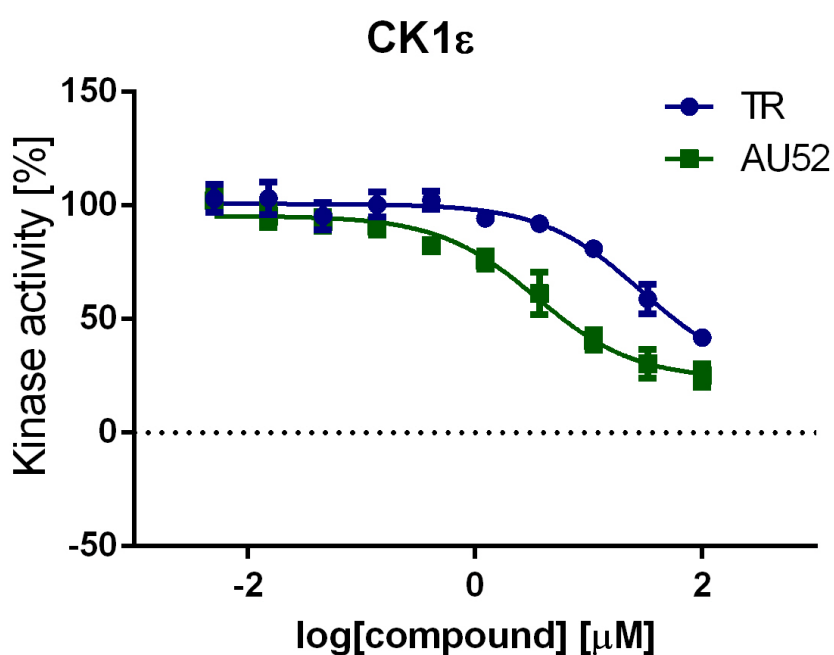
Figure 39. Dose-response curves of Triamterene and its derivative AU52 for the inhibition of CK1ε.

The IC$_{50}$ values were calculated to be 23.65 µM for TR and 5.36 µM for AU52.

Next, the ability of AU52 to promote the reversion of EpiSC was analyzed in further detail. Among a set of different compounds AU52 displayed the highest conversion efficiency based on OCT4-GFP and PECAM1 reactivation, almost 2-fold higher than TR and 3-fold higher than 2i (Figure 36). Interestingly, CH, as well as sodium butyrate, had a negliagible effect on the reactivation of OCT4-GFP and PECAM1 (Figure 36). AU52-converted cells exhibited cell morphology, OCT4-GFP expression, AP immunoreactivity, protein levels of Sox2, Nanog and Stella, and gene expression profile similar to those of ESC (Figure 40). Immunocytochemical characterization of AU52-converted cells was performed by Dr Miao Zhang.
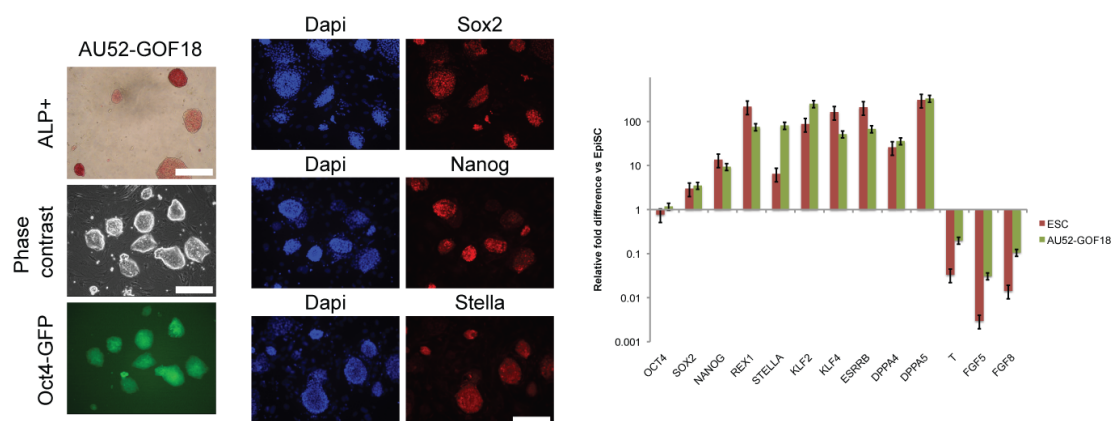
Figure 40. Characterization of AU52-converted cells.
Left panel) Morphology, OCT4-GFP and ALP expression in AU52-GOF18 cells (Scale bars: 300 µm). Middle panel) Immunofluorescence analysis for SOX2, NANOG, and STELLA (DPPA3) in AU52-GOF18 cells. DAPI was used for nuclear staining (Scale bar: 300 µm). Right panel) Comparison of gene expression patterns in ESC, AU52-GOF18 cells, and EpiSC. Expression levels are normalized to those of EpiSC (Data represent mean ± SD of triplicates; n = 3).

Most importantly, AU52-converted cells regained the ability to contribute to chimeras when injected into blastocysts (Figure 41). The chimeric mice were generated by Dr Guangming Wu by morula aggregation.

Figure 41. Chimeric mice derived from AU52-GOF18 cells upon blastocyst injection.

4.7   CK1δ/ε Inhibition Promotes the Activation/Maintenance of the ESC Pluripotency Gene Regulatory Network

Then, it was analysed how CK1δ/ε inhibiton influenced the expression of known pluripotency factors in EpiSC after treatment with TR for 2, 4, 6, and 8 days. Notably, *Klf2, Nanog*, and *Esrrb* were upregulated from day2, albeit with different expression dynamics (Figure 42).
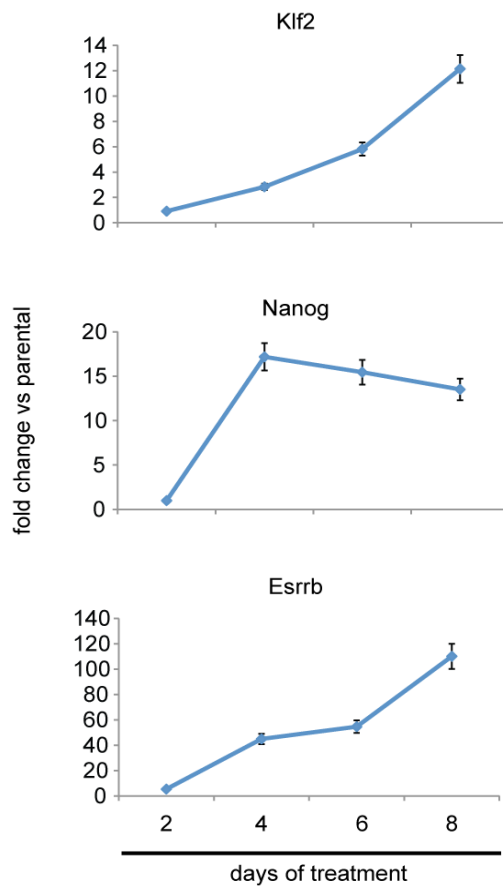
Figure 42. Timecourse for whole mRNA expression of *Klf2, Nanog*, and *Esrrb* in Triamterene-treated EpiSC.

Gene expression levels were normalized to those of untreated EpiSC samples (Data represent mean ± SD of triplicates; n = 3).

In the case of *Nanog* and *Esrrb*, the expression levels following 8 days of treatment with TR exceeded those in ESC. This result was recapitulated using D4476, another inhibitor of CK1δ/ε (Figure 43).
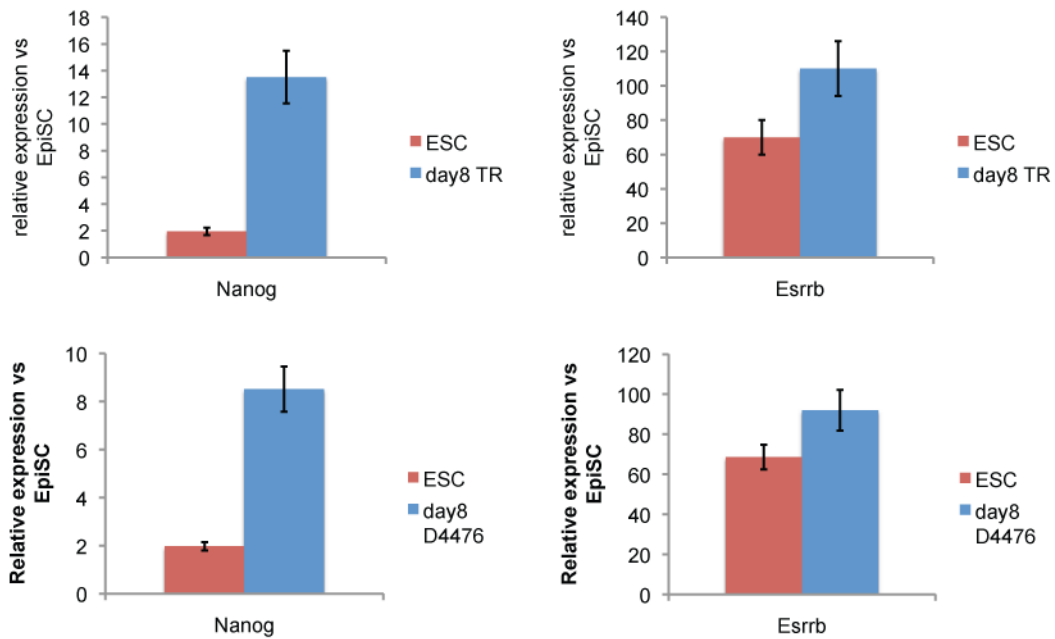
Figure 43. RT-qPCR analysis of TR-induced expression of *Nanog* and *Esrrb*.
Untreated EpiSC, ESC and EpiSC treated for 8 days with TR (upper panel), and D4476 (lower panel). Gene expression levels were normalized to those of untreated EpiSC samples (Data represent mean ± SD of triplicates; n = 3).

Then, the role of *Klf2*, *Nanog*, and *Esrrb* during AU52-based conversion was determined by shRNA-based knockdown (KD) experiments (Figure 44). Interestingly, *Nanog*-KD basically abolished conversion by AU52, and *Klf2*-KD significantly reduced the conversion, suggesting critical roles for both factors in the process. *Esrrb*-KD was less dramatic, but still reduced the conversion

efficiency of AU52 by about 30% (Figure 44). Transduction of shRNA was performed by Dr Kee Pyo Kim.
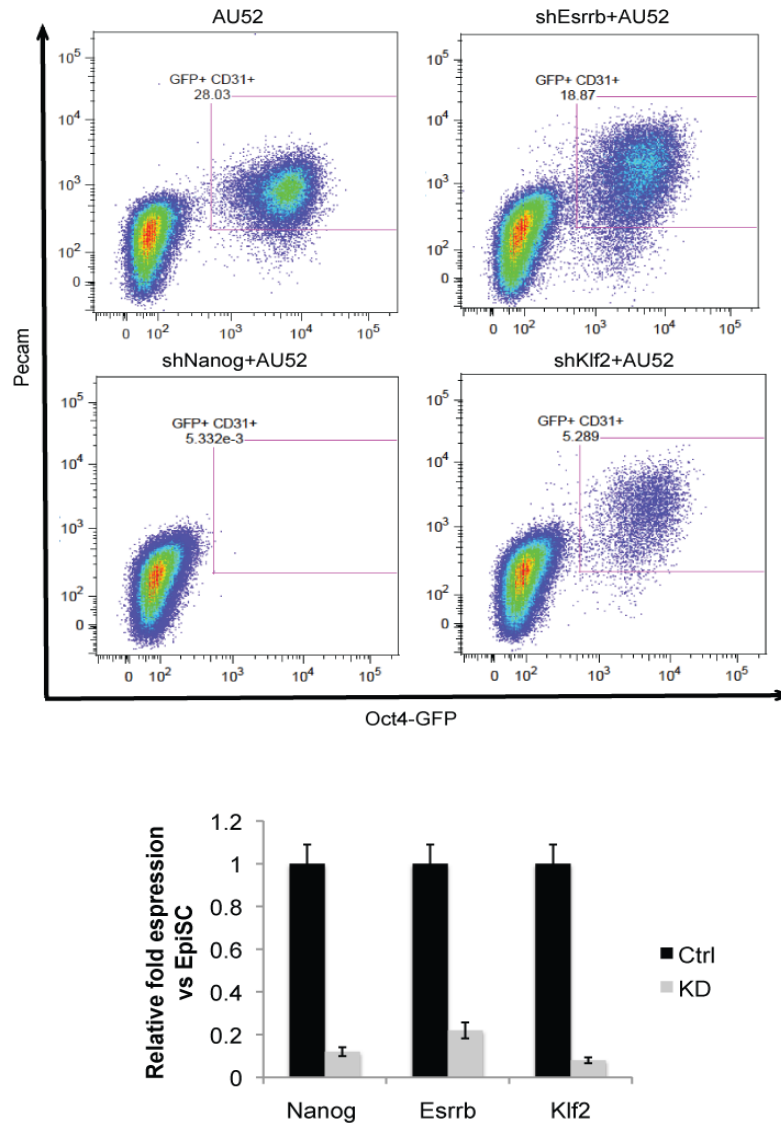
Figure 44. Knockdown of Esrrb, Nanog, and Klf2 in EpiSC during ESC conversion with AU52.

Upper panel) Percentage of OCT4-GFP and PECAM1 (CD31) double–positive cells after 6 days treatment with AU52 together with shRNA-based knock down of *Esrrb*, *Nanog*, and *Klf2* respectively, in EpiSC-GOF18 as measured by flow cytometry. Lower panel) Assessment of shRNA-based knock down efficiency by RT-qPCR analysis (Data represent mean ± SD of triplicates; n = 3).

Based on the effect of CK1δ/ε inhibitors on key pluripotency genes during the reversion of EpiSC to ESC-like cells, it was tested whether TR/AU52 had an effect on self-renewal by maintaining the pluripotency gene regulatory network. Too high levels of AU52 are toxic (data not shown). N2B27 medium alone is not permissible for ESC self-renewal. However, following a titration experiment an optimal working concentration of 2 μM AU52 in ESC was found at which the clonal expansion of ESC in N2B27 was promoted. Addition of either LIF or PD to AU52-supplemented media increased the self-renewal ability of the cells, whereas addition of CH to AU52-supplemented media decreased their self-renewal (Figure 45). Clonal assays were performed by Dr Rodrigo Osorno.
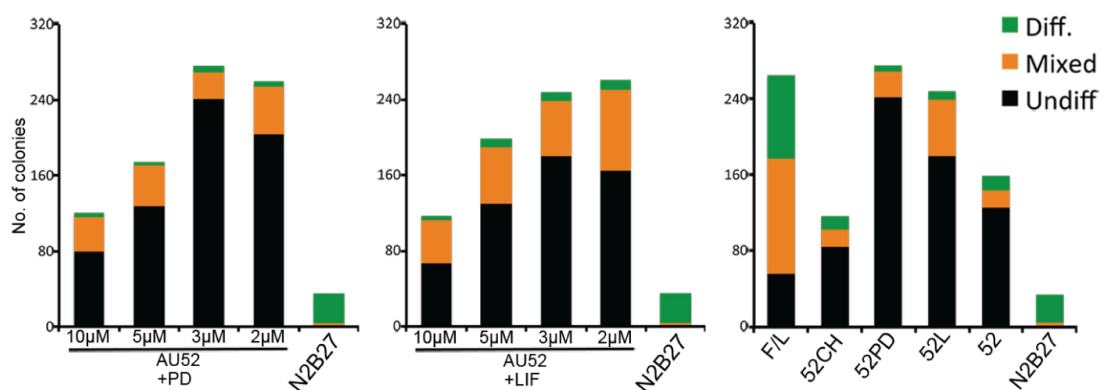
Figure 45. Clonal assay of ESC in the indicated culture conditions.
ESC were plated onto gelatin coated plates and cultured for 7 days, after which the cells were stained for alkaline phosphatase and counted. (F: FCS, L: LIF, 52: AU52)

Upon switch to EpiSC media (based on N2B27/ActivinA/bFGF), ESC acquire properties of primed pluripotency (Guo et al., 2009). Nanog-GFP ESC show progressive downregulation of Nanog-GFP under this condition (Chambers et al., 2007; Karwacki-Neisius et al., 2013). Wnt signaling has been reported to prevent the commitment of ESC into EpiSC (ten Berge et al., 2011). Consistent with this finding, it was found that downregulation of Nanog-GFP during EpiSC differentiation was blocked by the addition of TR with an efficiancy comparable to the Wnt agonist CH (Figure 46). The assay of figure 46 was performed by Dr Rodrigo Osorno.
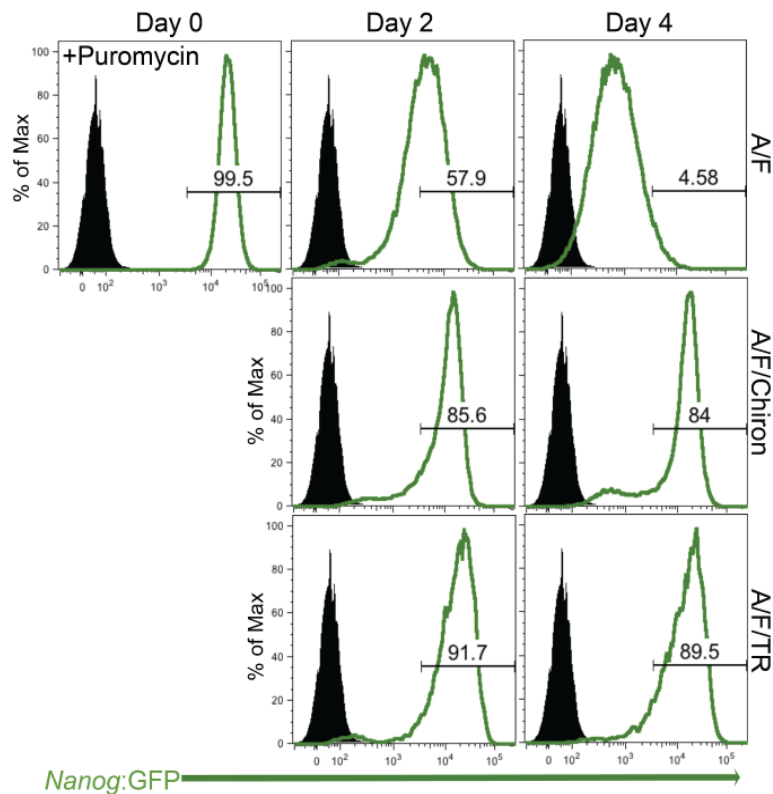
Figure 46. Differentiation of ESC into EpiSC is blocked by supplementation of TR.

Flow cytometry analysis of *Nanog*-GFP positive cells during EpiSC differentiation (A/F) and in the presence of either Chiron or TR. (A: ActivinA, F: bFGF, black cell population represents non-fluorescent control cells).

On the other hand, it has been shown that ESC cultured in the presence of serum and LIF result in transcription factor heterogeneity, coinciding with the presence of cells with different self-renewal capabilities (Chambers et al., 2007). To test the ability of TR/AU52 to maintain homogenous expression of ICM transcription factors, two reporter lines were used, Nanog-GFP and Esrrb-Tomato. TR treatment induced high, homogenous expression of Nanog-GFP and Esrrb-Tomato for the duration of the assay, whereas untreated controls gave rise to Nanog-GFP-negative and Esrrb-Tomato-negative cells (Figure 47). The heterogeneity assays of figure 47 using *Nanog*-GFP and *Esrrb*-Tomato reporter ESC were performed by Dr Rodrigo Osorno.
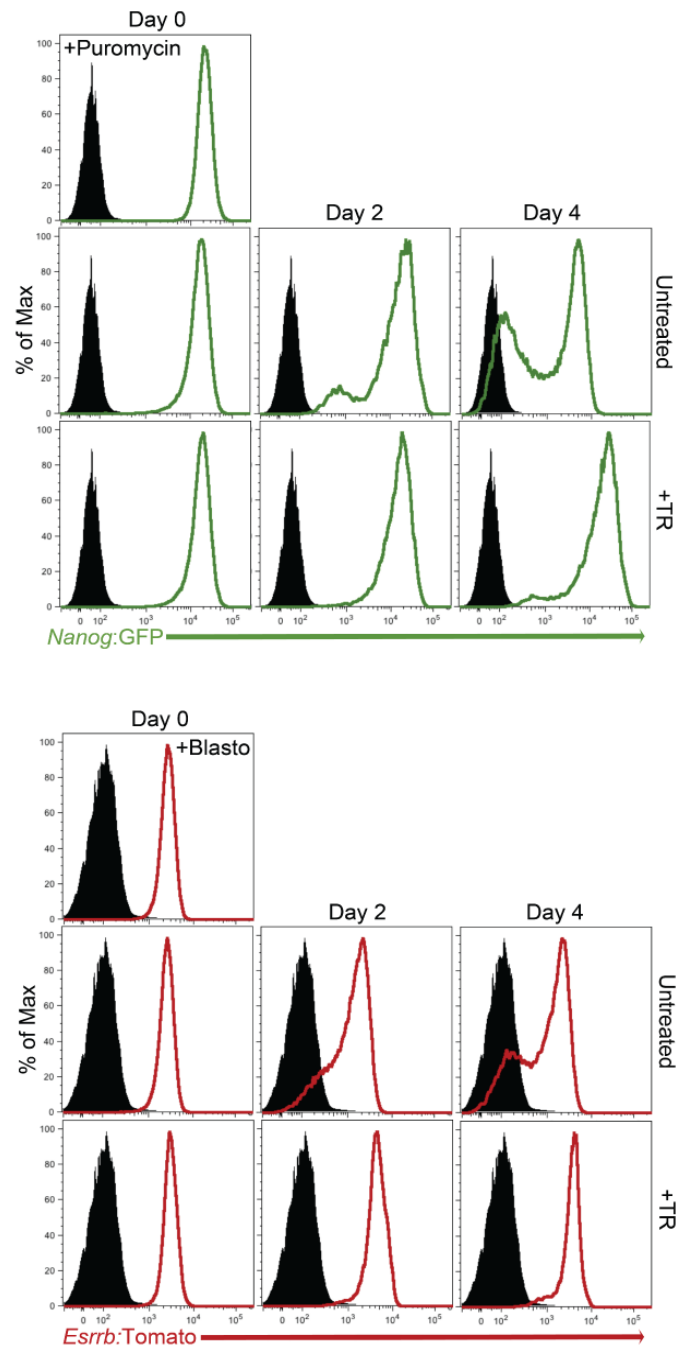
Figure 47. Heterogeneity of *Nanog*-GFP and *Esrrb*-Tomato is blocked by the presence of Triamterene.

Flow cytometry analysis of *Nanog*-GFP (left) and *Esrrb*-Tomato (right) reporter ESC cultured in GMEMβ/FCS/LIF/TR at low density for the indicated days (black cell population represents non-fluorescent control cells).

4.8   Inhibition of CK1ε Results in Simultaneous Activation of WNT Signaling and Inhibition of TGFβ/SMAD2 Signaling

Next, the mechanism by which inhibition of CK1δ/ε exerts its effects was investigated. Signaling pathways known to be involved in ESC pluripotency were analyzed upon treatment with CK1 inhibitors. It was found that AU52 prevented phosphorylation of β-CATENIN as well as SMAD2 (Figure 48). It also affected STAT3 phophorylation which is probably a result of the inhibition of PI3K which was identified by kinase profiling. In contrast, the ERK pathway was not affected (Figure 48). The western blot analysis was performed by Dr Juyong Yoon.
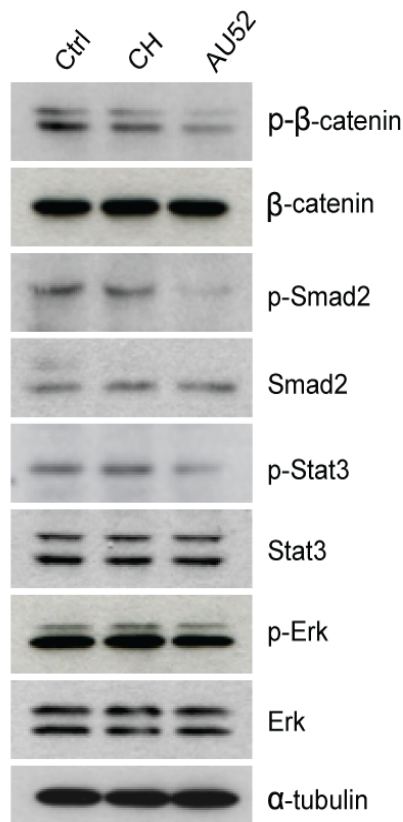
Figure 48. Western blot analysis showing the effects of AU52 and Chiron on β-CATENIN, SMAD2, STAT3, and ERK phosphorylation in EpiSC.
Cells were treated with either AU52 or Chiron for 30min.

Following the inhibition of phosphorylation of β-CATENIN the effect of TR/AU52 on the WNT pathway were further analyzed. To determine the enrichment of factors associated with signaling pathways, a gene ontology enrichment analysis was performed with the genes that were significantly upregulated within 12 hours of TR treatment of EpiSC. Based on this analysis the WNT receptor signaling pathway clearly ranked at the top of significantly enriched "biological process" terms (Figure 49). The bioinformatics analysis of microarray data was performed by Dr Marcos Jesus Arauzo Bravo.
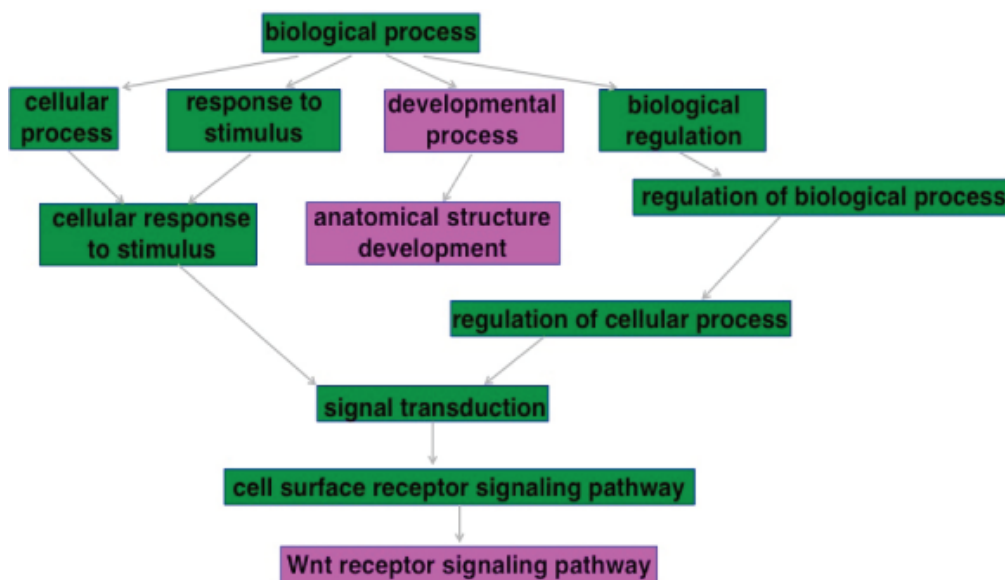
Figure 49. Direct acyclic graph (DAG) associated with the top 3 significantly enriched gene ontology terms.

The higher the significance of the term, the more red is the box framing the term. The significantly enriched terms are encircled by ellipses. The most significant term shown is Wnt receptor signaling pathway with the p-value of $8.3683e^{-8}$.

The known WNT/Tcf target genes *Axin2, Cdx1,* and *T-brachyury* were upregulated upon TR treatment (Figure 50) (Kelly et al., 2011).
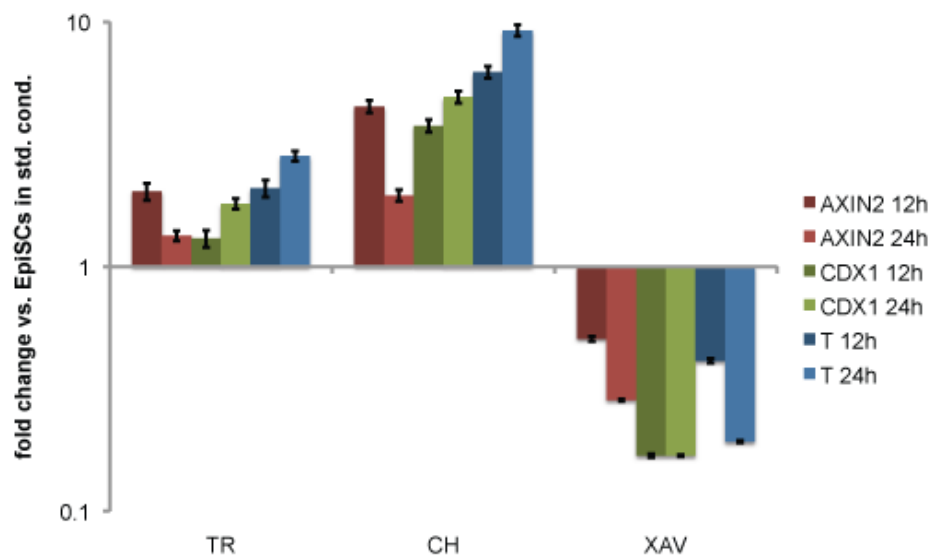
Figure 50. RT-qPCR analysis of the expression of WNT target genes in EpiSC upon treatment with Triamterene.

The gene expression levels are normalized to those of untreated samples. CHIR99021 and XAV939 were used as a positive and negative control, respectively (Data represent mean ± SD of triplicates; n = 3).

Then, I performed the TOPFlash Tcf-Luciferase assay to assess the WNT-inducing activity of AU52, and found that AU52 was more active than CH (Figure 51).
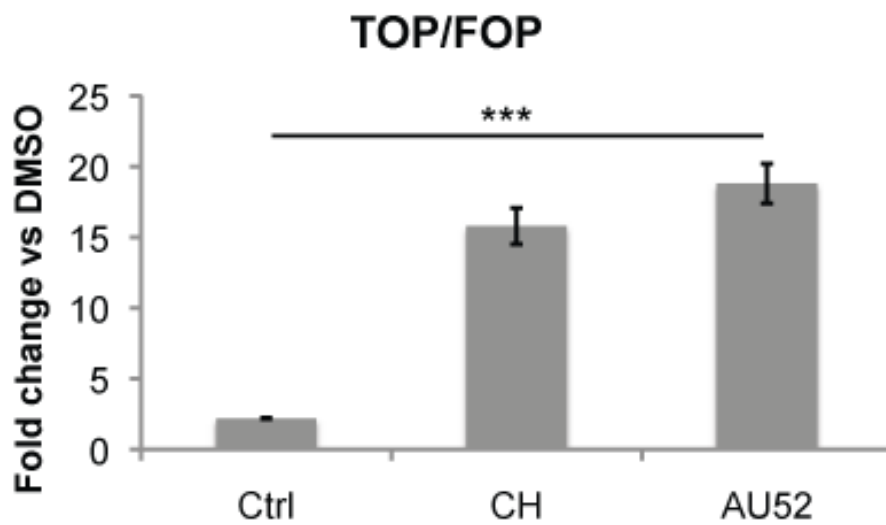
Figure 51. Luciferase assay of Tcf/Lef-mediated transcriptional activity in EpiSC as a result of AU52 and Chiron treatment.

Chiron was applied as a positive control. Columns depict TOP/FOP ratio (Data represent mean ± SD of triplicates; n = 3; p < 0.001).

Then, it was tested whether the positive effect on ESC self-renewal that was observed upon AU52 treatment depended on the Wnt/β-CATENIN pathway (Figure 45). To this end, an ESC line in which both *β-catenin* alleles have been floxed and that also carries a CreERT2 cassette inserted into the ROSA26 locus (*Bcatenin*$^{fl/fl}$) was used (Brault et al., 2001; Tsakiridis et al., 2014). Treatment of *Bcatenin*$^{fl/fl}$ ESC by 4-Hydroxytamoxifen induces deletion of both *β-catenin* alleles generating *Bcatenin*$^{-/-}$ ESC. *Bcatenin*$^{-/-}$ ESC are unable to self-renew in the presence of CH/PD (2i) or CH/LIF. In the absence of *β-catenin*, self-renewal is only supported by the combined presence of PD and LIF, though greatly diminished (Wray et al., 2011). Interestingly, though equally diminished by depletion of β-catenin, AU52 still mediated ESC self-renewal (Figure 52). Clonal assays were performed by Dr Rodrigo Osorno.
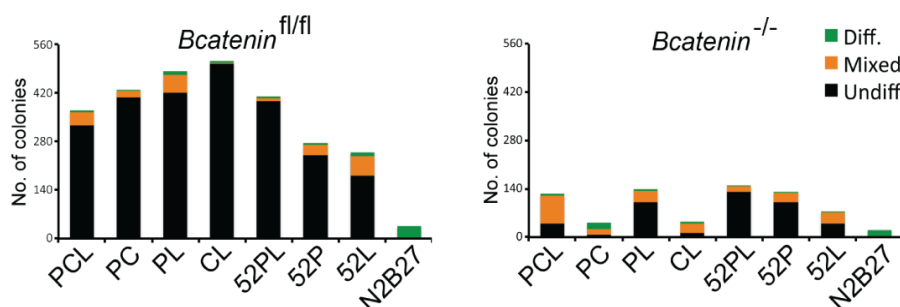
Figure 52. Clonal assay of Bcatenin$^{fl/fl}$ and Bcatenin$^{-/-}$ ESC in the indicated culture conditions.

Bcatenin$^{fl/fl}$ ESC were plated at clonal density (600 cells) onto gelatin coated plates and cultured for 7 days, after which the cells were stained for alkaline phosphatase and counted. In order to generate Bcatenin$^{-/-}$, Bcatenin$^{fl/fl}$ were plated just as described above. After 48hrs the cells were treated with 1 µM of 4-Hydroxytamoxifen for 24hrs to induce the Cre-excision of the floxed-Bcatenin. (P: PD, C: CH, L: LIF, 52: AU52).

Finally, the potential of TR/AU52 to modulate the WNT pathway *in vivo* was assessed. Zebrafish embryos from 7-48 hpf were kept in the presence of TR or AU52. At 48hpf the zebrafish embryos showed a typical phenotype that results from WNT over-activation during this period of development, including an impaired development of the eyes, the forehead, and the tail (Figure 53). The zebrafish assay was performed by Kathrin Grassme.
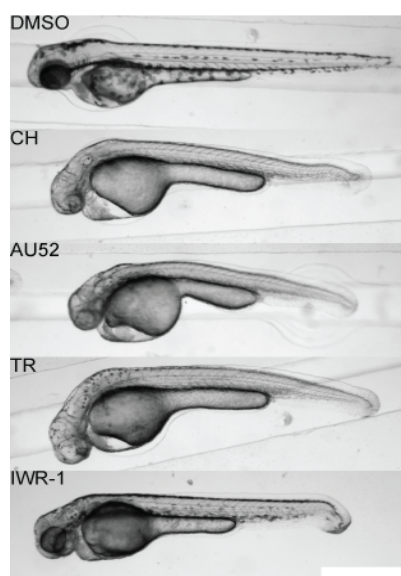
Figure 53. Phenotypes of zebrafish embryos at 48hpf.
The embryos were allowed to grow in the presence of the indicated inhibitors from 7hpf (hpf: hours post fertilization, scale bar: 500 μm).

SMAD2 was affected by TR/AU52 (Figure 48). Therefore, I determined the role of SMAD2 during conversion. I hypothesized that TR/AU52 acted via dual inhibition of phosphorylation of both β-CATENIN and SMAD2 and thus simulated this action by applying CH together with SB in order to convert EpiSC. Interestingly, while CH and SB alone had rather differentiating effects on EpiSC, together they gave rise to ESC-like colonies expressing OCT4-GFP and ICM marker genes comparable to ESC (Figure 54). Just like with TR/AU52 the conversion with CH/SB took six days and was accomplished under EpiSC culture conditions.
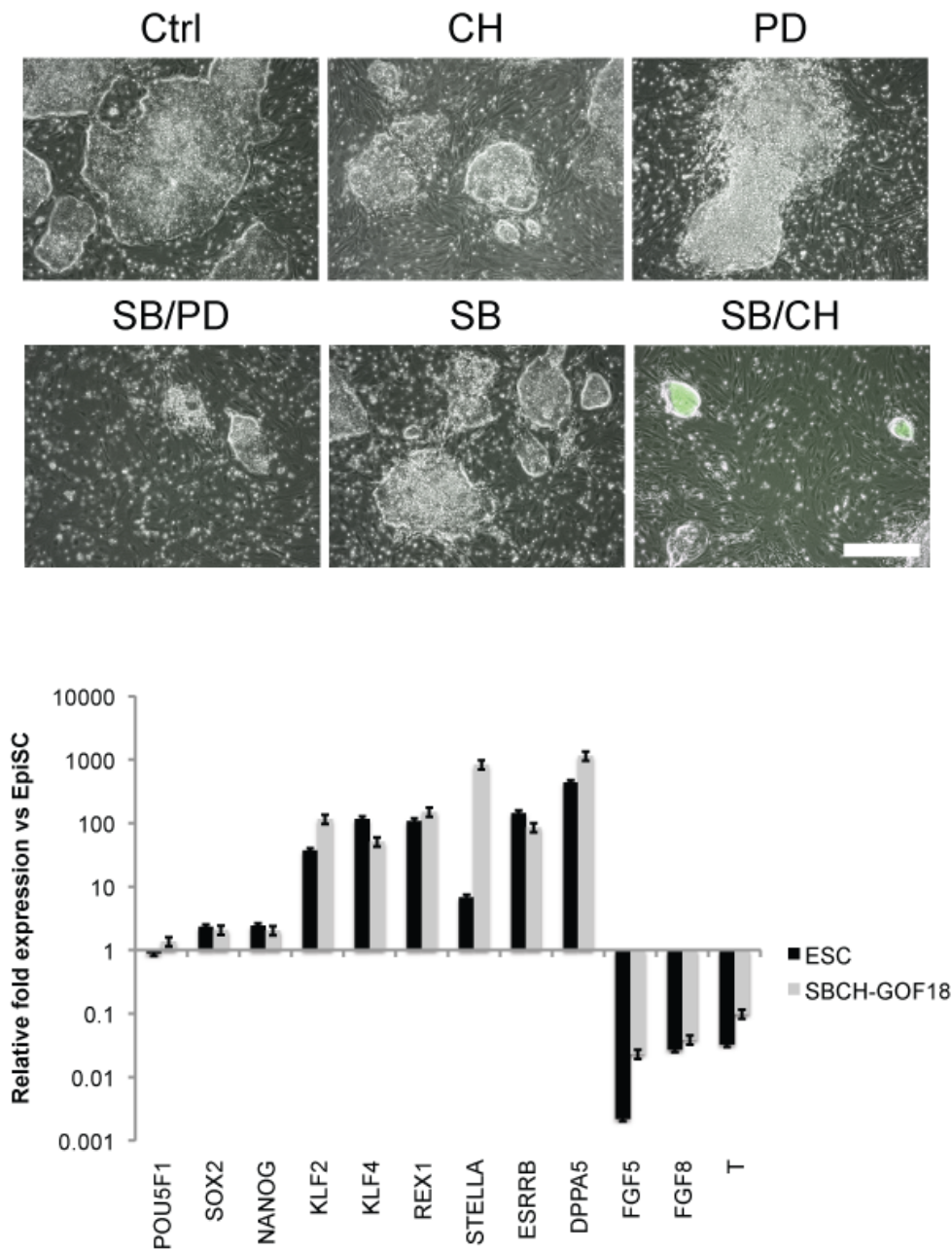
Figure 54. SB/CH-converted EpiSC.

Upper panel) Morphology and OCT4-GFP expression in EpiSC treated for 6 days with the indicated inhibitors (Scale bar: 200 µm). Lower panel) RT-qPCR analysis of ICM marker gene expression in SB/CH-treated cells, EpiSC and ESC. Gene expression levels were normalized to those of untreated EpiSC samples (Data represent mean ± SD of triplicates; n = 3).

A role for CK1δ/ε in β-catenin and Smad2 phosphorylation was previously reported (Amit et al., 2002; Waddell et al., 2004). To determine whether CK1δ/ε was involved in β-catenin and Smad2 phosphorylation, an shRNA-based KD of CK1δ and CK1ε in EpiSC was performed. Most strikingly, KD of CK1ε, and not CK1δ, gave rise to OCT4-GFP-positive cells, and Western blot analysis revealed that KD of CK1ε hindered phophorylation of both β-catenin and Smad2 (Figure 55). Given the fact that TR did not inhibit GSK3β and ALK (Appendix 1), these findings suggest that TR/AU52 acts on β-catenin and Smad2 phosphorylation via CK1ε. Transduction of shRNA was performed by Dr Kee Pyo Kim. Western blot analysis was performed by Dr Juyong Yoon.
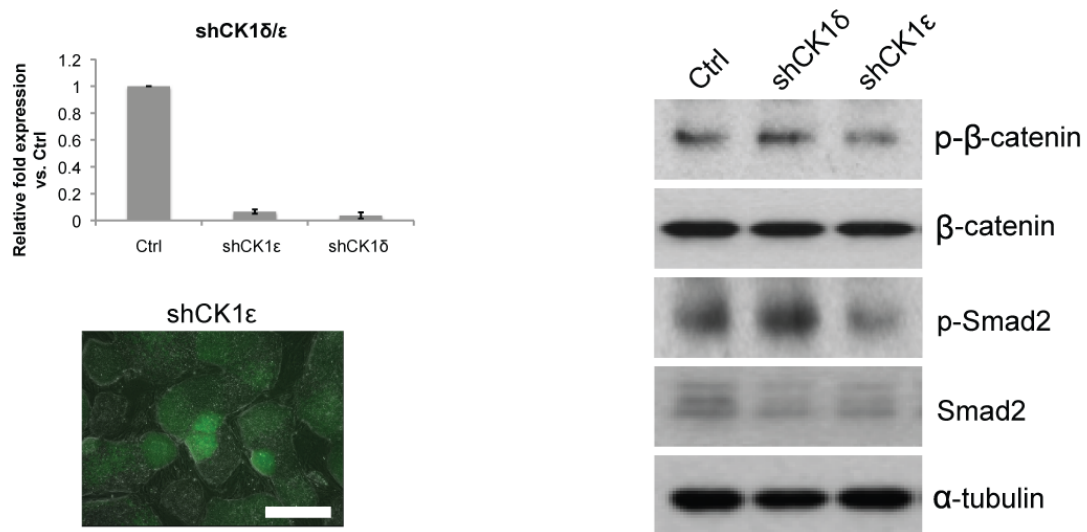
Figure 55. Knockdown of *CK1δ* and *CK1ε* in EpiSC.
Left panel) Assessment of shRNA-based knock down efficiency by RT-qPCR analysis (above, data represent mean ± SD of triplicates; n = 3) and OCT4-GFP expression in EpiSC-GOF18 after shRNA-based knock down of *CK1ε* (below, scale bar: 250 µm). Right panel) Western blot analysis of β-catenin and Smad2 phosphorylation in EpiSC after shRNA-based knock down of *CK1δ* and *CK1ε*.

Finally, the role of LIF during the conversion was left to be clarified. TR was found to inhibit PI3K which could explain the blocked Stat3 phophorylation pointing toward a redundancy of this pathway during conversion (Figure 48 and Appendix 1). Moreover, ESC could be maintained with AU52 alone, i.e. without LIF, for an extended period, and SB/CH could equally maintain ESC without LIF (Figure 56).
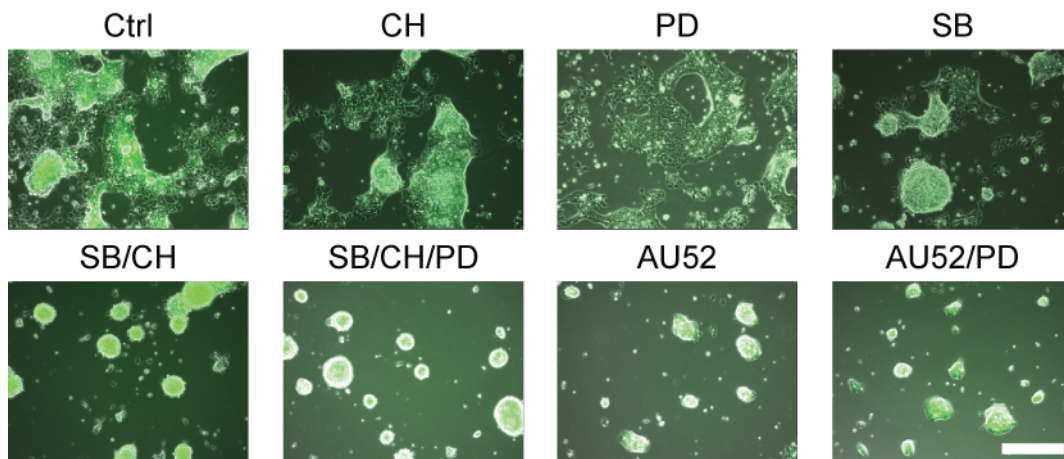
Figure 56. Morphology and OCT4-GFP expression in ESC cultured for 8d under the indicated conditions.

(Scale bar: 100 µm).

To categorically determine whether LIF/Stat3 signaling is involved in AU52-mediated self-renewal *Stat3*^{-/-} ESC were used. These ESC can only be propagated by the supplementation of CH/PD (2i) (Ying et al., 2008). In the absence of *Stat3*, AU52-mediated self-renewal was severely reduced in the presence of either LIF or CH (Figure 57). In contrast, the dual inhibition of Erk and CK1 (N2B27/PD/AU52), promoted a robust propagation of *Stat3*^{-/-} ESC for more than two months (Figure 57). Clonal assay was performed by Dr Rodrigo Osorno.
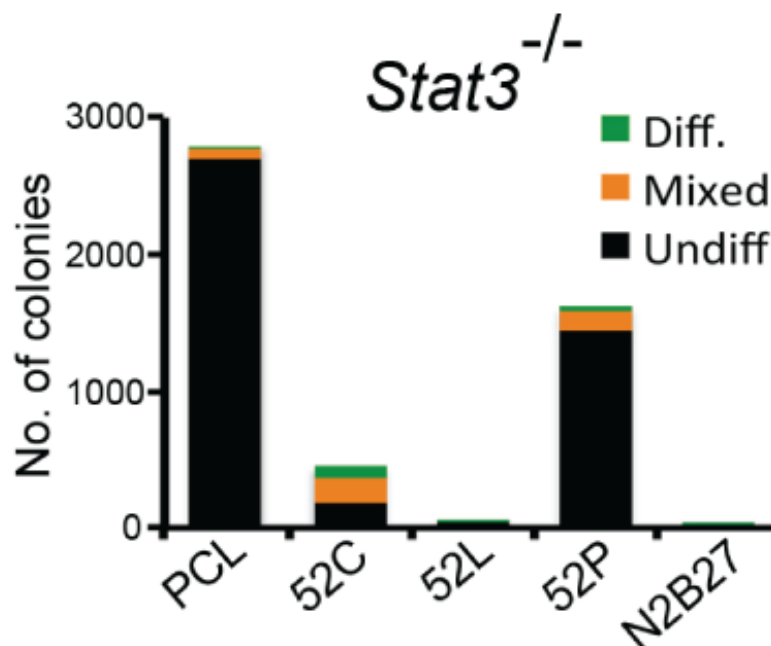
Figure 57. Colony formation of Stat3-/- ESC after clonal density plating and 7 days culture under the indicated conditions.
(P: PD, C: CH, L: LIF, 52: AU52).

Stat3$^{-/-}$ ESC cultured for more than two months in PD/AU52 retain robust expression of OCT4, NANOG, ESRRB and KLF4 proteins, and give rise to chimeric mice upon blastocyst injection (Figures 58). Immunocytochemical characterization was performed by Dr Rodrigo Osorno.
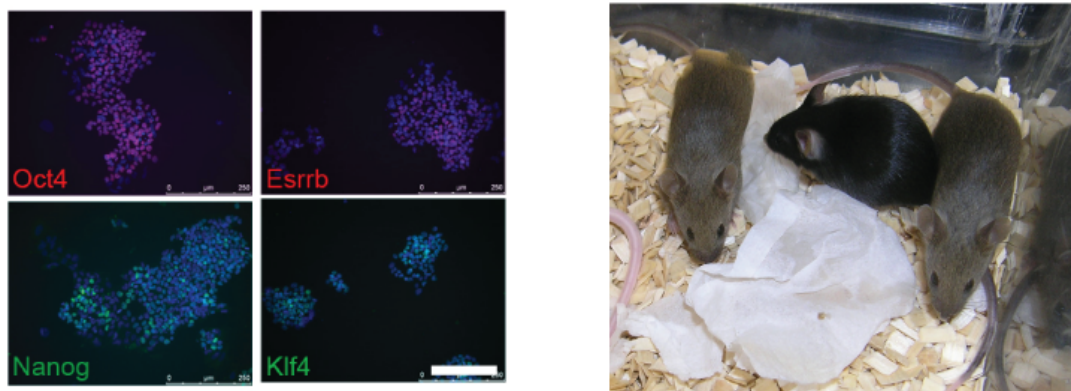
Figure 58. Stat3-/- ESC maintained in AU52/PD exhibit chimera-grade pluripotency.
Left panel) Immunofluorescence analysis of Oct4, Nanog, Esrrb, and Klf4 in Stat3-/-
ESC cultured for two months in the presence of PD/AU52 (Scale bar: 200 µm). Right
panel) Chimeric mice derived from the injection of Stat3-/- MF1 ESC into BL6
blastocyst. Prior to blastocyst injection the
Stat3-/- ESC were cultured for two months in the presence of PD/AU52.

Taken together, the data of this thesis suggest a concise mechanism of action for TR/AU52 that is based on β-catenin and Smad2 modulation via inhibition of CK1ε (Figure 59).
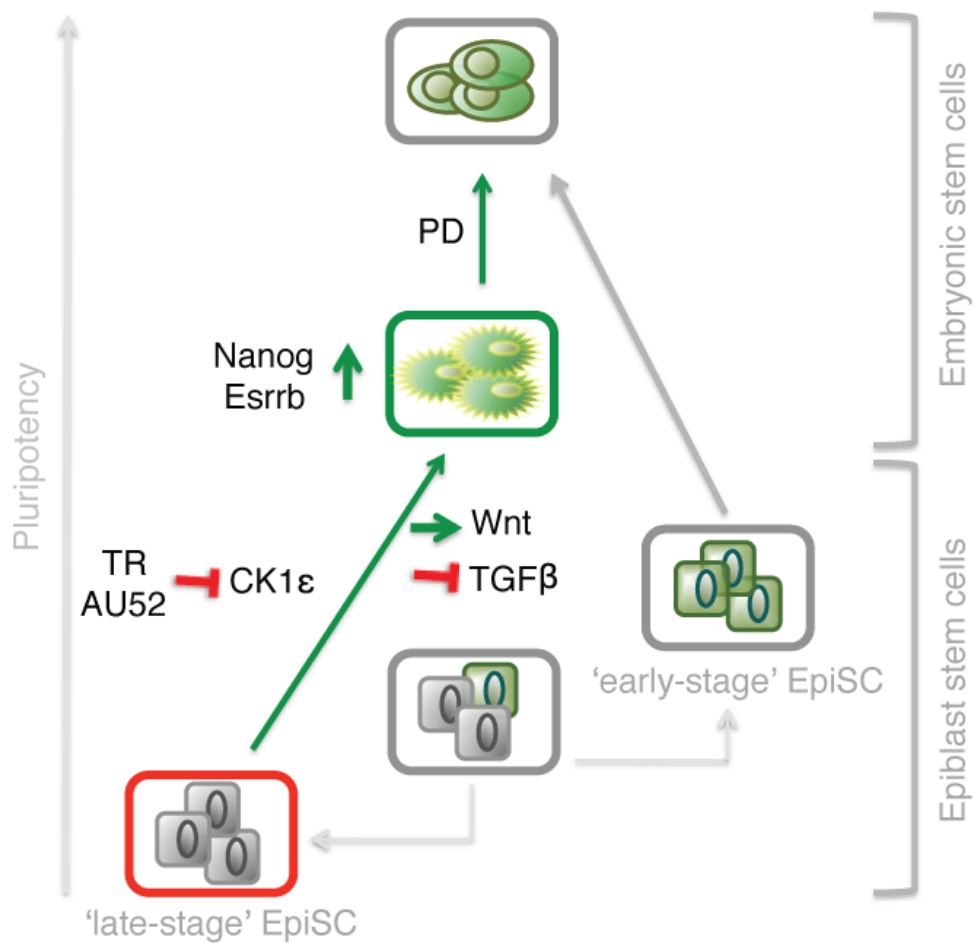
Figure 59. Schematic model of the mechanism through which TR/AU52 reverts recalcitrant EpiSC into ESC pluripotency.

See text for discussion.

5. Discussion

5.1 Recalcitrant Late-Stage EpiSC

It has been shown that EpiSC are heterogeneous within a given cell line, and to different degrees among cell lines (Bao et al., 2009; Bernemann et al., 2011; Han et al., 2010; Tsakiridis et al., 2014). Only a small subpopulation of EpiSC displays features of the early post-implantation epiblast (Bao et al., 2009; Han et al., 2010), whereas the vast majority of EpiSC functionally represent late stages of the postimplantation epiblast. Early-stage EpiSC are susceptible to media-induced reversion to an ESC-like state, whereas late-stage EpiSC are refractory to this process (Figures 4, 5) (Bernemann et al., 2011; Han et al., 2010). In this study, using a small-molecule library screen, I found a novel compound able to induce the conversion of early- and late-stage EpiSC into ESC-like cells, and I describe how this is accomplished. To my knowledge this is the first study showing the robust conversion of recalcitrant late-stage EpiSC to ESC through chemical means alone.

The starting point for this project was the wide acceptance of an unsubstantiated notion within scientists studying naïve and primed pluripotency that basically all EpiSC can be reverted into naïve pluripotent cells with the current protocols. In particular, the misconception lies in the assumption that the methods by which naïve pluripotency can be induced actually apply to all EpiSC. In stark contrast to this assumption, the most widely accepted conversion method based on culture conditions, namely the presence of 2i/LIF in the culture medium, is far from being a universal conversion method for EpiSC. Inhibition of MEK and GSK3β, together with the presence of LIF, can convert only a select fraction of EpiSC (Figures 1, 4) -

a specific fraction that demonstrates features of naïve pluripotency such as ICM integration and chimeric competence (Han et al., 2010).

5.2 Small Molecule Screening Assay

Following a chemical genetic approach I developed a small molecule screening assay to identify ligands capable of converting recalcitrant late-stage EpiSC into naïve pluripotency. By identifying the protein targets of such ligands I tried to define the mechanism governing conversion of late-stage EpiSC to a naïve pluripotent state. I screened the LOPAC library of known pharmacologically active compounds. The advantages of the LOPAC library are the cell penetrating capacity of the screened compounds, the broad range of target classes that are covered, and the known biological activity of the inhibitors. At the same time the known biological activity of the compounds promised to facilitate later target identification efforts.

I developed a screening assay based on fluorescent reporter gene expression under the control of *Oct4*. Two *Oct4* reporter lines were available: the OG2 and GOF18 (E3) cell lines. EpiSC-GOF18 contain a GFP transgene under the control of the entire regulatory region of the *Oct4* gene (Yeom et al., 1996). In EpiSC-OG2 the GFP reporter is solely under the control of the distal enhancer (DE) of the *Oct4* gene, i.e. the construct lacks the proximal enhancer (*Oct4*-ΔPE-GFP) (Yeom et al., 1996). The distal enhancer of *Oct4* contains a dense binding locus for key ESC-specific transcription factors (Chen et al., 2008). The fact that EpiSC preferentially utilize the PE over the DE, and that the *Oct4*-ΔPE-GFP is only active in ESC and not in EpiSC suggests that EpiSC must be lacking some of the key ESC-specific transcription factors (Tesar et al., 2007; Yeom et al., 1996). Accordingly, under their respective normal culture condition ESC (OG2) exhibit strong OCT4-GFP expression whereas OG2-EpiSC do not express OCT4-GFP (Figure 1). Theoretically, EpiSC-GOF18 containing both the PE and the DE should be OCT4-GFP positive.

However, only a very low percentage of established EpiSC-GOF18 expresses OCT4-GFP which probably results from epigenetic modifications during the adaptation to the in vitro culture conditions affecting the *Oct4-GFP* transgene, but not the endogenous *Oct4* (Figures 1, 3). I made use of the differential expression of the OCT4-GFP reporter in EpiSC and ESC to detect converted cells in the screening assay and hence active compounds.

I chose to keep the EpiSC in CM and not in mESC medium supplemented with LIF that is used for the conversion with 2i. This EpiSC culture condition was more stringent in two ways: Through the absence of additional LIF spontaneous conversion was prevented, and the presence of FGF2 represented an additional "barrier" toward naïve pluripotency. Thus, I was able to design an assay with a satisfactory screening window (Figures 8, 9). Once a hit compound had been identified, the converted cells needed to be extensively characterized as authentic naïve pluripotent stem cells. A high-content imager was used for the readout to identify converted naïve stem cells. Dissociation into single cells prior to the readout allowed me not only to detect cells with a GFP intensity equal to ESC, but also to quantify them. Hence, the readout was based on the number of single cells with a GFP intensity equivalent to those in ESC.

5.3   Triamterene

Our screening assay yielded a pteridine derivative known as Triamterene (Figures 10, 11), which blocks the epithelial sodium channel (ENaC), and is clinically used as a diuretic (Busch et al., 1996). The fact that despite the small library size Triamterene turned out as a hit that could subsequently be validated in secondary assays was a great surprise.

The screen was initially performed with unsorted EpiSC-GOF18. The next step after identifiying Triamterene was to confirm its activity on late-stage EpiSC. Triamterene induced transgenic *Oct4-GFP* expression in recalcitrant

EpiSC of both the EpiSC-GOF18 and EpiSC-OG2 lines (Figure 12). The TR-treated EpiSC changed their morphology toward smaller dome-shaped colonies. This newly acquired dome-shaped morphology could not be retained if cultured under EpiSC conditions, indicating that they had been converted to a state different to that of EpiSC (Figures 13-15). Furthermore, the activity of TR could be shown also for two other late-stage EpiSC lines, T9 and C1a1, through expression of the ESC-specific markers PECAM1, KLF4, and ESRRB (Figure 18) (Bernemann et al., 2011). The conversion was done in EpiSC medium, i.e. CM without addition of LIF. It is remarkable that Triamterene could induce the reversion of late-stage EpiSC despite the presence of FGF2 which is known to prime ESC for differentiation (Burdon et al., 1999; Kunath et al., 2007; Stavridis et al., 2007). Gene expression analyses by qRT-PCR revealed that other ESC specific markers were upregulated, such as *Nanog*, *Rex1*, *Stella*, *Dppa4*, and *Dppa5* (Figure 16). Consistently, early lineage markers like *Fgf5*, *Fgf8*, and *T* were downregulated. An overall assimilation of the global gene expression pattern toward that of ESC could be observed (Figure 17).

The TR-induced conversion of EpiSC from primed to naïve pluripotency displays several striking features distinct from the 2i-based conversion. After a relatively short exposure period to induce naïve pluripotency (6-8 days), TR-converted cells could be clonally expanded and maintained in LIF-supplemented ESC medium - without further addition of TR. Notably, TR induces the expression of OCT4-GFP in EpiSC cultured in CM medium despite the presence of FGF2 and without added LIF. This is likely to be possible as MEF-conditioned medium contains LIF. However, it was found that TR also inhibits PI3K-mediated STAT3 phosphorylation indicating a redundancy of this pathway during the conversion (Figure 48). Furthermore, STAT3-null ESC could be stably maintained and expanded in AU52/PD, or TR/PD, and even maintained the capacity to give rise to chimeric mice (Figures 57, 58).

Despite the apparent assimilations toward the naïve pluripotent state cells derived with TR alone failed to contribute to chimerism. The lack of homogenous high expression of OCT4-GFP in all TR-derived cells already raised suspicion whether the cells were fully converted (Figure 13). Global gene expression analysis then indeed pointed out that gene expression was not identical to that of ESC (Figure 17, 27). I do not want to exclude that chimera competent cells can be derived from recalcitrant EpiSC through the conversion with TR alone. Maybe the presence of FGF2 during the conversion, which is known to prime ESC for differentiation, counteracts the effect of TR (Burdon et al., 1999; Kunath et al., 2007; Stavridis et al., 2007). I was also able to convert late-stage EpiSC in N2B27-based ESC medium and in KO-DMEM-based ESC medium in the absense of FGF2. Proper selection of cell colonies with high OCT4-GFP expression and repeated subcloning might yield homogenous strongly OCT4-GFP-expressing cells capable of chimera contribution. Another important issue in this context is the passage number of the late-stage EpiSC before conversion. It could be that cells of an earlier passage revert more readily to cells that can contribute to chimeras.

5.4   FGF/ERK Inhibition

Activation of the FGF/ERK pathway predisposes ESC to undergo differentiation (Burdon et al., 1999; Kunath et al., 2007; Stavridis et al., 2007). In contrast, ERK-inhibition in combination with LIF and/or CH supports the maintenance of undifferentiated ESC (Ying et al., 2008). The presence of FGF2 in the EpiSC culture medium that was used for the conversion might have been a hindering factor toward full reprogramming. This is why I tried to complete conversion by inhibition of the FGF/ERK pathway. Inhibition of this pathway in TR-converted cells facilitated the transition of these cells to naïve pluripotency (Figures 20-32). ERK inhibition lead to strong downregulation of many lineage markers including *Fgf5* and *Fgf8*, and simultaneous

upregulation of ESC-specific marker genes like *Klf4*, *Tbx3*, and *Tcl1* (Figure 29). An overall assimilation to the ESC-like state was observed including changes in the epigenetic markup and Oct4 promoter utilization (Figures 24, 30). Most importantly TR/PD-converted cells resulted in chimera competent cells capable of germline contribution (Figure 32). It is important to state that ERK inhibition merely completes TR-induced conversion. TR/PD-based ESC conversion is a two-step procedure that is initiated by TR and completed by Erk inhibition. Neither does ERK inhibition alone induce naïve pluripotency even in early-stage EpiSC (Figure 54), nor is it necessary at the beginning of the TR-induced conversion (Figures 12, 18). Even the combined inhibition of ERK and GSK3β (2i) does not suffice to convert late-stage EpiSC (Figures 4, 5). As discussed earlier I cannot exclude that under certain favourable conditions chimera competent ESC-like cells can be derived from late-stage EpiSC through the conversion with TR alone. As ERK inhibition merely completes the conversion of recalcitrant EpiSC to naïve pluripotent cells, I consider it straightforward to hypothesize that for the most part conversion can be attributed to the effects of TR.

5.5 Casein Kinase 1ε (CK1ε)

Pteridin derivatives were known to inhibit protein kinases (Doukas et al., 2009; Gomtsyan et al., 2004; Leung et al., 2006). It was, therefore, hypothesized that a kinase may be the target of TR, and TR was profiled against a set of selected protein kinases which were previously reported to be relevant in stem cell biology.

Several kinase inhibitors were reported to support induced pluripotent stem (iPS) cell generation, or to promote ground-state pluripotency (Ichida et al., 2009; Li and Rana, 2012; Maherali and Hochedlinger, 2009; Sato et al., 2004; Ying et al., 2008). I tested TR against the reported kinases, but none were affected by TR (Appendix 1). Notably, TR did not inhibit GSK3β, MEK/ERK

nor ALK4/5, which are all known targets that promote the reversion of EpiSC to ESC-like cells (Greber et al., 2010; Zhou et al., 2010) (Appendix 1). This observation suggested that TR might be working through the regulation a different kinase.

Kinase profiling revealed that TR inhibited CK1δ/ε and PI3KC2γ (Appendix 1). Notably, however, none of the PI3K inhibitors tested were able to induce OCT4-GFP expression in EpiSC (Figures 33, 34). Therefore, I excluded PI3K as the effective target of TR-induced reversion of EpiSC. In contrast, a structurally unrelated CK1δ/ε inhibitor (D4476) was able to induce OCT4-GFP, and promote *Nanog* and *Esrrb* expression in EpiSC (Figures 33, 34, 36, 43). Profiling of TR against different isoforms of the Casein kinase family revealed affinity to $CK1\delta$ and $CK1\varepsilon$ (Figure 38). This is not surprising given the highly conserved protein sequences of these two isoforms. The IC_{50} values were 7.95 μM and 23.65 μM for $CK1\delta$ and $CK1\varepsilon$, respectively (Figures 37, 39). Importantly, knockdown of CK1ε (and not knockdown of CK1δ) gave rise to OCT4-GFP positive colonies, and resulted in a reduction of β-CATENIN and SMAD2 phosphorylation, thus, further substantiating the role for CK1ε in the reprogramming process (Figure 55).

Taken together, I report the first chemical conversion of late-stage EpiSC to the naïve pluripotent state and also define for the first time a role for CK1ε in this process.

5.6   AU52

In collaboration with Andrei Ursu, who synthesized the Triamterene derivatives, I performed a structure-activity-relationship analysis with TR with the aim to study the structural requirements needed for naïve conversion. Detailed information concerning the synthesis of the Triamterene derivatives will be part of Andrei Ursu's dissertation and will not be discussed here (Ursu, 2014). The aim of the SAR study was to explore potential room for synthetic

improvement of activity and to detect the indispensable substituents with regard to the design of pulldown probes for follow-up studies. The phenyl ring in position 6 of the pteridine scaffold proved to be sensitive to synthetic modifications with regard to the compound's conversion efficiency. The *para*-position of the phenyl ring was particularly sensitive, as insertions of any substituents resulted in a dramatic decrease of compound activity. Introducing substituents in the *meta*-position, on the other hand, such as fluorine, chlorine, bromine, or methyl, resulted in more active compounds with the chlorine derivative showing the highest conversion efficiency (AU52, Figure 35). Consistently, the higher biological activity was accompanied by obviously stronger inhibition of CK1δ and CK1ε with IC_{50} values of 0.44 µM and 5.36 µM, respectively (Figures 37, 39). AU52 showed a kinase inhibition profile similar to TR and was subsequently used as a substitute for TR. I could show that AU52 was capable of converting late-stage EpiSC into ESC-like cells sharing the features of naïve pluripotency (Figure 40). Most importantly, AU52 converted cells contributed to chimeric mice (Figure 41).

5.7   WNT and TGFβ Signaling

CK1 family members are known to exert both negative and positive effects on WNT signaling (Price, 2006). Potential contact points for negative regulation of WNT signaling via phosphorylation by CK1 include β-CATENIN (Amit et al., 2002; Liu et al., 2002), APC (Rubinfeld et al., 2001), and LRP5/6 (Swiatek et al., 2006). However, members of the CK1 family are also known to be involved in numerous other processes including p53 and E-CADHERIN modifications, nuclear-cytoplasmic shuttling of transcription factors and TGFβ signaling (Dupre-Crochet et al., 2007; Knippschild et al., 1997; Rena et al., 2004; Waddell et al., 2004). The agonistic effect of TR/AU52 on the WNT pathway was confirmed *in vitro* (Figures 48-52) and *in vivo* (Figures 53).

However, the finding that TR/AU52 simultaneously modulate WNT/β-CATENIN and TGFβ/SMAD2 signaling via inhibition of CK1ε is of special importance. By this I show that only activation of the WNT pathway together with the simultaneous inhibition of SMAD2 signaling can reproduce the TR/AU52-based reprogramming.,which is in contrast to affecting the individual pathway (Figures 48, 54, 55). This finding helps us to understand why neither SB, nor CH alone can convert EpiSC to a naïve pluripotent state. Neither the CK1ε pathway nor the TGFβ/SMAD2 pathway to date were known to be involved in naïve conversion of late-stage EpiSC. Thus, I also demonstrate why WNT modulation alone, or even 2i/LIF is incompetent in this regard. The missing link in 2i/LIF-based conversion indeed is inhibition of TGFβ/SMAD2 signaling.

5.8   *Klf2, Nanog*, and *Esrrb*

TR-treatment of EpiSC coincided with strong upregulation of the key ESC-specific pluripotency markers *Klf2*, *Nanog* and *Esrrb* (Figures 42, 43). Interestingly, KD of *Klf2* or *Nanog* significantly impaired TR/AU52-based conversion, highlighting their importance during this process (Figure 44). *Esrrb*-KD reduced by half the number of AU52-induced OCT4-GFP-positive cells (Figure 44). However, it should be noted that the shRNA probes for *Esrrb* were less efficient than those for *Nanog* and *Klf2* (Figure 44). In any case, these three factors may indeed be necessary in the chemical-induced reversion of EpiSC, which is consistent with previous reports that they promote the efficient conversion when expressed in EpiSC (Festuccia et al., 2012; Hall et al., 2009; Silva et al., 2009).

Taken together, I have developed a simple and efficient method for the conversion of recalcitrant EpiSC into an ESC-like state. The here presented findings reveal novel insights into the mechanisms governing the transition between primed and naïve pluripotency. Notably, I introduce CK1ε as a key

player in the regulation of naïve pluripotency, through the direct modulation of WNT/β-CATENIN and TGFβ/SMAD2 signaling which results in induction of the ESC-specific transcription factors *Klf2*, *Nanog* and *Esrrb* that drive the necessary change in the gene expression pattern of late-stage EpiSC.

5.9 Summary

EpiSC contain subpopulations within a given cell line, and to different degrees among cell lines. These subpopulations functionally correspond to an early and late stage of postimplantation development (Figure 59). Interestingly, the subpopulation, that normally is smaller in number and that represents early-stage EpiSC, was found to contribute to chimeras when injected into the ICM at the blastocyst stage, which is considered a hallmark feature of preimplantation pluripotent cells. So far, late-stage EpiSC which represent the vast majority of EpiSC and cannot contribute to chimera development when introduced into the ICM were recalcitrant to chemical reprogramming to naïve pluripotency.

The aim of the presented study was to enable the reversion of recalcitrant late-stage EpiSC to a naïve pluripotent state and to elucidate the molecular mechanism underlying the reversion. The questions that I was interested in were: Can recalcitrant late-stage EpiSC be reverted to a naïve ESC-like state by chemical means alone, i.e. without genetically invasive methods? If so, which extrinsic factors can accomplish naïve conversion of late-stage EpiSC? What is the underlying mechanism that such extrinsic factor exerts?

Following a chemical genetic approach I discovered Triamterene to be able to induce the conversion of late-stage EpiSC to naïve pluripotent cells (Figure 59). An SAR study in collaboration with Andrei Ursu revealed AU52 as a more potent Triamterene derivative capable of converting late stage EpiSC to naive pluripotency (Ursu, 2014). The data of the presented thesis demonstrate that Triamterene acts via a dual mechanism through the inhibition of CK1ε (Figure

59). The inhibition of CK1ε, namely, results in simultaneous inhibition of β-CATENIN and SMAD2 phosphorylation which actuates WNT and attenuates TGFβ signaling (Figure 59). The simultaneous modulation of the two signaling pathways results in the induction of the ESC-specific transcription factors *Klf2, Nanog* and *Esrrb* which eventually drive the conversion to naïve pluripotency (Figure 59).

Following up on the findings of the presented work there are several interesting aspects to be investigated to gain better understanding of the mechanisms governing naïve pluripotency. I introduce for the first time CK1ε as a new player in naïve pluripotency. It would be interesting to determine whether the role of CK1 in the regulation of naïve pluripotency is conserved across species. It must be noted, however, that the ESC-specific markers *Klf2, Nanog* and *Esrrb* which are induced by the inhibition of CK1ε and which were shown to convert EpiSC to naïve pluripotency in the mouse system are already expressed in hESC.

It has been demonstrate that inhibition of CK1ε results in simultaneous modulation of β-CATENIN and SMAD2 phosphorylation directly associating SMAD2 signaling with late-stage EpiSC. Inhibition of SMAD2 together with ERK signaling was recently shown to promote ESC derivation from non-permissive mouse strains (Hassani et al., 2014). BMP4 signaling can be augmented in these cells which might indicate a crosstalk between SMAD2 and BMP4-directed SMAD1.

Finally, the role of ERK inhibition has to be studied in more detail to determine whether chimera competent naïve pluripotent cells can be obtained through TR/AU52 treatment alone (Figure 59). As suggested earlier key to that might be proper selection of converted colonies, and conversion media free of FGF. In the same sense, it might be possible to identify the minimal key set of genes that establish and control chimera competence.

6.   References

Amit, S., Hatzubai, A., Birman, Y., Andersen, J.S., Ben-Shushan, E., Mann, M., Ben-Neriah, Y., and Alkalay, I. (2002). Axin-mediated CKI phosphorylation of beta-catenin at Ser 45: a molecular switch for the Wnt pathway. Genes & development *16*, 1066-1076.

Bao, S., Tang, F., Li, X., Hayashi, K., Gillich, A., Lao, K., and Surani, M.A. (2009). Epigenetic reversion of post-implantation epiblast to pluripotent embryonic stem cells. Nature *461*, 1292-1295.

Bernemann, C., Greber, B., Ko, K., Sterneckert, J., Han, D.W., Arauzo-Bravo, M.J., and Scholer, H.R. (2011). Distinct developmental ground states of epiblast stem cell lines determine different pluripotency features. Stem Cells *29*, 1496-1503.

Bradley, A., Evans, M., Kaufman, M.H., and Robertson, E. (1984). Formation of germ-line chimaeras from embryo-derived teratocarcinoma cell lines. Nature *309*, 255-256.

Brault, V., Moore, R., Kutsch, S., Ishibashi, M., Rowitch, D.H., McMahon, A.P., Sommer, L., Boussadia, O., and Kemler, R. (2001). Inactivation of the beta-catenin gene by Wnt1-Cre-mediated deletion results in dramatic brain malformation and failure of craniofacial development. Development *128*, 1253-1264.

Brons, I.G., Smithers, L.E., Trotter, M.W., Rugg-Gunn, P., Sun, B., Chuva de Sousa Lopes, S.M., Howlett, S.K., Clarkson, A., Ahrlund-Richter, L., Pedersen, R.A.*, et al.* (2007). Derivation of pluripotent epiblast stem cells from mammalian embryos. Nature *448*, 191-195.

6. References

Buecker, C., Chen, H.H., Polo, J.M., Daheron, L., Bu, L., Barakat, T.S., Okwieka, P., Porter, A., Gribnau, J., Hochedlinger, K.*, et al.* (2010). A murine ESC-like state facilitates transgenesis and homologous recombination in human pluripotent stem cells. Cell stem cell *6*, 535-546.

Bunin, B.A., and Ellman, J.A. (1992). A General and Expedient Method for the Solid-Phase Synthesis of 1,4-Benzodiazepine Derivatives. J Am Chem Soc *114*, 10997-10998.

Burdon, T., Stracey, C., Chambers, I., Nichols, J., and Smith, A. (1999). Suppression of SHP-2 and ERK signalling promotes self-renewal of mouse embryonic stem cells. Developmental biology *210*, 30-43.

Busch, A.E., Suessbrich, H., Kunzelmann, K., Hipper, A., Greger, R., Waldegger, S., Mutschler, E., Lindemann, B., and Lang, F. (1996). Blockade of epithelial Na+ channels by triamterenes - underlying mechanisms and molecular basis. Pflugers Archiv : European journal of physiology *432*, 760-766.

Canessa, C.M., Schild, L., Buell, G., Thorens, B., Gautschi, I., Horisberger, J.D., and Rossier, B.C. (1994). Amiloride-sensitive epithelial Na+ channel is made of three homologous subunits. Nature *367*, 463-467.

Chambers, I., Silva, J., Colby, D., Nichols, J., Nijmeijer, B., Robertson, M., Vrana, J., Jones, K., Grotewold, L., and Smith, A. (2007). Nanog safeguards pluripotency and mediates germline development. Nature *450*, 1230-1234.

Chen, X., Xu, H., Yuan, P., Fang, F., Huss, M., Vega, V.B., Wong, E., Orlov, Y.L., Zhang, W., Jiang, J.*, et al.* (2008). Integration of external signaling pathways with the core transcriptional network in embryonic stem cells. Cell *133*, 1106-1117.

6.   References

_____

Chou, Y.F., Chen, H.H., Eijpe, M., Yabuuchi, A., Chenoweth, J.G., Tesar, P., Lu, J., McKay, R.D., and Geijsen, N. (2008). The growth factor environment defines distinct pluripotent ground states in novel blastocyst-derived stem cells. Cell *135*, 449-461.

Doukas, J., Eide, L., Stebbins, K., Racanelli-Layton, A., Dellamary, L., Martin, M., Dneprovskaia, E., Noronha, G., Soll, R., Wrasidlo, W.*, et al.* (2009). Aerosolized phosphoinositide 3-kinase gamma/delta inhibitor TG100-115 [3-[2,4-diamino-6-(3-hydroxyphenyl)pteridin-7-yl]phenol] as a therapeutic candidate for asthma and chronic obstructive pulmonary disease. The Journal of pharmacology and experimental therapeutics *328*, 758-765.

Dupre-Crochet, S., Figueroa, A., Hogan, C., Ferber, E.C., Bialucha, C.U., Adams, J., Richardson, E.C., and Fujita, Y. (2007). Casein kinase 1 is a novel negative regulator of E-cadherin-based cell-cell contacts. Molecular and cellular biology *27*, 3804-3816.

Evans, M.J., and Kaufman, M.H. (1981). Establishment in culture of pluripotential cells from mouse embryos. Nature *292*, 154-156.

Festuccia, N., Osorno, R., Halbritter, F., Karwacki-Neisius, V., Navarro, P., Colby, D., Wong, F., Yates, A., Tomlinson, S.R., and Chambers, I. (2012). Esrrb is a direct Nanog target gene that can substitute for Nanog function in pluripotent cells. Cell stem cell *11*, 477-490.

Gafni, O., Weinberger, L., Mansour, A.A., Manor, Y.S., Chomsky, E., Ben-Yosef, D., Kalma, Y., Viukov, S., Maza, I., Zviran, A.*, et al.* (2013). Derivation of novel human ground state naive pluripotent stem cells. Nature *504*, 282-286.

Gillich, A., Bao, S., Grabole, N., Hayashi, K., Trotter, M.W., Pasque, V., Magnusdottir, E., and Surani, M.A. (2012). Epiblast stem cell-based system reveals reprogramming synergy of germline factors. Cell stem cell *10*, 425-439.

Gomtsyan, A., Didomenico, S., Lee, C.H., Stewart, A.O., Bhagwat, S.S., Kowaluk, E.A., and Jarvis, M.F. (2004). Synthesis and biological evaluation of pteridine and pyrazolopyrimidine based adenosine kinase inhibitors. Bioorganic & medicinal chemistry letters *14*, 4165-4168.

Greber, B., Coulon, P., Zhang, M., Moritz, S., Frank, S., Muller-Molina, A.J., Arauzo-Bravo, M.J., Han, D.W., Pape, H.C., and Scholer, H.R. (2011). FGF signalling inhibits neural induction in human embryonic stem cells. Embo J *30*, 4874-4884.

Greber, B., Wu, G., Bernemann, C., Joo, J.Y., Han, D.W., Ko, K., Tapia, N., Sabour, D., Sterneckert, J., Tesar, P.*, et al.* (2010). Conserved and divergent roles of FGF signaling in mouse epiblast stem cells and human embryonic stem cells. Cell stem cell *6*, 215-226.

Guo, G., and Smith, A. (2010). A genome-wide screen in EpiSCs identifies Nr5a nuclear receptors as potent inducers of ground state pluripotency. Development *137*, 3185-3192.

Guo, G., Yang, J., Nichols, J., Hall, J.S., Eyres, I., Mansfield, W., and Smith, A. (2009). Klf4 reverts developmentally programmed restriction of ground state pluripotency. Development *136*, 1063-1069.

Hakkim, A., Fuchs, T.A., Martinez, N.E., Hess, S., Prinz, H., Zychlinsky, A., and Waldmann, H. (2011). Activation of the Raf-MEK-ERK pathway is required for neutrophil extracellular trap formation. Nature chemical biology *7*, 75-77.

6.   References

Hall, J., Guo, G., Wray, J., Eyres, I., Nichols, J., Grotewold, L., Morfopoulou, S., Humphreys, P., Mansfield, W., Walker, R.*, et al.* (2009). Oct4 and LIF/Stat3 additively induce Kruppel factors to sustain embryonic stem cell self-renewal. Cell stem cell *5*, 597-609.

Han, D.W., Tapia, N., Joo, J.Y., Greber, B., Arauzo-Bravo, M.J., Bernemann, C., Ko, K., Wu, G., Stehling, M., Do, J.T.*, et al.* (2010). Epiblast stem cell subpopulations represent mouse embryos of distinct pregastrulation stages. Cell *143*, 617-627.

Hanna, J., Cheng, A.W., Saha, K., Kim, J., Lengner, C.J., Soldner, F., Cassady, J.P., Muffat, J., Carey, B.W., and Jaenisch, R. (2010). Human embryonic stem cells with biological and epigenetic characteristics similar to those of mouse ESCs. Proceedings of the National Academy of Sciences of the United States of America *107*, 9222-9227.

Hanna, J., Markoulaki, S., Mitalipova, M., Cheng, A.W., Cassady, J.P., Staerk, J., Carey, B.W., Lengner, C.J., Foreman, R., Love, J.*, et al.* (2009). Metastable pluripotent states in NOD-mouse-derived ESCs. Cell stem cell *4*, 513-524.

Hassani, S.N., Totonchi, M., Sharifi-Zarchi, A., Mollamohammadi, S., Pakzad, M., Moradi, S., Samadian, A., Masoudi, N., Mirshahvaladi, S., Farrokhi, A.*, et al.* (2014). Inhibition of TGFbeta signaling promotes ground state pluripotency. Stem cell reviews *10*, 16-30.

Hayashi, K., and Surani, M.A. (2009). Self-renewing epiblast stem cells exhibit continual delineation of germ cells with epigenetic reprogramming in vitro. Development *136*, 3549-3556.

6. References

Ichida, J.K., Blanchard, J., Lam, K., Son, E.Y., Chung, J.E., Egli, D., Loh, K.M., Carter, A.C., Di Giorgio, F.P., Koszka, K.*, et al.* (2009). A small-molecule inhibitor of tgf-Beta signaling replaces sox2 in reprogramming by inducing nanog. Cell stem cell *5*, 491-503.

Irizarry, R.A., Hobbs, B., Collin, F., Beazer-Barclay, Y.D., Antonellis, K.J., Scherf, U., and Speed, T.P. (2003). Exploration, normalization, and summaries of high density oligonucleotide array probe level data. Biostatistics *4*, 249-264.

Karwacki-Neisius, V., Goke, J., Osorno, R., Halbritter, F., Ng, J.H., Weisse, A.Y., Wong, F.C., Gagliardi, A., Mullin, N.P., Festuccia, N.*, et al.* (2013). Reduced Oct4 expression directs a robust pluripotent state with distinct signaling activity and increased enhancer occupancy by Oct4 and Nanog. Cell stem cell *12*, 531-545.

Kehat, I., Kenyagin-Karsenti, D., Snir, M., Segev, H., Amit, M., Gepstein, A., Livne, E., Binah, O., Itskovitz-Eldor, J., and Gepstein, L. (2001). Human embryonic stem cells can differentiate into myocytes with structural and functional properties of cardiomyocytes. The Journal of clinical investigation *108*, 407-414.

Kelly, K.F., Ng, D.Y., Jayakumaran, G., Wood, G.A., Koide, H., and Doble, B.W. (2011). beta-catenin enhances Oct-4 activity and reinforces pluripotency through a TCF-independent mechanism. Cell stem cell *8*, 214-227.

Klockgether-Radke, A.P. (2002). F. W. Serturner and the discovery of morphine. 200 years of pain therapy with opioids. Anasth Intensiv Notf *37*, 244-+.

6. References

Knippschild, U., Milne, D.M., Campbell, L.E., DeMaggio, A.J., Christenson, E., Hoekstra, M.F., and Meek, D.W. (1997). p53 is phosphorylated in vitro and in vivo by the delta and epsilon isoforms of casein kinase 1 and enhances the level of casein kinase 1 delta in response to topoisomerase-directed drugs. Oncogene *15*, 1727-1736.

Koch, M.A., Schuffenhauer, A., Scheck, M., Wetzel, S., Casaulta, M., Odermatt, A., Ertl, P., and Waldmann, H. (2005). Charting biologically relevant chemical space: a structural classification of natural products (SCONP). Proceedings of the National Academy of Sciences of the United States of America *102*, 17272-17277.

Koehler, A.N. (2010). A complex task? Direct modulation of transcription factors with small molecules. Current opinion in chemical biology *14*, 331-340.

Kunath, T., Saba-El-Leil, M.K., Almousailleakh, M., Wray, J., Meloche, S., and Smith, A. (2007). FGF stimulation of the Erk1/2 signalling cascade triggers transition of pluripotent embryonic stem cells from self-renewal to lineage commitment. Development *134*, 2895-2902.

Leung, S.Y., Niimi, A., Noble, A., Oates, T., Williams, A.S., Medicherla, S., Protter, A.A., and Chung, K.F. (2006). Effect of transforming growth factor-beta receptor I kinase inhibitor 2,4-disubstituted pteridine (SD-208) in chronic allergic airway inflammation and remodeling. The Journal of pharmacology and experimental therapeutics *319*, 586-594.

Li, Z., and Rana, T.M. (2012). A kinase inhibitor screen identifies small-molecule enhancers of reprogramming and iPS cell generation. Nature communications *3*, 1085.

Liu, C., Li, Y., Semenov, M., Han, C., Baeg, G.H., Tan, Y., Zhang, Z., Lin, X., and He, X. (2002). Control of beta-catenin phosphorylation/degradation by a dual-kinase mechanism. Cell *108*, 837-847.

Maherali, N., and Hochedlinger, K. (2009). Tgfbeta signal inhibition cooperates in the induction of iPSCs and replaces Sox2 and cMyc. Current biology : CB *19*, 1718-1723.

Martin, G.R. (1981). Isolation of a pluripotent cell line from early mouse embryos cultured in medium conditioned by teratocarcinoma stem cells. Proceedings of the National Academy of Sciences of the United States of America *78*, 7634-7638.

Merrifield, B. (1997). Concept and early development of solid-phase peptide synthesis. Methods in enzymology *289*, 3-13.

Nichols, J., and Smith, A. (2009). Naive and primed pluripotent states. Cell stem cell *4*, 487-492.

Nie, B., Wang, H., Laurent, T., and Ding, S. (2012). Cellular reprogramming: a small molecule perspective. Current opinion in cell biology *24*, 784-792.

Niwa, H., Ogawa, K., Shimosato, D., and Adachi, K. (2009). A parallel circuit of LIF signalling pathways maintains pluripotency of mouse ES cells. Nature *460*, 118-122.

Ong, S.E., Blagoev, B., Kratchmarova, I., Kristensen, D.B., Steen, H., Pandey, A., and Mann, M. (2002). Stable isotope labeling by amino acids in cell culture, SILAC, as a simple and accurate approach to expression proteomics. Molecular & cellular proteomics : MCP *1*, 376-386.

Pera, M.F., and Tam, P.P. (2010). Extrinsic regulation of pluripotent stem cells. Nature *465*, 713-720.

6. References

Price, M.A. (2006). CKI, there's more than one: casein kinase I family members in Wnt and Hedgehog signaling. Genes & development *20*, 399-410.

Rena, G., Bain, J., Elliott, M., and Cohen, P. (2004). D4476, a cell-permeant inhibitor of CK1, suppresses the site-specific phosphorylation and nuclear exclusion of FOXO1a. EMBO reports *5*, 60-65.

Rossant, J. (2008). Stem cells and early lineage development. Cell *132*, 527-531.

Rubinfeld, B., Tice, D.A., and Polakis, P. (2001). Axin-dependent phosphorylation of the adenomatous polyposis coli protein mediated by casein kinase 1epsilon. The Journal of biological chemistry *276*, 39037-39045.

Sato, N., Meijer, L., Skaltsounis, L., Greengard, P., and Brivanlou, A.H. (2004). Maintenance of pluripotency in human and mouse embryonic stem cells through activation of Wnt signaling by a pharmacological GSK-3-specific inhibitor. Nature medicine *10*, 55-63.

Schreiber, S.L. (2000). Target-oriented and diversity-oriented organic synthesis in drug discovery. Science *287*, 1964-1969.

Schreiber, S.L. (2005). Small molecules: the missing link in the central dogma. Nature chemical biology *1*, 64-66.

Schust, J., Sperl, B., Hollis, A., Mayer, T.U., and Berg, T. (2006). Stattic: a small-molecule inhibitor of STAT3 activation and dimerization. Chemistry & biology *13*, 1235-1242.

6. References

Silva, J., Nichols, J., Theunissen, T.W., Guo, G., van Oosten, A.L., Barrandon, O., Wray, J., Yamanaka, S., Chambers, I., and Smith, A. (2009). Nanog is the gateway to the pluripotent ground state. Cell *138*, 722-737.

Spring, D.R. (2005). Chemical genetics to chemical genomics: small molecules offer big insights. Chemical Society reviews *34*, 472-482.

Stavridis, M.P., Lunn, J.S., Collins, B.J., and Storey, K.G. (2007). A discrete period of FGF-induced Erk1/2 signalling is required for vertebrate neural specification. Development *134*, 2889-2894.

Stockwell, B.R. (2000). Chemical genetics: ligand-based discovery of gene function. Nature reviews Genetics *1*, 116-125.

Swiatek, W., Kang, H., Garcia, B.A., Shabanowitz, J., Coombs, G.S., Hunt, D.F., and Virshup, D.M. (2006). Negative regulation of LRP6 function by casein kinase I epsilon phosphorylation. The Journal of biological chemistry *281*, 12233-12241.

Tai, C.I., and Ying, Q.L. (2013). Gbx2, a LIF/Stat3 target, promotes reprogramming to and retention of the pluripotent ground state. Journal of cell science.

Takahashi, K., Tanabe, K., Ohnuki, M., Narita, M., Ichisaka, T., Tomoda, K., and Yamanaka, S. (2007). Induction of pluripotent stem cells from adult human fibroblasts by defined factors. Cell *131*, 861-872.

Takeda, K., Noguchi, K., Shi, W., Tanaka, T., Matsumoto, M., Yoshida, N., Kishimoto, T., and Akira, S. (1997). Targeted disruption of the mouse Stat3 gene leads to early embryonic lethality. Proceedings of the National Academy of Sciences of the United States of America *94*, 3801-3804.

6. References

Tan, D.S., Foley, M.A., Shair, M.D., and Schreiber, S.L. (1998). Stereoselective synthesis of over two million compounds having structural features both reminiscent of natural products and compatible with miniaturized cell-based assays. J Am Chem Soc *120*, 8565-8566.

ten Berge, D., Kurek, D., Blauwkamp, T., Koole, W., Maas, A., Eroglu, E., Siu, R.K., and Nusse, R. (2011). Embryonic stem cells require Wnt proteins to prevent differentiation to epiblast stem cells. Nature cell biology *13*, 1070-1075.

Tesar, P.J., Chenoweth, J.G., Brook, F.A., Davies, T.J., Evans, E.P., Mack, D.L., Gardner, R.L., and McKay, R.D. (2007). New cell lines from mouse epiblast share defining features with human embryonic stem cells. Nature *448*, 196-199.

Thomson, J.A., Itskovitz-Eldor, J., Shapiro, S.S., Waknitz, M.A., Swiergiel, J.J., Marshall, V.S., and Jones, J.M. (1998). Embryonic stem cell lines derived from human blastocysts. Science *282*, 1145-1147.

Tsakiridis, A., Huang, Y., Blin, G., Skylaki, S., Wymeersch, F., Osorno, R., Economou, C., Karagianni, E., Zhao, S., Lowell, S.*, et al.* (2014). Distinct Wnt-driven primitive streak-like populations reflect in vivo lineage precursors. Development *141*, 1209-1221.

Ursu, A. (2014). planned Dissertation. TU Dortmund.

Waddell, D.S., Liberati, N.T., Guo, X., Frederick, J.P., and Wang, X.F. (2004). Casein kinase Iepsilon plays a functional role in the transforming growth factor-beta signaling pathway. The Journal of biological chemistry *279*, 29236-29246.

Wagers, A.J., and Weissman, I.L. (2004). Plasticity of adult stem cells. Cell *116*, 639-648.

6. References

Ware, C.B., Wang, L., Mecham, B.H., Shen, L., Nelson, A.M., Bar, M., Lamba, D.A., Dauphin, D.S., Buckingham, B., Askari, B.*, et al.* (2009). Histone deacetylase inhibition elicits an evolutionarily conserved self-renewal program in embryonic stem cells. Cell stem cell *4*, 359-369.

Watanabe, K., Ueno, M., Kamiya, D., Nishiyama, A., Matsumura, M., Wataya, T., Takahashi, J.B., Nishikawa, S., Nishikawa, S., Muguruma, K.*, et al.* (2007). A ROCK inhibitor permits survival of dissociated human embryonic stem cells. Nature biotechnology *25*, 681-686.

Wetzel, S., Bon, R.S., Kumar, K., and Waldmann, H. (2011). Biology-oriented synthesis. Angew Chem Int Ed Engl *50*, 10800-10826.

Wetzel, S., Klein, K., Renner, S., Rauh, D., Oprea, T.I., Mutzel, P., and Waldmann, H. (2009). Interactive exploration of chemical space with Scaffold Hunter. Nature chemical biology *5*, 581-583.

Wray, J., Kalkan, T., Gomez-Lopez, S., Eckardt, D., Cook, A., Kemler, R., and Smith, A. (2011). Inhibition of glycogen synthase kinase-3 alleviates Tcf3 repression of the pluripotency network and increases embryonic stem cell resistance to differentiation. Nature cell biology *13*, 838-845.

Xu, R.H., Sampsell-Barron, T.L., Gu, F., Root, S., Peck, R.M., Pan, G., Yu, J., Antosiewicz-Bourget, J., Tian, S., Stewart, R.*, et al.* (2008). NANOG is a direct target of TGFbeta/activin-mediated SMAD signaling in human ESCs. Cell stem cell *3*, 196-206.

Yeom, Y.I., Fuhrmann, G., Ovitt, C.E., Brehm, A., Ohbo, K., Gross, M., Hubner, K., and Scholer, H.R. (1996). Germline regulatory element of Oct-4 specific for the totipotent cycle of embryonal cells. Development *122*, 881-894.

6.   References

Ying, Q.L., Nichols, J., Chambers, I., and Smith, A. (2003). BMP induction of Id proteins suppresses differentiation and sustains embryonic stem cell self-renewal in collaboration with STAT3. Cell *115*, 281-292.

Ying, Q.L., Wray, J., Nichols, J., Batlle-Morera, L., Doble, B., Woodgett, J., Cohen, P., and Smith, A. (2008). The ground state of embryonic stem cell self-renewal. Nature *453*, 519-523.

Zhang, J.H., Chung, T.D., and Oldenburg, K.R. (1999). A Simple Statistical Parameter for Use in Evaluation and Validation of High Throughput Screening Assays. Journal of biomolecular screening *4*, 67-73.

Zhang, S.C., Wernig, M., Duncan, I.D., Brustle, O., and Thomson, J.A. (2001). In vitro differentiation of transplantable neural precursors from human embryonic stem cells. Nature biotechnology *19*, 1129-1133.

Zhou, H., Li, W., Zhu, S., Joo, J.Y., Do, J.T., Xiong, W., Kim, J.B., Zhang, K., Scholer, H.R., and Ding, S. (2010). Conversion of mouse epiblast stem cells to an earlier pluripotency state by small molecules. The Journal of biological chemistry *285*, 29676-29680.

Ziegler, S., Pries, V., Hedberg, C., and Waldmann, H. (2013). Target identification for small bioactive molecules: finding the needle in the haystack. Angew Chem Int Ed Engl *52*, 2744-2792.

7. Abstract

7.1 Background

Embryonic stem cells (ESC) are derived from the inner cell mass (ICM) of preimplantation embryos. They are capable of contributing to the development of chimeric mice when injected back into the ICM. This particular ability is called naïve or ground state pluripotency. Epiblast stem cells (EpiSC) are derived from the epiblast of postimplantation embryos. While they equally represent pluripotent cells capable of teratoma formation they do not contribute to the development of chimeras when injected into the ICM. This somewhat restricted pluripotency of the slightly more advanced embryo was termed primed, i.e. ready for lineage commitment. EpiSC are heterogenous within and among cell lines. They were shown to comprise at least two subpopulations which are functionally equivalent to the early and late stage of postimplantation development. The small fraction representing the early stage is even chimera competent while the vast majority representing the late stage is not chimera competent. Until now these late-stage EpiSC could not be reprogrammed to naïve pluripotency through chemical inhibitors alone. In contrast to early-stage EpiSC, late-stage EpiSC were recalcitrant to the 2i/LIF condition which is widely known to stabilize the ground state of pluripotency based on GSK3β and MEK inhibition.

7.2 Aim of the Study

The aim of the presented study was to identify a novel chemical means for the conversion of recalcitrant late-stage EpiSC into naïve pluripotency.

Through the study of the mechanism-of-action of the discovered inhibitors I aimed at the elucidation of the mechanism governing the establishment of ground state pluripotency in late-stage EpiSC.

7.3 Methods

Toward this end, I applied a chemical genetic approach. I developed a small molecule screening assay and used the LOPAC library of known pharmacologically active compounds to discover a hit compound. The hit compound was validated in secondary assays through full characterization of the converted cells using FACS, qRT-PCR, global transcription analysis, immunocytochemistry, teratoma and chimera assays. Target identification efforts included kinase profiling, testing of structurally diverse inhibitors, microarray and gene ontology analyses, structure-activity-relationship analyses and IC_{50} value determinations. Further investigations of the mechanism-of-action and target validation involved biochemical assays like western blotting, genetic knockdown experiments, and *in vivo* phenotypic zebrafish assays.

7.4 Results

I developed a 96-well plate small molecule screening assay based on the differential expression of the *OCT4-GFP* reporter in EpiSC-GOF18 and ESC using a high-content imager. I discovered Triamterene (TR) as a hit compound, a known diuretic pteridine derivative. Validation of the hit compound revealed that TR was capable of converting several late-stage EpiSC lines into a state that shared many features with ESC. The converted cells, however, did not yield chimeric mice when injected in blastocysts. This imparity could be overcome through complementation of TR-induced

conversion by the simultaneous inhibition of ERK signaling to yield ESC-like cells with full chimera competence. Kinase profiling identified CK1δ/ε and PI3Kclass2γ as potential targets of TR. Subsequent gene knockdown experiments confirmed the isoform CK1ε as the target of TR-induced conversion, and structure-activity-relationship analysis lead to the synthesis of a significantly more potent inhibitor capable of naïve conversion, termed AU52. Biochemical analyses revealed that inhibition of CK1ε resulted in simultaneous inhibition of β-CATENIN and SMAD2 phosphorylation. The concurrent stimulation of WNT and attenuation of TGFβ signaling lead to the induction of the ESC-specific transcription factors *Klf2*, *Nanog*, and *Esrrb* which eventually effected the naïve conversion.

7.5   Conclusion

Taken together, the findings of this thesis represent the first chemical condition for the conversion of late-stage EpiSC to naïve pluripotency. I introduce CK1ε as a novel player to affect the core regulatory network of ground state pluripotency and elucidate the mechanism-of-action of TR/AU52-induced naïve conversion. Finally, I offer a novel chemical platform as a convenient tool for further investigations of the two states of naïve and primed pluripotency.

8.   Zusammenfassung (German)

8.1   Einleitung

Embryonale Stammzellen (ES-Zellen) werden aus der inneren Zellmasse (IZM) von Präimplantationsembryonen gewonnen. Sie sind in der Lage, zur Entwicklung von chimärischen Mäusen beizutragen, wenn sie in die IZM zurücktransplantiert werden. Diese besondere Fähigkeit wird als naive Pluripotenz oder als der Grundzustand der Pluripotenz bezeichnet. Epiblast-Stammzellen (EpiS-Zellen) werden aus dem Epiblasten von Postimplantationsembryonen gewonnen. Während sie ebenfalls pluripotente Stammzellen darstellen, die in der Lage sind, Teratomen zu generieren, tragen sie nicht zur Entwicklung von chimärischen Mäusen bei, wenn sie in die IZM zurücktransplantiert werden. Diese etwas beschränkte Pluripotenz des geringfügig weiter entwickelten Embryos wird "primed" Pluripotenz genannt, d.h. bereit für die Festlegung auf ein Keimblatt. EpiS-Zellen sind heterogen sowohl innerhalb von, als auch zwischen Zelllinien. Es wurde gezeigt, dass sie aus mindestens zwei Subpopulationen bestehen, die funktional der frühen bzw. der späten Postimplantationsentwicklung entsprechen. Der kleine Anteil, der das frühe Stadium repräsentiert, ist sogar fähig Chimären zu generieren, während der allergrößte Teil, der das späte Stadium repräsentiert, nicht zur Entwicklung von Chimären beitragen kann. Bis jetzt konnten diese EpiS-Zellen des späten Stadiums nicht, allein durch chemische Inhibitoren, in naive Pluripotenz reprogrammiert werden. Im Gegenteil zu EpiS-Zellen des frühen Stadiums widersetzten sich EpiS-Zellen des späten Stadiums der 2i/LIF-Bedingung, mit dem die Stabilisierung des Grundzustands der Pluripotenz durch Inhibition von GSK3β und MEK erreicht werden kann.

8.2   Ziel der vorliegenden Arbeit

Ziel der vorliegenden Arbeit war, eine neue chemische Methode für die Konvertierung von inerten EpiS-Zellen des späten Stadiums in naive Pluripotenz zu identifizieren. Im Rahmen der Untersuchungen des Wirkmechanismus der entdeckten aktiven Verbindungen sollte der Mechanismus, der der Etablierung des Grundzustands der Pluripotenz in EpiS-Zellen des späten Stadiums zugrunde liegt, aufgeklärt werden.

8.3   Methoden

Zu diesem Zweck wählte ich einen chemisch-genetischen Ansatz. Ich entwickelte ein systematisches Testverfahren (screening assay) zur Identifizierung von niedermolekularen Verbindungen (small molecules) und benutzten die LOPAC-Bibliothek von bekannten pharmakologisch aktiven Verbindungen, um "Treffer" (hits) zu finden. Der Hit wurde in Sekundärtestverfahren durch vollständige Charakterisierung der konvertierten Zellen mittels FACS, qRT-PCR, globaler Genexpressionsanalyse, Immunozytochemie und Teratom- und Chimärentest validiert. Untersuchungen zur Zielidentifizierung umfassten Kinaseprofilierung, Testierung weiterer Inhibitoren mit abweichenden chemischen Strukturen, Microarray- und Gene Ontology-Analysen, Untersuchungen zur Struktur-Aktivitätsbeziehung und IC50-Wertbestimmungen. Die weitere Erforschung des Wirkmechanismus und die Zielvalidierung umfassten biochemische Testverfahren, wie Westernblot, genetische Knock-down-Experimente, und *in vivo* phänotyp-basierte Testverfahren am Zebrafischmodell.

8.4 Ergebnisse

Ich entwickelte ein Testverfahren (screening assay) in 96-Well-Mikrotiterplatten basierend auf der unterschiedlichen Exprimierung des *OCT4-GFP*-Reportergens in GOF18 EpiS-Zellen und ES-Zellen für die Identifizierung von aktiven niedermolekularen Verbindungen (small molecules). Für die Auslese wurde ein High-content-Lesegerät für Mikrotiterplatten verwendet. Ich identifizierte Triamteren (TR), ein bekanntes Pteridinderivat, das als Diuretikum verwendet wird, als Trefferverbindung. Die Validierung der Trefferverbindung zeigte, dass TR mehrere EpiS-Zelllinien des späten Stadiums in einen Zustand konvertieren konnte, der viele Eigenschaften mit ES-Zellen teilte. Die konvertierten Zellen waren jedoch nicht in der Lage, zur Entwicklung von Chimären beizutragen, wenn sie in Blastozysten injiziert wurden. Dieses Defizit konnte durch die Ergänzung der TR-induzierten Konvertierung durch gleichzeitige Inhibition des ERK-Signalwegs überwunden werden, was in der Gewinnung von ES-Zell-ähnlichen Zellen mit vollständiger Chimärenkompetenz resultierte. Kinaseprofilierung identifizierte CK1δ/ϵ und PI3Kclass2γ als mögliche Zielmoleküle von TR. Anschließende Gen-knock-down-Experimente bestätigten die Isoform CK1ϵ als das Zielmolekül der TR-induzierten Konvertierung. Untersuchungen der Struktur-Aktivitätsbeziehung führte zur Synthese eines deutlich potenteren Inhibitors, genannt AU52, mit der Fähigkeit der naiven Zellkonvertierung. Biochemische Analysen zeigten, dass die Inhibition von CK1ϵ in der gleichzeitigen Inhibition der Phosphorylierung von β-CATENIN and SMAD2 resultierte. Die zeitgleiche Stimulierung des WNT und Blockierung des TGFβ Signalwegs führten zur Aktivierung der ES-Zell-spezifischen Transkriptionsfaktoren *Klf2*, *Nanog* und *Esrrb*, die schließlich die naive Konvertierung bewerkstelligten.

143

8.5   Schlussfolgerung

Zusammenfassend stellen die vorliegenden Ergebnisse das erste chemische Protokoll für die Reprogrammierung von EpiS-Zellen des späten Stadiums in naive Pluripotenz dar. Ich zeige, dass CK1ε einen Einfluss auf das Kernnetzwerk der Regulierung des Grundzustands der Pluripotenz hat, und erläutere den Wirkmechanismus der TR/AU52-induzierten naiven Konvertierung. Letztendlich stelle ich eine neue chemische Methode für die weitere Erforschung der zwei Stadien der "naïve" und "primed" Pluripotenz vor.

9. Appendix

Appendix 1. Kinase Profiling of Triamterene and AU52 Against a Selected Set of ESC-Related Kinases

Kinase	Residual kinase activity [%]	
	TR @ 10µM	AU52 @ 10 µM
Abl	98	92
Abl (m)	97	91
Akt1	100	102
Akt2	112	94
Akt3	95	71
ALK	86	79
ALK4	93	86
ALK5	107	102
Aurora A	103	66
Aurora B	101	98
Aurora C	90	86
CDK1/cyclinB	103	101
CDK2/cyclinA	103	100
CDK2/cyclinE	101	85
CDK3/cyclinE	96	97
CDK5/p25	97	85
CDK5/p35	103	86
CDK6/cyclinD3	93	98
CDK7/cyclinH/MAT1	86	139
CDK9/cyclin T1	87	101
CK1γ1	98	86
CK1γ2	95	85
CK1γ3	110	90
CK1δ	28	-7
CK2	95	86
CK2α2	109	79
cSRC	97	102
FAK	105	105
Fer	111	96

Appendix 1 cont.

FGFR1	93	116
FGFR2	104	93
FGFR3	99	84
FGFR4	99	100
GSK3-alpha	102	95
GSK3-beta	114	95
IKK-alpha	103	96
IKK-beta	93	71
JAK2	94	104
JAK3	118	86
JNK1α1	104	101
JNK2α2	102	89
JNK3	90	59
LIMK1	89	92
Lyn	88	86
Lyn (m)	97	103
MAPK1	115	84
MAPK2	108	94
MAPK2 (m)	102	90
MAPK12	107	93
MAPK13	87	76
MEK1	107	117
MKK4 (m)	129	120
MKK6	108	111
MKK7-beta	114	135
MLCK	89	82
MLK1	88	71
MST1	101	99
MST2	99	85
MST3	102	89
mTOR	83	94
NLK	93	84
p38 alpha	100	93
p38 beta	92	89
p70S6K	91	94
PAK2	107	103
PAK4	94	103
PAK5	100	82
PAK6	89	85
PDK1	103	83

Appendix 1 cont.

PI3 Kinase (p110b/p85a)	100	93
PI3 Kinase (p120g)	58	60
PI3 Kinase (p110d/p85a)	81	51
PI3 Kinase (p110a/p85a) (m)	89	90
PI3 Kinase (p110a/p65a) (m)	91	90
PI3 Kinase (p110a(E545K)/p85a) (m)	91	82
PI3 Kinase (p110a(H1047R)/p85a) (m)	96	91
PI3 Kinase (p110b/p85b) (m)	98	88
PI3 Kinase (p110b/p85a) (m)	97	90
PI3 Kinase (p110d/p85a) (m)	60	66
PI3 Kinase (p110a(E542K)/p85a) (m)	89	83
PI3 Kinase (p110a/p85a)	82	79
PI3 Kinase (p110a(E542K)/p85a)	81	91
PI3 Kinase (p110a(H1047R)/p85a)	81	95
PI3 Kinase (p110a(E545K)/p85a)	75	84
PI3 Kinase (p110a/p65a)	86	87
PI3KC2a	107	76
PI3KC2g	35	23
PKA	103	104
PKCα	110	88
PKCβI	101	98
PKCβII	93	90
PKCγ	103	102
PKCδ	107	93
PKCε	106	87
PKCμ	106	88
PKCη	105	95
PKCι	102	86
PKCμ	100	96
PKCθ	107	97
PKCζ	123	100
PIP4K2a	98	86
PIP5K1a	95	87
PIP5K1g	76	73
ROCK-I	105	80
ROCK-II	100	102
Src(1-530)	96	94
Syk	92	89

Appendix 2. Primer Sequences for qRT-PCR

Gene	Fwd primer 5'-3'	Rev primer 5'-3'
Axin2	TAGGCGGAATGAAGATGGAC	CTGGTCACCCAACAAGGAGT
beta-Act	ACTGCCGCATCCTCTTCCTC	CCGCTCGTTGCCAATAGTGA
Cdx1	GGGGTCACTGTGGACAAACT	GGCCTAGGACACAAGAGCTG
Dppa4	CGGGCGTCATAACCAGTTCA	GACATGCATGCGGAGGCTAC
Dppa5	TGTGTCTCCGACCTGGATGC	CACATCAGAATGCGCAGCAG
Esrrb	AGGCTCTCATTTGGGCCTAGC	ATCCTTGCCTGCCACCTGTT
Fgf5	CCTTGCGACCCAGGAGCTTA	CCGTCTGTGGTTTCTGTTGAGG
Fgf8	TCGCGAAGCTCATTGTGGA	GCCGTTGCTCTTGGCAATTAG
Gapdh	CCAATGTGTCCGTCGTGGAT	TGCCTGCTTCACCACCTTCT
Klf4	TGTGTCGGAGGAAGAGGAAGC	ACGACTCACCAAGCACCATCA
Nanog	GAACGGCCAGCCTTGGAAT	GCAACTGTACGTAAGGCTGCAGAA
Oct4	TGTTCCCGTCACTGCTCTGG	TTGCCTTGGCTCACAGCATC
Rex1	GGCTGCGAGAAGAGCTTTATTCA	AGCATTTCTTCCCGGCCTTT
Sox1	GGCCGAGTGGAAGGTCATGT	TCCGGGTGTTCCTTCATGTG
Sox2	TTCGAGGAAAGGGTTCTTGCTG	TCCTTCCTTGTTTGTAACGGTCCT
Stella (Dppa3)	GCCGCACAGCAGATGTGAA	AAATCTGGATCGTTGTGCATCCT
T	TTGAACTTTCCTCCATGTGCTGA	TCCCAAGAGCCTGCCACTTT

10. Abbreviations

°C	degree Celsius
μg	microgram
μl	microliter
μM	micromolar
2i	PD0325901 and CHIR99021
ALP	alkaline phosphatase
AP	alkaline phosphatase
bFGF	basic fibroblast growth factor; also FGF2
BIOS	biology-oriented synthesis
BMP4	bone morphogenetic protein 4
BSA	bovine serum albumin
cDNA	copy deoxyribonucleic acid
CH	CHIR99021
cm	centimeter
CM	conditioned medium
CRISPR	clustered regularly interspaced short palindromic repeats
Ctrl	control
Da	Dalton
DE	distal enhancer
DMEM	Dulbecco's Modified Eagle's Medium
DNA	deoxyribonucleic acid
DOS	diversity-oriented synthesis
dpc	days post coitum; also E3.5
E3.5	embryonic day 3.5; also 3.5 dpc
ENaC	epithelial sodium channel
EpiSC	epiblast stem cell

FCS	fetal calf serum
FGF2	fibroblast growth factor 2; also bFGF
FRET	fluorescence resonance energy transfer
GFP	green fluorescent protein
GO	gene ontology
GPCR	G protein-coupled receptor
H&E	hematoxylin and eosin stain
hESC	human embryonic stem cell
hpf	hours post fertilization
HRP	horseradish peroxidase
hrs	hours; also hr
HTRF	homogeneous time resolved fluorescence
ICM	inner cell mass
ID	identification
KD	knockdown
KOSR	knockout serum replacement
LIF	leukemia inhibitory factor
MEF	mouse embryonic fibroblasts
mESC	mouse embryonic stem cell
mg	milligram
min	minute
ml	milliliter
mm	millimeter
mM	millimolar
ng	nanogram
NMR	nuclear magnetic resonance
PBS	phosphate buffered saline
PD	PD0325901
PE	proximal enhancer
PFA	paraformaldehyde
PSSC	protein structure similarity clustering

10. Abbreviations

PVDF	polyvinylidene difluoride
qRT-PCR	quantitative reverse transcription polymerase chain reaction
RNA	ribonucleic acid
rpm	revolutions per minute
RT	room temperature
SAR	structure-activity-relationship
SB	SB431542
SCONP	structural classification of natural products
SD	standard deviation
SDS-PAGE	sodium dodecyl sulfate polyacrylamide gel electrophoresis
shRNA	short hairpin ribonucleic acid
SILAC	stable isotope labeling by/with amino acids in cell culture
TALEN	transcription activator-like effector nucleases
TBST	tris buffered saline with Tween 20
TOS	target-oriented synthesis
TR	Triamterene

11.   Curriculum Vitae

Personal Data

Name:	Damir Jacob Illich
Date of Birth:	November 1, 1984
Place of Birth:	Banja Luka, Republic of Srpska
Nationality:	German

Graduate Education

Jan 2010 - present	Doctoral research studies under the supervision of Prof. Dr. Herbert Waldmann and Prof. Dr. Hans R. Schöler, Max-Planck Institute for Molecular Biomedicine, Münster, Germany "Discovery and Mechanistic Studies of Triamterene-induced Naïve Conversion of Late-Stage Epiblast Stem Cells"

Undergraduate Education

Mar 2009 - Dec 2009	Diploma thesis under the supervision of Prof. Dr. Jürgen Hescheler and Dr. Dr. Tomo Saric, Institute for Neurophysiology, Uniclinic Cologne, Cologne, Germany "Enhancing the Generation of Induced Pluripotent Stem (iPS) Cells With Small Molecules"
Oct 2007 - Mar 2009	Hauptstudium in Medicinal Chemistry, University of Regensburg, Regensburg, Germany
Oct 2004 - Oct 2007	Grundstudium in Chemistry, University of Erlangen/Nürnberg, Erlangen, Germany

Pre-University Education

Sep 1995 - Jun 2004	Aventinus Gymnasium, Burghausen, Germany
Sep 1991 - Jul 1995	Grundschule, Burghausen, Germany

153

Extracurricular Internships

Aug/Sep 2007   Research Internship under the supervision of Prof.
                       Dr. Markus Kaiser, Chemical Genomics Center of
                       the Max-Planck Society, Dortmund, Germany

Mar/April 2007   Research Internship under the supervision of Prof.
                       Dr. Christoph Thiele, Max-Planck Institute of
                       Molecular Cell Biology and Genetics, Dresden,
                       Germany